USING COMPUTATIONAL MODELS TO SCALE SUBLETHAL EFFECTS OF STRESSORS TO ADVERSE POPULATION OUTCOMES IN FISH

By

Brandon M. Armstrong

A DISSERTATION

Submitted to

Michigan State University
In partial fulfillment of the requirements
For the degree of

Fisheries and Wildlife – Doctor of Philosophy
Environmental Toxicology – Dual Major

2016

ABSTRACT

COMPUTATIONAL MODELS TO SCALE FROM SUBLETHAL EFFECTS OF STRESSORS TO ADVERSE FISH POPULATION RELEVANT OUTCOMES

By

Brandon M. Armstrong

Obtaining whole-animal or population-level data to evaluate the thousands of anthropogenic chemicals that exist is impractical. The U.S. National Research Council (NRC) recommended that new, predictive approaches be developed to examine toxicant effects ranging from molecular level changes in individuals to impacts on entire populations. One approach that can help meet the goals of the NRC is the adverse outcome pathway (AOP), a conceptual framework linking a single molecular initiating event to an adverse outcome at the level of the population considered relevant for risk assessment. My research is focused on the development of two AOPs; 1) Reduced fecundity in female fish due to an impairment of vitellogenin production following exposure to select neurotoxicants and 2) Reduced survival and growth of early life stage fish as a result of behavioral impairments following neurotoxicant exposure.

Much of the AOP focus has been on fish reproduction, specifically the initiation of the hormonal cascade within the hypothalamic-pituitary-gonadal (HPG) axis and the formation of vitellogenin, an egg yolk precursor protein. Previous efforts modeling fish vitellogenin production were driven by gonadotropin production and did not incorporate components that influenced its release. Many end products of this hormonal cascade are controlled by the upstream production of neurotransmitters, such as gamma-aminobutyric acid and dopamine. Inclusion of a neurotransmission compartment can increase the predictive power and accuracy of the fish vitellogenin model. I hypothesized that several environmental toxicants will interact with and disrupt the function of neurotransmitter receptors and enzymes that have critical roles in

vertebrate reproduction and could cause population level effects. Specifically, I explored two case studies, methylmercury (MeHg) and pulp and paper mill effluent (PPME) and their potential for neurotoxic effects on subsequent vitellogenin production. My goal was to incorporate a neurotransmission compartment into the existing fish vitellogenesis model using results from cell-free high throughput bioassays to predict adverse reproductive outcomes following exposure to contaminants. This model highlighted the importance of understanding pathway differences between species and showed a proof of principle concept for determining how perturbations to physiological systems could enhance or inhibit fish reproduction.

Additionally, there is a current need for developing an AOP for fish early-life-stage toxicity as conducting traditional early-life stage tests are labor- and resource-intensive and do not provide essential information regarding a chemical's mode of action. Toxicants have been shown to cause adverse effects on larval fish behavior well below exposure concentrations that induce mortality. Behavior can be incorporated into an individual-based model (IBM) to predict how adverse effects on an individual's behavior cause ramifications at the population level. Previous research has shown that MeHg exposure can impair larval fish behavior. I hypothesized that growth rate and survival of a larval fish population will be reduced due to impaired swimming speed and reduced foraging efficiency following MeHg exposure. My approach was to adapt a previously built IBM in order to link these sublethal behavioral effects to population relevant outcomes such as survival and growth. The last chapter uses the IBM to explore several ecological factors that may explain the recent low recruitment of yellow perch in Lake Michigan. This work highlighted the importance of assessing complex mixtures of stress including both abiotic and biotic sources which can interact and adversely affect the pelagic larval fish community.

This dissertation is dedicated to my wife, Kristen, and our children for their endless love, patience and support. It is also dedicated to my parents, Brian and Vickie, who opened the door to my education.

ACKNOWLEDGMENTS

First and foremost I must acknowledge many of the people whom without this work would not be possible. Cheryl Murphy[1], my graduate advisor, was crucial in providing support, expertise and dedication toward the success of my Dissertation. Dan Hayes, Karen Chou and Richard Balander served on my graduate committee and provided critical advice and guidance throughout my research. My colleagues Niladri Basu[2], Jessica Head[2], Adeline Arini[2], Krittika Mittal[2], Michael Carvan III[3], Francisco Mora[3], Abby Debofsky[3], Rebekah Klingler[3], Scott McNaught[4] and Frederick Goetz[5] not only performed most of the experimental and field sampling behind this work but also provided valuable feedback on modeling design and development. Sara Smith[1] and Kathleen Jensen[6] advised and assisted in laboratory methods. Several undergraduate assistants including Jake Young[1], Karishma Chopra[1], and Erin Smigielski[1] assisted in either performing modeling exercises or provided assistance in the laboratory. James Lazorchak[6] offered his expertise and assistance toward my professional development. The Institute for Integrative Toxicology including Bob Roth, the Council of Graduate Students, the Graduate School, College of Lyman Briggs, College of Natural Resources and Dr. Howard Tanner at Michigan State University in addition to the Society of Environmental Toxicology and Chemistry presented me with numerous assistantships in support of my research. Finally, I would like to thank everyone in the Fisheries and Wildlife Department at MSU for over 15 years of enjoyable and unforgettable memories.

Michigan State University[1],McGill University[2],University of Wisconsin-Milwaukee[3],Central Michigan University[4],National Oceanic and Atmospheric Administration[5], United States Environmental Protection Agency[6]

TABLE OF CONTENTS

LIST OF TABLES

LIST OF FIGURES

KEY TO ABBREVIATIONS

AOP	Adverse outcome pathway
D2	Dopamine D2 receptor
DA	Dopamine
DDE	Dichlorodiphenyl dichloroethylene
E2	17β-estradiol
ER	Estrogen receptor
CPUE	Catch per unit effort
GABA	γ-aminobutyric acid
$GABA_A$	γ-aminobutyric acid A receptor
GABA-T	γ-aminobutyric acid transaminase
GnRH	Gonadotropin releasing hormone
Hg	Mercury
HPGL	Hypothalamic-pituitary-gonadal-liver
IBM	Individual based model
LH	Luteinizing hormone
MAO	Monoamine oxidase
MeHg	Methylmercury
NOAEC	No-observable-adverse-effect concentration
NRC	National Research Council
ODD	Overview, design concepts and details
OFAT	One factor at a time analysis

PCBs	Polychlorinated biphenyls
PPME	Pulp and paper mill effluent
PVPP	Polyvinylpolypyrrolidone
qPCR	Quantitative polymerase chain reactions
SBP	Steroid binding proteins
T	Testosterone
TSCA	Toxic Substances Control Act
U.S. EPA	United States Environmental Protection Agency
VTG	Vitellogenin
YOY	Young of the year

INTRODUCTION

One significant adverse effect of contaminants on Great Lakes fish is the death of large, commercially valuable resident species, however, little is known about the population implications of subtle or sublethal effects. Often stressors, such as contaminants that do not cause a direct mortality, can exert sublethal effects; however these responses can be more difficult to measure. Sublethal stressors can interfere with behavior, bioenergetics, endocrine function and immunity of individuals which can have repercussions at the population level.

There are over 85,000 registered chemicals on the U.S. Environmental Protection Agency's TSCA Chemical Substance Inventory (U.S. EPA 2015), making it impractical to rely solely on *in vivo* toxicology moving forward. Computational models can be a tool used to extrapolate from *in vitro* data to *in vivo* responses. *In vitro* assays can be used to determine multiple modes of action of compounds over a wide concentration range (NRC 2007) and can be used to understand toxicity of complex mixtures (Basu et al. 2009). Adverse outcome pathways (AOPs) are a conceptual framework that can be used to relate a single molecular initiating event to an adverse outcome relevant to risk assessment (Ankley et al. 2010). Computational models can then create quantitative linkages between key events within an AOP to link *in vitro* molecular data to *in vivo* adverse outcomes at the individual or population level.

Computational modeling is an important tool that can be used to estimate the damage of fish and wildlife populations caused by contaminant exposure. Several modeling techniques are available to predict mortality following contaminant exposure (Hallam et al. 1990, Mayer et al. 1994, Sun et al. 1995, Field et al. 2002); however, it is just as important to understand the population implications following exposure to sublethal contaminant concentrations. Linking

sublethal effects to population outcomes is a recent development in ecological risk assessment, and such an exercise has not been performed for the fish inhabiting the Great Lakes.

Much of the focus of my Dissertation centers on evaluating potential reasons for the yellow perch, *Perca flavescens*, decline in Lake Michigan. Since the late 1990's yellow perch in Lake Michigan have experienced poor recruitment (Dettmers et al. 2003, Clapp & Dettmers 2004, Santucci Jr et al. 2014) which has been attributed to food web changes following exotic species introductions (Shroyer & McComish 2000, Marsden & Robillard 2004) and other abiotic factors (Clapp & Dettmers 2004). However, I hypothesized that contaminant exposure may be another factor contributing to the yellow perch decline. Recently, computational models have been developed for other systems which extrapolate from sublethal effects following contaminant exposure to population relevant indices such as fecundity, growth and survival (Murphy et al. 2005, Miller et al. 2007, Murphy et al. 2008, Watanabe et al. 2009, Li et al. 2011). Therefore my goal was to adapt and develop similar computational models for yellow perch in Lake Michigan to evaluate sublethal effects of contaminant exposure on their population.

The first two chapters of my dissertation focus on the effects of contaminants on the fish neuroendocrine system which can have implications in egg production. *In vitro* screening assays and whole animal *in vivo* studies combined with modeling determined the subtle effects of contaminants found within the Great Lakes on fish population dynamics. A physiological model was developed to link the results from *in vitro* screening assays with individual-level outcomes concerning fish reproduction. Specifically, this model linked the process of vitellogenesis in a female fish with neuroendocrine biomarkers of effect including dopamine and gamma-aminobutyric acid processes within the hypothalamus. The cumulative vitellogenin produced by

this model was then used to estimate the total number of eggs produced as a means to scale to population-level implications following contaminant exposure.

The last two chapters take an individual based modeling (IBM) approach to evaluate effects of stressors on larval yellow perch recruitment in Lake Michigan. Contaminants that evoke sublethal effects on an individual's behavior can have significant implications on the population. For example, reductions in larval yellow perch swimming speed and foraging efficiency following methylmercury exposure (Mora et al. 2015) may affect an individual's ability to grow and survive through predator-prey interactions. Additionally, suboptimal habitat conditions have been shown to reduce tolerances of individuals to various contaminant exposures (Thrush et al. 2008). Therefore, I also investigated whether methylmercury exposure and/or habitat conditions in Lake Michigan may be having an adverse effect on larval yellow perch recruitment.

This project assisted in the development of a multi-tiered experimental approach and framework that can be used to assess ecological exposures and effects of many contaminants within the Great Lakes and their potential impacts on fish population dynamics. With this research, we have a better understanding of how contaminants affect our fisheries and the information will be invaluable for developing guidelines for acceptable contaminant loads for a healthy Great Lakes ecosystem. These efforts will support improvements in the Great Lakes as the models allow for a linkage of individual effects to population indices which can begin to estimate the damage contaminants can cause to a fish population.

CHAPTER 1

INCORPORATING A NEUROTRANSMISSION COMPARTMENT INTO THE FISH VITELLOGENESIS MODEL: A PULP AND PAPER MILL EFFLUENT CASE STUDY

ABSTRACT

Many environmental contaminants may cause adverse reproductive effects through disruption of the neuroendocrine system. Pulp and paper mill effluent can contain up to 250 different contaminants and has been linked to reproductive impairment in fish. We used data from an *in vitro* study that characterized the potential neurochemical effects of pulp and paper mill effluent, to model vitellogenin production after exposure to different effluent fractions. We hypothesized that disrupted *in vitro* GABA and DA signaling could be modeled to simulate reproductive impairment in fish, specifically reduced vitellogenin production. These neurotransmitters are involved in the release of gonadotropin releasing hormone from the hypothalamus which stimulates downstream processes related to vitellogenin production in the liver of female fish. In0 our approach, we integrated the *in vitro* results into a fish vitellogenesis model to predict adverse reproductive outcomes at the individual level. Our model results indicate that exposure to toxicants within pulp and paper mill effluent which interfere with neurotransmission may cause harmful reproductive effects by impairing vitellogenin production. While the model has yet to be validated, our proof of principle approach highlights the use of computational modeling as a means to integrate results from *in vitro* studies that assess complex mixtures to potentially adverse effects on fish reproduction

1.0 INTRODUCTION

Aquatic organisms are exposed to complex mixtures of stressors in their environment derived from both natural and anthropogenic sources. Predatory cues, food limitations, temperature fluctuations, hypoxia and salinity are just a few of the stressors that exist within

aquatic environments (Holmstrup et al. 2010, Hooper et al. 2013). Anthropogenic sources can also include the release of chemical compounds through household and industrial wastes and agricultural practices (Kolpin et al. 2002, Adams 2005). For example, in a recent survey of 139 streams across the United States, over 80 organic wastewater contaminants, including personal care products, agricultural, industrial and household compounds and pharmaceuticals were detected and at least one of these compounds was detected in 80% of the streams sampled (Kolpin et al. 2002). Understanding how these stressors interact with one another in a complex mixture to produce biological effects remains a difficult yet pressing task for ecotoxicology.

Complex mixtures may cause long-term adverse effects on communities inhabiting aquatic environments. A commonly measured adverse effect is mortality; however sublethal effects may occur following exposures to doses lower than those that induce mortality. Often, contaminants impair behavior, gene expression and physiological function (Laws, 2000) which may interfere with bioenergetics, endocrine and neuroendocrine functions and immunity of organisms. Chemical interactions within complex mixtures may result in adverse effects even below their individual no-observable-adverse-effect concentration (NOAEC; Monosson 2005). For example, Armstrong et al. (2015) determined that a mixture of unionized ammonia (NH_3; 0.03 mg/L) and the pharmaceutical 17α-ethinylestradiol (EE2; 0.25 ng/L) at their respective NOAEC resulted in increased fathead minnow mortality during a 21 day exposure.

Traditionally, toxicological studies have assessed the effects of a single contaminant on a single organismal species. Many of these studies were conducted in laboratory settings offering optimal environmental conditions for the chosen organism that could survive in a laboratory setting. Additionally, these studies focused on laboratory model species which aren't necessarily predictive of wild species. Lastly, many of them did not assess the interactions that may occur

between stressors and that these interactions may culminate in cumulative, synergistic, antagonistic or additive effects. Therefore, effect concentrations derived from single contaminant exposures may fall short in protecting aquatic organisms inhabiting environments where complex mixtures of environmental stressors exist.

Assessing the biological effects of chemical mixtures is a challenge as there are currently over 85,000 registered chemicals on the U.S. Environmental Protection Agency's Toxic Substances Control Act (TSCA) chemical substance inventory (U.S. EPA 2015). Fully assessing the biological effects of each chemical on every species inhabiting aquatic environment is not attainable. It is also impractical to determine the effects of every possible combination of chemicals found in a complex mixture using traditional approaches. Chemical instrumentation analyses can determine the types and quantities of each chemical associated with a chemical mixture; however this technique offers little or no information on biological effects stemming from an exposure to that mixture. Biological methods can be used to derive effect concentrations for various endpoints however these methods cannot determine which chemical in the mixture (or their interactions) are producing the observed biological effect.

Exposure to contaminants that evoke sublethal effects within individuals can indicate exposure through identifiable profiles, known as biomarkers, which can be measured at the molecular, biochemical or cellular level (U.S. EPA, 2012). Biomarkers are quantifiable biological responses used to indicate the biological state of an organism or cell (Carvan 2008). These biomarkers are generally easier to measure than conducting whole-organism and/or population-level studies, and so, a goal of toxicology today is to extrapolate from mechanistically relevant molecular and subcellular biomarkers to whole individual and population/community level effects.

Biomarkers are not without their own set of limitations. Biomarkers only provide a measurement at a single time point and due to the complexity of organismal systems one must consider the temporal dependence of a biomarker from the onset of exposure (Forbes et al. 2006). Measuring multiple biomarkers at any given time may only lead to ambiguity as individual biomarkers likely have different dose-response curves (Depledge 1994, Forbes et al. 2006). Forbes et al. (2006) suggested that suites of biomarkers must be linked to a mechanistic model tied to some measurement of fitness in order to be useful. When coupled with a mechanistic model anchored to an exposure or toxicologically relevant phenotype, biomarkers measured in an individual can be useful predictors of population risk (Carvan 2008).

For ecotoxicological purposes, sublethal effects must be translated to population level impacts. There are significant limitations to obtaining population-level data to evaluate the thousands of anthropogenic chemicals, many have been recognized by the U.S. National Research Council (NRC 2007) who suggested that new, predictive approaches be developed to examine toxicant effects. These recommendations range from molecular level changes in individuals to impacts on entire populations (NRC 2007). The NRC suggested that researchers and regulators move away from the reliance on *in vivo* studies to *in vitro* model systems. One approach that can help meet these goals is the adverse outcome pathway (AOP), a conceptual framework linking molecular initiating events caused by contaminant exposures to adverse outcomes at higher levels of organization considered relevant to risk assessment (Ankley et al. 2010).

An AOP framework approach can be used to assess the risks of environmental contaminant mixtures to fish and wildlife by scaling molecular data to the individual and also to the population level (Watanabe et al. 2011). This framework could help population modeling and

ecological risk assessment efforts by linking ecotoxicology data with mechanistic predictors of effects to reproduction and population survival (Kramer et al. 2011). Currently, AOPs are being developed to relate chronic toxicity to impaired fish growth (Groh et al. 2015) and reproduction (Ankley et al. 2010). As further AOPs are established, modeling approaches will be needed to link several AOPs into an integrated key event network (Murphy et al. 2017). This linkage process is necessary as it is unlikely that exposure to a chemical will result in only a single AOP being activated, especially considering the wide range of molecular targets within complex organisms.

In this chapter we investigated a pulp and paper mill effluent case study to show, as proof of principle, a way to integrate *in vitro* neurochemical data into a fish vitellogenesis model to predict adverse reproductive effects following exposure to complex mixtures. The vitellogenesis model was adapted from Murphy et al. (2005) to include the release of neurotransmitters specific to fish reproduction and their binding to associated receptors which influence the downstream production of sex steroids. We included processes for γ-aminobutyric acid (GABA) and dopamine (DA) as they are the two primary neurotransmitters involved in controlling gonadotropin production in fish. Neurotransmitters binding to their respective receptors and the activity of their associated degrading enzymes can be measured using cell-free *in vitro* assays. We leveraged data from an *in vitro* study (Basu et al. 2009) which exposed common goldfish whole brain extracts to fractionated PPME and characterized subsequent impairments to GABA and DA receptor binding and enzyme activity. Our objective was to incorporate the *in vitro* neurochemical data into the mathematical model and simulate the HPGL axis of a generic female fish by predicting cumulative vitellogenin production over one spawning season. Model

simulations for each effluent fraction were then compared against a control to determine if an impairment of vitellogenin production would result from PPME exposure.

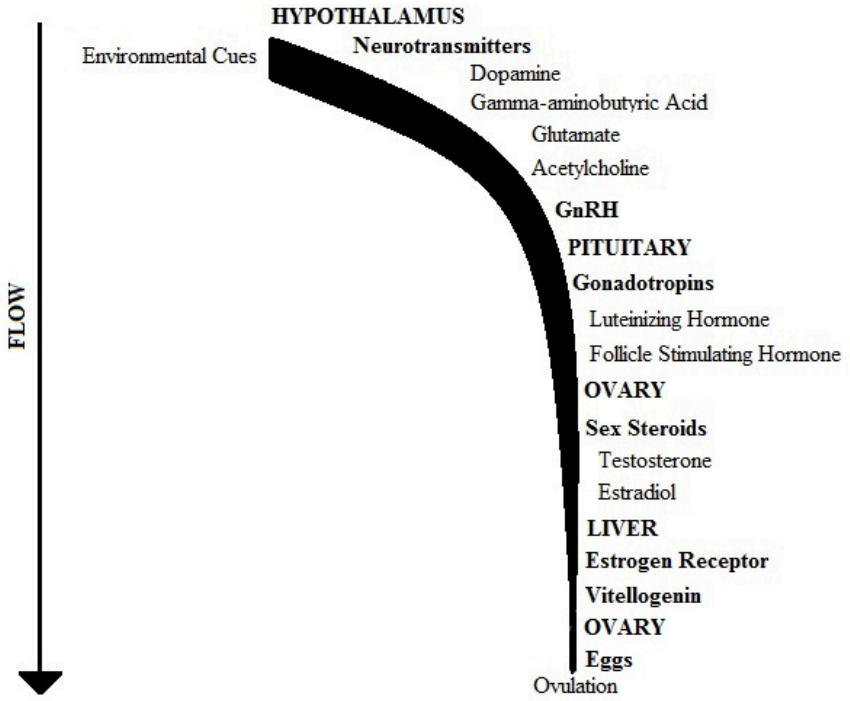

Figure 1: The hormonal cascade of the fish hypothalamic-pituitary-gonadal-liver axis and subsequent reproduction

Vertebrate reproduction is controlled by many hormones and compounds within the hypothalamic-pituitary-gonadal-liver (HPGL) axis, Figure 1 (Van Der Kraak et al., 1998; Trudeau et al. 2000). Environmental cues, such as temperature and photoperiod, stimulate the release of neurotransmitters. Neurotransmitters facilitate the body's communication system, including reproduction, by acting as chemical messengers and activating specific receptors in post synaptic cells, Figure 2, (Lauder et al. 1993).

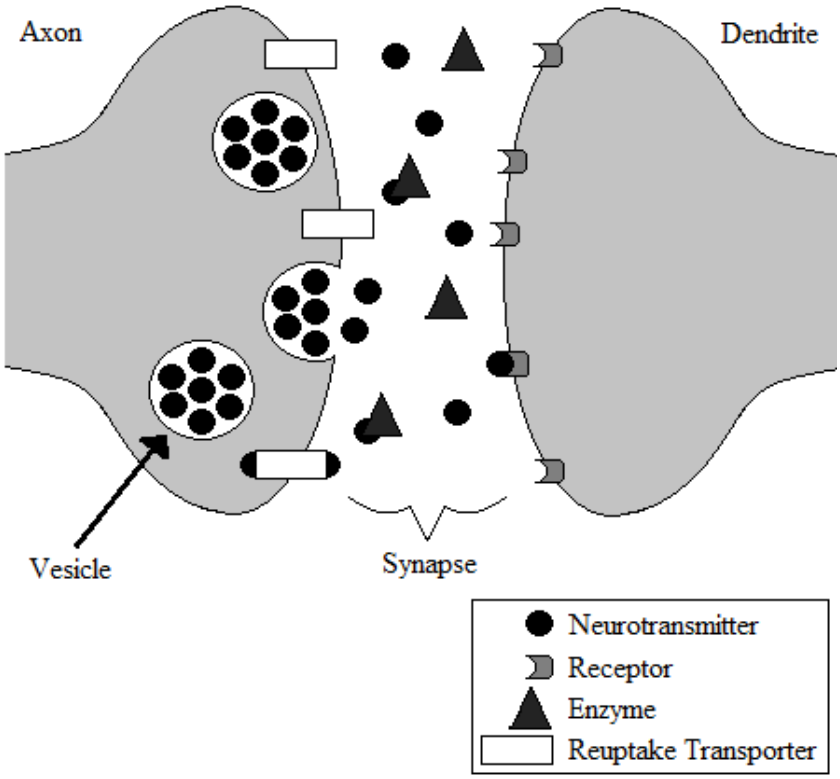

Figure 2: Neurotransmission

Neural cells transmit information from one cell to another at the synapse, the narrow space between the axon of the initiating cell and recipient cell (McGeer et al. 2013). The initiating cell generates an action potential that travels through the axon to the terminal triggering the release of neurotransmitters from the axon into the synapse. The neurotransmitters then bind to post-synaptic receptors of the recipient cell and depolarize the cell membrane. The chemical signal is converted back to an electrical signal and either destroyed or cleared. There are three major classes of neurotransmitters: biogenic amines, amino acids and neuropeptides (Kurreck & Stein 2015).

There are a number of mechanisms in which toxicants can cause neurotoxicity. Once released, neurotransmitters must then bind to receptors to initiate the signaling process. Toxicants can impede the cell signaling by binding or activating these receptors and/or inhibiting

neurotransmitter release. Inactivation of free (unbound) neurotransmitters within the synaptic cleft occurs through enzymatic degradation. Toxicants may disrupt enzyme activity within the hypothalamus (Basu et al. 2009). Disruption of neurotransmitter receptor binding or enzyme activity may cause downstream effects including altered sex hormone dynamics which may impair reproduction (Figure 1).

Dopamine (DA) is a biogenic amine neurotransmitter that acts directly at the pituitary cell level to inhibit the release of gonadotropin through interaction with the gonadotrope D2 receptor (Zohar et al., 2010). In some species such as the goldfish, *Carassius auratus,* DA has been shown to inhibit both gonadotropin release directly as well as gonadotropin releasing hormone (GnRH) mediated gonadotropin secretion (Popesku et al., 2008). This is thought to be an evolutionary mechanism to prevent spawning during periods of poor environmental conditions (Zohar et al., 2010). Once released, free DA is subject to reuptake into the presynaptic terminal by DA transporters or degradation by the enzyme monoamine oxidase (MAO) (Bortolato et al. 2008). The role of DA is dependent on the fish species. For example, dopamine inhibition of GnRH was found to be very high in cyprinids and was much less pronounced in salmonids and nearly absent in Atlantic croaker, *Micropogonias undulates* (Van Der Kraak 2009) and percids (Zakes & Demska-Zakes 2005, Dabrowski et al. 1994, Żarski et al. 2015) which suggests dopamine's role in fish reproduction is a species-dependent process (Levavi-Sivan et al. 2010)

Gamma-aminobutyric acid (GABA) is an amino acid neurotransmitter found in the brain of vertebrates (Zohar et al., 2010). Once released it is reabsorbed by the presynaptic terminal, degraded by the enzyme GABA-transaminase (GABA-T) or bound to post synaptic terminal receptors (Treiman 2001). In mammals, GABA acts as an inhibitory neurotransmitter within the brain and, through interactions with GnRH neurons, GABA inhibits GnRH release (Smith & Jennes 2001). However, in fish, GABA has a stimulatory role in reproduction by promoting

GnRH secretion from the hypothalamus through exciting GnRH neurons and inhibiting DA release (Popesku et al. 2008, Watanabe et al. 2014). For example, rainbow trout injected with a single dose of GABA exhibited increased LH release from the pituitary (Levavi-Sivan et al. 2010) likely through actions on the hypothalamic GnRH neurons which directly innervate the pituitary (Peter et al. 1990). There are two types of GABA receptors localized throughout the hypothalamus, $GABA_A$ and $GABA_B$ (Maffucci & Gore, 2010). While the specific functions of these two receptor types aren't completely understood, mammalian research has shown that activation of the $GABA_A$ receptor blocks the proestrus LH surge and release whereas in fish, $GABA_A$ receptor activation excites GnRH neurons (Watanabe 2014).

The conversion of wood fibers into paper products generates a large amount of pollution (Ali & Sreekrishnan 2001) with up to 100 million kg of pollutants released into the environment each year (Dey et al. 2013). Additionally, the industry is one of the largest in terms of water consumption as the formation of paper products requires an expansive amount of freshwater (Thompson et al. 2001). Pulp and paper mill effluents (PPME) can contain over 250 different chemicals at various stages of the treatment process (Ali & Sreekrishnan 2001) including chlorinated compounds, fatty acids, tannins, organic polymers and sulfuric compounds (Zayas et al. 2011).

Several studies have shown that exposure to PPME can impair fish reproduction. For example, female largemouth bass exposed to PPME (≥ 20% effluent) for 56 days exhibited reduced 17β-estradiol and vitellogenin production (Sepulveda et al. 2003). Additionally, fathead minnow egg production was significantly reduced following a 5-day exposure to 100% PPME (Waye et al. 2014). The chemicals found in PPME can also alter *in vitro* neurochemical signaling in fish (Basu et al. 2009) which may be a mechanism for disrupted reproduction in fish exposed

to the effluent (Kovacs et al. 2013). In this case study, we will focus on the neurochemical effects of PPME reported by Basu et al. (2009).

Basu et al. (2009) assessed the potential neurochemical effects of PPME in goldfish brain tissue by measuring changes in GABA and DA neurotransmitter receptor binding and associated enzyme activities (Basu et al. 2009). The PPME was collected following primary treatment (clarifier) and secondary treatment (conventional activated sludge) from a facility in Eastern Canada and fractionated into different chemical components using classic solvent polarity (hexane, ethyl acetate and water) and polyphenolic extraction (Polyvinylpolypyrrolidone, PVPP) methods. While the fractionation process used did not identify the exact active compounds within the effluent, it did separate out chemicals into different classes based on unique properties of the individual compounds. Using an *in vitro* technique which measured changes in receptor binding and enzyme activity, Basu et al. (2009) reported that chemicals in both the primary and secondary PPME extracts can disrupt the function of neurotransmission in fish brains *in vitro* (Table 1). The data collected by Basu et al. (2009), by itself, is hard to interpret on higher levels of biological organization, such as an individual's reproductive potential, as some receptors were increased while their respective enzymes were also increased. For example, the hexane fraction of the primary effluent increased GABA binding to the $GABA_A$ receptor by 289 %, which may indicate increased gonadotropin production. However, GABA-transaminase activity was also increased 169 %, which may inhibit gonadotropin production. It is difficult to determine if reproduction would be impaired based on this *in vitro* information alone.

Table 1: Summary of *in vitro* mean neurochemical results expressed as a % of control samples following PPME exposure (Basu et al. 2009)

Neurochemical		Primary Effluent					Secondary Effluent				
		Solvent Series			PVPP		Solvent Series			PVPP	
		Ethyl Acetate	*Water*	*Hexane*	*Water*	*Ethanol*	*Ethyl Acetate*	*Water*	*Hexane*	*Water*	*Ethanol*
Receptors	D2	126.0*	148.3*	65.2	74	124.4	61.4	121.7*	99.9	144.9*	71.7
	$GABA_A$	104.8	92.1	288.9*	71.4	50.8	73	34.9*	73	33.3*	42.9
Enzymes	MAO	72.3*	103.7	53.3*	98.8	52.1*	96.7	85.6*	99.6	63.5*	100.1
	GABA-T	120.9*	66.6*	168.6*	158.1*	150.5*	108.3	123.7	112.7	67.1*	80.3

Samples were incubated with either primary or secondary stage treated pulp and paper mill effluent. *In vitro* assays were conducted on male and female pooled whole brains collected from 100 common goldfish. N = 3 assay runs per neurochemical.
D2 dopamine receptor, $GABA_A$ γ-aminobutyric acid A receptor; MAO monoamine oxidase, GABA-T γ-aminobutyric acid transaminase, PVPP Polyvinylpolypyrrolidone * indicates significant differences ($p < 0.05$) from controls

Linking neurochemical changes with vitellogenin production may provide a scheme to better interpret the aforementioned work. Vitellogenin is a precursor protein for egg yolk in oviparous organisms (Arukwe & GoskØyr, 2003) and is directly related to fecundity and egg quality in an individual fish (Miller et al. 2007). Thus, vitellogenin is an important biomarker of exposure to endocrine disrupting contaminants. The neurochemical effects of PPME reported by Basu et al. (2009) may lead to downstream effects along the HPG axis and disrupt reproduction, specifically vitellogenin production. The results from Basu et al. (2009) suggest that dopamine in the brain may be increased due to the general trend of decreased MAO activity. Female rainbow trout exposed to 0.01 mg/L hydrogen cyanide for 12 days exhibited increased brain dopamine levels which correlated with reduced plasma vitellogenin levels and smaller oocytes (Ruby et al. 1986, Szabo et al. 1991). The GABA results reported by Basu et al. (2009) are hard to determine if there would be an increase or decreased effect on GnRH production as there was a general increase in GABA-T activity but decrease in $GABA_A$ receptor binding. In another study, injection of the GABA receptor agonist, muscimol (0.1 μg/g) increased serum LH in female goldfish after 30 minutes (Trudeau et al. 1993). Similarly, a single injection of the GABA-T inhibitor, γ-vinyl-GABA (300 μg/g), in female goldfish increased serum LH at days 1, 7 and 14 which returned to baseline levels by day 21 (Trudeau et al. 1993). We assume that both of these results would lead to increased vitellogenin production.

Based on these prior studies, we hypothesized that exposure to PPME and its subsequent GABA and DA signaling disruption (as determined using cell-free *in vitro* methods) within the hypothalamus will lead to reduced liver vitellogenin production in female fish. Therefore, the goal of this study was to incorporate a neurochemical compartment to an existing fish

vitellogenesis computational model (Murphy et al. 2009) to link neurochemical changes to impaired fish vitellogenin production using an AOP framework.

2.0 METHODS

2.1 Model State Variables and Scales

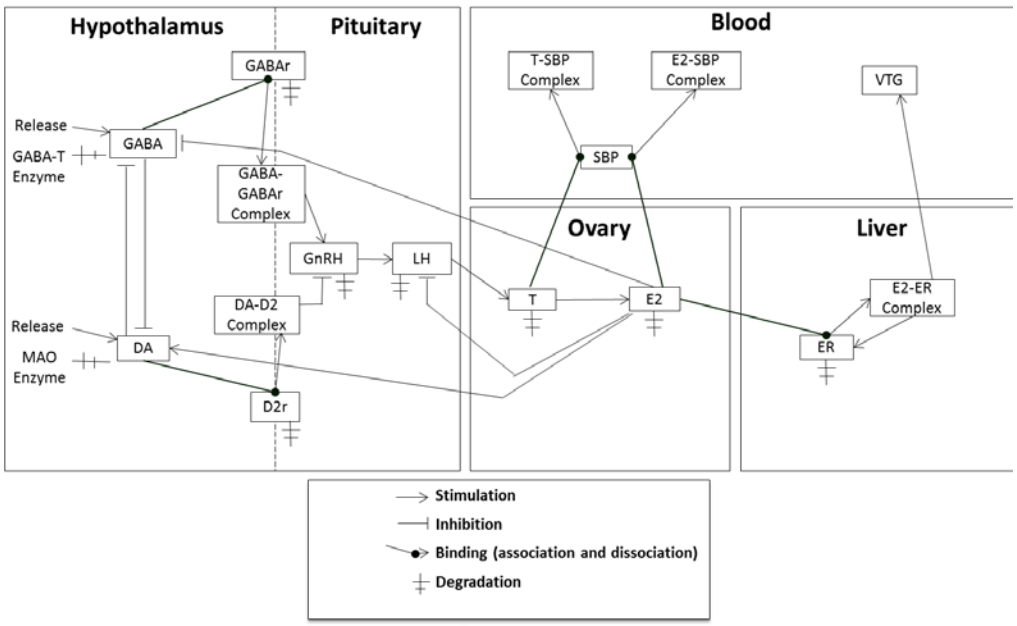

Figure 3: Conceptual compartmentalized computational model of a generic female fish HPGL axis with dopamine inhibition on GnRH.

The model consisted of a series of differential equations which determined the rate of change of 11 state variables within five compartments; Hypothalamus, Pituitary, Ovary, Liver and Blood. Hypothalamic state variables included GABA and DA (nmol/mg) neurotransmitters, $GABA_A$ and D2 receptors (nM) and GnRH (ng/ml). LH release into circulation (ng/ml) was the sole state variable in the pituitary compartment. The gonad compartment consisted of T and E2 sex steroid concentration (ng/ml). The liver compartment contained the state variables estrogen receptor (nM) and the blood compartment contained the state variables steroid binding proteins (nM) and vitellogenin (mg/ml).

The model schematic (Figure 3) and specific processes for each state variable are further described in Section 2.4: Submodels. A description of all variables, parameters, initial values and associated units used in the model are listed in Table 9 (Appendix). The simulations ran for six months to correspond to the period of vitellogenesis in a generic female fish (Murphy et al. 2005). Fourth-order Runge-Kutta integration with a time step of 0.0001 h was used to solve the model. The model was developed in FORTRAN 90 with the Lahey Fujitsu compiler (version 7.3) to perform simulation experiments.

2.2 Submodels

2.2.1 Hypothalamus Compartment

The model was driven by the release of the neurotransmitters GABA (*Syn[GABA]*; Equation 1, nmol/mg/h) and DA (*Syn[DA]* Equation 2, nmol/mg/h). Many neurochemicals are released in a pulsatile manner (Terasawa 1994) including GABA (Maffucci & Gore 2010) and DA (van den Pol 2010). Additionally, the circadian rhythm of many hormones is believed to be caused by a diurnal circle of hypothalamic neurotransmitters (Macho et al. 1986) and GABA and DA have been shown have a circadian rhythm in other brain regions (Castaneda et al. 2004). Therefore we characterized the neurotransmitter release using a slightly modified diurnal cycling function (Murphy et al. 2005) which included neurotransmitter inhibition parameters. Neurotransmitters were released into the system for the first two months of the simulation to correspond to the period of gonadal recrudescence (Murphy et al. 2005). The release of GABA and DA were subjected to either a DA (inh_{DA}) or GABA (inh_{GABA}) inhibition rate, respectively (Popesku et al. 2008). During vitellogenesis, E2 has been shown to stimulate the production of DA in salmonids (Zohar et al., 2010) and therefore our model included an E2 derived DA stimulation rate ($Stim_{E2DA}$). Additionally, it was reported that GABA transmission to GnRH

neurons is reduced by E2 (Watanabe et al. 2014), therefore we included an E2 inhibition (Inh_{E2GABA}) rate in the GABA release function.

$$Syn[GABA] = \frac{500[1-1.0*\frac{\cos 2\pi(t-6.0)}{24.0}]}{1.0+[DA]*inh_{DA}+E2*inh_{E2GABA}} \quad (1)$$

$$Syn[DA] = \frac{500[1-1.0*\frac{\cos 2\pi(t-6.0)}{24.0}*[E2]*Stim_{E2DA}]}{1.0+[GABA]*inh_{GABA}} \quad (2)$$

Once released, the concentration of free (unbound) GABA and DA neurotransmitters (*[GABA]*, Equation 3; *[DA]*, Equation 4, nmol/mg) within the hypothalamus compartment were bound to a receptor, degraded by an enzyme or cleared from the synapse via a reuptake transporter. GABA was bound to $GABA_A$ receptors or degraded by the GABA-T enzyme whereas DA was bound to D2 receptors or degraded by MAO. The concentration of free neurotransmitters was calculated based on the amount being released, adding the concentration disassociating from the receptor and subtracting the concentration bound to a receptor, degraded by an enzyme or undergoing reuptake by a transporter.

$$\frac{dGABA}{dt} = Syn[GABA] - ka_{GABA}[GABA][GABA-A] + kd_{GABA}[GABA\_GABA-A] - Up_{GABA} - Deg_{GABA} \quad (3)$$

$$\frac{dDA}{dt} = Syn[DA] - ka_{DA}[DA][D2] + kd_{DA}[DA\_D2] - Up_{DA} - Deg_{DA} \quad (4)$$

Enzymatic degradation (*Deg*; Equations 5 & 6; nmol/mg/h) and synaptic reuptake (*Up*; Equations 7 & 8, nmol/mg/h) of both GABA and DA followed Michaelis-Menten kinetics as has been reported in other studies (Wheeler & Hollingsworth, 1979, Venten et al. 2003) using the parameters *V* (maximum rate) and *k* (half saturation rate). Enzyme degradation multipliers ($Mult_{GABA\text{-}T}$ and $Mult_{MAO}$) were incorporated to simulate MeHg exposure, further detailed in Section 2.2. We assumed that *in vitro* enzyme activity was directly related to degradation rates of the neurotransmitters.

$$Deg_{GABA} = \frac{V_{GABAT}*[GABA]}{k_{GABAT}+[GABA]} * Mult_{GABA\text{-}T} \quad (5)$$

$$Deg_{DA} = \frac{V_{MAO}*[DA]}{k_{MAO}+[DA]} * Mult_{MAO} \quad (6)$$

$$Up_{GABA} = \frac{V_{GABA}*[GABA]}{k_{GABA}+[GABA]} \quad (7)$$

$$Up_{DA} = \frac{V_{DA}*[DA]}{k_{DA}+[DA]} \quad (8)$$

Additionally, we assumed that ligand-receptor binding followed a generalized mathematical formula (Murphy et al. 2005). For example, the concentration ligand bound receptors (*[GABA_GABA-A]*, Equation 9; *[DA_D2]*, Equation 10, nmol/mg/h) was calculated as the association rate constant (*ka;* Table 9; Appendix) multiplied by the number of open receptors ([GABA-A] or [D2]) and the concentration of unbound ligand ([GABA] or [DA]). The concentration dissociating from the receptor was calculated by multiplying the dissociation rate constant (*kd;* Table 9; Appendix) by the concentration of ligand bound receptors.

$$\frac{dGABA\_GABA-A}{dt} = ka_{GABA}[GABA][GABA-A] - kd_{GABA}[GABA\_GABA-A] \quad (9)$$

$$\frac{dDA\_D2}{dt} = ka_{DA}[DA][D2] - kd_{DA}[DA\_D2] \quad (10)$$

The concentration of open neurotransmitter receptors *[GABA-A*; equation 11*]* and *[DA-D2*; equation 12*]* were calculated based on a basal receptor induction rate (*kind*, 1/h), the amount of ligand associating or disassociating to the receptor and a basal elimination rate of the receptor (*kelim*, 1/h). Neurotransmitter receptor binding multipliers ($Mult_{GABA\text{-}A}$ and $Mult_{D2R}$) were incorporated to simulate MeHg exposure, further detailed in Section 2.2.

$$\frac{dGABA-A}{dt} = (kind_{GABA-A}[GABA-A] - ka_{GABA}[GABA][GABA-A] + kd_{GABA}[GABA_{GABA}-A] - kelim_{GABA-A}) * Mult_{GABA\text{-}A} \quad (11)$$

$$\frac{dD2}{dt} = (kind_{D2}[D2] - ka_{DA}[DA][D2] + kd_{DA}[DA\_D2] - kelim_{D2}) * Mult_{D2R} \quad (12)$$

The release of GnRH was a ratio of *GABAStim* to *DAInhib* (Equation 13, ng/ml) Where *GABAStim* (Equation 14) and *DAInhib* (Equation 14) were second order Michaelis-Menten kinetic equation, similar to what has been used in LH simulations (Blum 2000). The amount of free GnRH in the system (*[GnRH]*, Equation 16, ng/ml) was calculated by subtracting the amount being converted into luteinizing hormone (LH) from the amount of GnRH being released.

$$Syn[GnRH] = GabaStim/DAInhib \tag{13}$$

$$GABAStim = \frac{5*[GABA\_GABA-BZ]^2}{2.0+[GABA\_GABA-BZ]^2} \tag{14}$$

$$DAInhib = \frac{5*[DA\_D2]^2}{2.0+[DA\_D2]^2} \tag{15}$$

$$\frac{dGnRH}{dt} = Syn[GnRH] - Syn[LH] \tag{16}$$

2.2.2 Pituitary Compartment

The GnRH stimulated LH release rate (*GnRHStim*, Equation 17, ng/ml) was calculated as a second-order Michaelis-Menten kinetic equation (Blum et al. 2000). Circulating E2 can diffuse through pituitary tissue and inhibit the release of LH (Van Der Kraak 2009). Therefore the actual amount of LH being released into the system (*SynLH*, Equation 18, ng/ml) included an E2 inhibition rate (Murphy et al. 2005). The concentration of free LH (*[LH]*, Equation 19, ng/ml) was calculated by subtracting the amount of LH being converted into testosterone (T) from the concentration of LH being synthesized.

$$GnRHStim = \frac{5*[GnRH]^2}{2.0+[GnRH]^2} \tag{17}$$

$$Syn[LH] = \frac{GnRHStim}{1+\frac{[E2]}{10}} \tag{18}$$

$$\frac{dLH}{dt} = Syn[LH] - Syn[T] \tag{19}$$

2.2.3 Gonad Compartment

Once LH was released into the blood it traveled to the ovary to promote T synthesis (*Syn[T]*, Equation 20, ng/ml) within the gonad which was calculated as a Hill function (Murphy et al. 2005). The concentration of T in the system (*[T]*, Equation 21, ng/ml) was calculated by subtracting the enzymatic degradation rate (*kdegT*, ng/ml/h), the concentration being bound by steroid binding proteins (SBP) and the amount of T being converted into E2 (*Syn[E2]*, ng/ml) from the amount of T being synthesized and dissociated from SBP (Murphy et al. 2005).

$$Syn[T] = \frac{V_T * [LH]^{H_T}}{{k_T}^{H_T} + [LH]^{H_T}} \quad (20)$$

$$\frac{dT}{dt} = Syn[T] - kdeg_T[T] + kd_T[SBP\_T] - Syn[E2] - ka_T[T][SBP] \quad (21)$$

The synthesis of E2 from the aromatization of T (*Syn[E2]*, Equation 22, ng/ml) was defined by a Hill function (Murphy et al. 2005). The concentration of free E2 in the system (*[E2]*, Equation 23, ng/ml) was dependent upon *Syn[E2]* and the concentration being degraded by enzymes, associated to and dissociated from the liver estrogen receptors (ER) and the concentration associating to and disassociating from blood SBP (Murphy et al. 2005). It is important to note that we only characterized the initial surge of E2 production which occurs during the early vitellogenic period. We did not model the ovulatory surge that occurs prior to spawning.

$$Syn[E2] = \frac{V_{E2} * [T]^{H_{E2}}}{{k_{E2}}^{H_{E2}} + [T]^{H_{E2}}} \quad (22)$$

$$\frac{dE2}{dt} =$$

$$syn[E2] - kdeg_{E2}[E2] + k\_1[ER\_E2] + kd_{E2}[SBP_{E2}] - k1[E2][ER] - ka_{E2}[E2][SBP] \quad (23)$$

2.2.4 Blood Compartment

SBP are located in the plasma of teleost fish which bind to free sex steroid hormones (T and E2) to prevent their metabolic degradation (Murphy et al. 2005). We assumed free and

bound steroid hormones are at equilibrium in the blood, however, only the free hormone is physiologically active (Hammond 2016). In the model, the concentration of unbound SBP in the blood (*[SBP]*; Equation 24, nM) was calculated by subtracting the concentration of E2 and T being associated to unbound SBP from the concentration of E2 and T dissociating from bound SBP (Murphy et al. 2005). The concentration of bound SBP to T and E2 (*[SBP-T]* & *[SBP-E2]*, Equations 25 & 26, nM, respectively) was calculated by subtracting the concentration of ligands being dissociated from the amount of ligands associating to unbound SBP (Murphy et al. 2005).

$$\frac{dSBP}{dt} = kd_T[SBP_T] + kd_E[SBP_{E2}] - ka_T[T][SBP] - ka_E[E2][SBP] \quad (24)$$

$$\frac{dSBP\_T}{dt} = ka_T[SBP][T] - kd_T[SBP\_T] \quad (25)$$

$$\frac{dSBP\_E2}{dt} = ka_{E2}[SBP][E2] - kd_{E2}[SBP\_E2] \quad (26)$$

2.2.5 Liver Compartment

Once the free E2 reached the liver it bound to an open estrogen receptor (ER), forming the ER-E2 complex (Murphy et al. 2005). Unbound ER concentration (*[ER]*, Equation 27, nM) was calculated by subtracting the amount of E2 being associated to unbound ER from the concentration of E2 dissociating from bound ER. k1 and k_1 are the association and dissociation rate constants for E2 to ER (Murphy et al. 2005). Estrogen receptor multipliers ($Mult_{ER}$) were incorporated to simulate MeHg exposure, further detailed in Section 2.2. Additionally, we assumed a background degradation rate (*kdegu*) of unbound ER and an induction rate (*k2*) where activated ER lead to further production of unbound ER (Murphy et al. 2005). Fish have three distinct ERs, ERα, ERβ and ERγ (Sabo-Attwood et al., 2004). Each receptor type has its own distinct physiological action and its concentration depends on the species and tissue (Leaños-Castañeda & Van Der Kraak, 2007). In our model, we assume all of the vitellogenin production

comes from the binding of E2 to the ERβ subtype (Leaños-Castañeda & Van Der Kraak, 2007, Nelson et al. 2013).

$$\frac{dER}{dt} = 1.15 * k2[ER_{E2}] - kdegu[ER] + k\_1[ER\_E2] \ - k1[ER][E2]*Mult_{ER} \quad (27)$$

$$\frac{dER\_E2}{dt} = k1[E2][ER] - kdega[ER\_E2] - k1[ER\_E2] - k2[ER\_E2] \quad (28)$$

Once ER was bound by E2, the model assumed a forward rate constant (*k3*) of vitellogenin production (*[VTG]*, Equation 29, ng/ml) (Murphy et al. 2005). Vitellogenin is a good indicator of egg production because as the oocyte is growing, it is continually being filled with vitellogenin derived yolk proteins. Therefore we assumed a direct relationship between cumulative vitellogenin predicted by the model and fecundity (Miller et al. 2007).

$$\frac{dVTG}{dt} = k3[ER\_E2] \quad (29)$$

2.3 PPME Simulation Conditions

Basu et al. (2009) assessed the potential neurochemical effects of both primary and secondary effluent from an Eastern Canadian pulp and paper mill. Both effluents were fractionated into four extracts by two methods of extraction; classic polarity and polyphenolic extraction. Whole brain tissues from male and female common goldfish were incubated with the effluent extracts for 30 minutes. Radioligand binding to both GABA and DA receptors were measured *in vitro* for each effluent extract using male and female common goldfish whole brain tissue. MAO and GABA-T proteins concentration was determined in whole brain tissue. GABA-T enzyme activity was determined by incubating 5 µg of protein homogenates in 100mM potassium pyrophosphate buffer containing 5 mM α-ketoglutarate, 4 mM NAD, 3.5 mM 2-mercaptoethanol, 10 µM pyridoxal-5′-phosphate, pH 8.6 for 15 minutes at 37 ºC. 10mM GABA was added and the absorbance was observed every 10 s for 2 min and maximal velocity of the enzyme reaction calculated. A final effluent concentration of 0.5 mg/ml was added and the

enzyme activity measured. Similarly, MAO activity was measured by mixing 5 μg of protein with 100 μM 10-acetyl-3,7-dihydroxyphenoxazine, 200 mU horseradish peroxidase and 100 mM tyramine. Samples were incubated for 30 minutes and the production of resorufin was monitored between 30 and 50 minutes.

The neurotransmitter receptor binding and enzyme activity data obtained from Basu et al. (2009) were incorporated into the model as multipliers, expressed as a percent change from the control (Table 1). Neurochemical receptor binding multipliers were added to the state variable equations 2, 5, and 14 (Chapter 1: Dissertation), respectively. Additionally, multipliers for enzyme activity were incorporated in the enzyme degradation equations 22 and 23 (Chapter 1: Dissertation) for GABA-T and MAO, respectively. Five separate simulations were run for both the primary and secondary PPME, one for each fraction.

3.0 RESULTS

3.1 Modeled Effects of PPME on the Fish HPGL Axis

3.1.1 Neurochemicals

The model predicted that free GABA would reach its highest concentration on day 14 following the onset of gonadal recrudescence at 2120 nmol/mg in the control brain tissue (Figure 4). The PVPP water and PVPP ethanol fractions from the primary effluent increased the maximum concentration of free GABA by 29.1% and 80.3%, respectively, compared to the control (Figure 4A). The increase was likely due to the decreased number of receptor sites available for GABA binding, 71.4 and 50.8% of the control, respectively. The hexane fraction decreased the maximum concentration of free GABA by 68.1%. This decrease in free GABA resulted due to the increased number of receptor sites (288.9% of the control) and increased GABA-T enzyme activity (168.6% of the control). The remaining primary effluent fractions,

ethyl acetate and water, slightly reduced the maximum concentration of free GABA by 10.5% and 0.1 %, respectively. The secondary PPME resulted in increased GABA concentrations during all modeled fraction simulations (Figure 4B). The highest concentration of free GABA was increased by 23.9%, 41.9%, 216.0%, 266.7% and 278.3% nmol/mg in the ethyl acetate, hexane, PVPP ethanol, water only and PVPP water fractions, respectively, compared to the control. These increases were likely due to the fact that all fractions reduced *in vitro* GABA receptor binding compared to the control (Table 1).

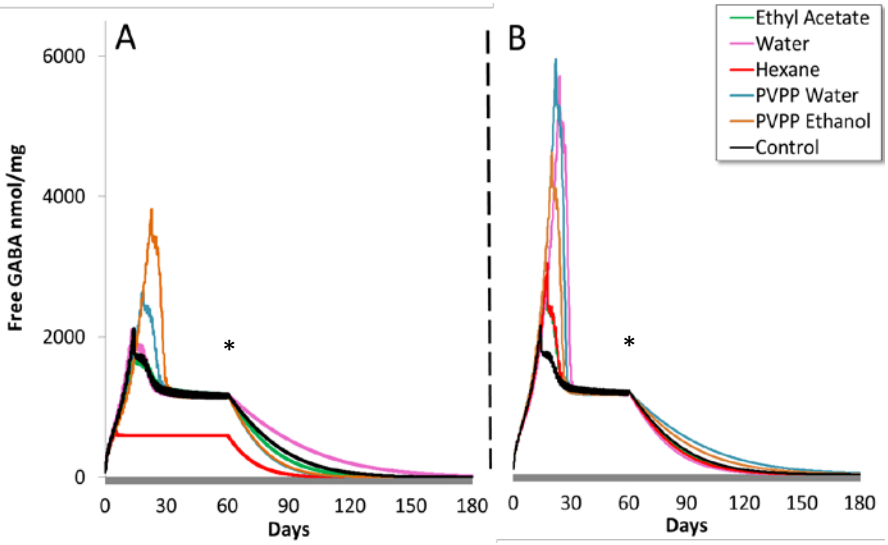

Figure 4: Simulated effects of primary (A) and secondary (B) pulp and paper mill effluent on modeled free gamma-aminobutyric acid (GABA) in a generic female fish during vitellogenesis. * indicates when the neurotransmitter release function was turned off.

Modeled free DA reached a maximum concentration by day 3 at 127 nmol/mg in the control brain tissue. This maximum concentration was followed by a quick decline to 39.8 nmol/mg at day 20 in the controls due to the increased free GABA concentration and subsequent DA inhibition. As E2 increased in circulation which inhibited GABA release, the free DA then increased to 58.4 nmol/mg in the control brain tissue by day 60. The model predicted that exposure to the primary effluent would result in a slight increase in the maximum concentration of free DA by 103.2 %, 104.6 %, 106.8 %, 107.2 % and 107 % nmol/mg in the ethyl acetate,

PVPP water, PVPP ethanol, and hexane fractions, respectively, compared to the control (Figure 5A). The water fraction resulted in a 2.4 % decrease in maximum concentration of DA. The low concentration of free DA at day 30 due to GABA inhibition was reduced by 12.1 %, 23.1 %, and 47.5 % nmol/mg in the water, PVPP water and PVPP ethanol fractions, respectively and increased by 17.8 % and 38.2 % in the hexane and ethyl acetate fractions, respectively, compared to the control. Interestingly, even after the neurotransmitter release was shut off at day 60, dopamine was still present in the hexane fraction for an additional 60 days. Overall, the highest concentration of the free dopamine increased by 0.02 %, 1.1 % and 3.1 % in the ethyl acetate, hexane and water only simulations and decreased by 0.4 % and 1.8 % in the PVPP water and PVPP ethanol simulations, respectively. However, because all of the secondary PPME effluent fractions increased the amount of free GABA, all fraction simulations predicted a lower concentration at day 30 in free DA (Figure 5B). The subsequent free DA low concentration was reduced by 22.3 %, 26.6 %, 52.0 %, 63.3 % and 66.38 % in the ethyl acetate, hexane, PVPP ethanol, PVPP water and water only simulation, respectively, compared to the control.

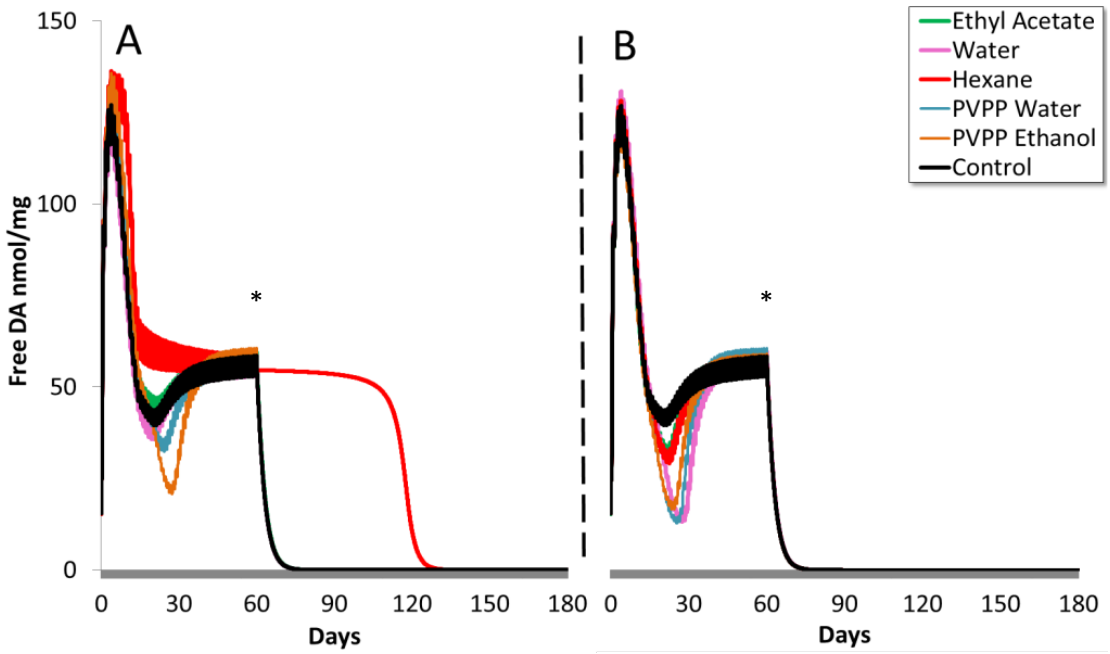

Figure 5: Simulated effects of primary (A) and secondary (B) pulp and paper mill effluent on modeled free dopamine (DA) in a generic female fish during vitellogenesis. * indicates when the neurotransmitter release function was turned off.

3.1.2 Sex Steroid and Vitellogenin Production

Free plasma E2 production reached the highest concentration of 5.0 ng/ml in the control simulation. The maximum concentration was slightly increased by 2.3%, 4.5% and 5.7% in the water only, PVPP water and PVPP ethanol fractions of the primary PPME, respectively. The ethyl acetate and hexane fractions reduced the maximum concentration of free E2 compared to the control by 10.0 and 81.2 %, respectively, in the primary PPME. All simulated fractions from the secondary PPME slightly increased free E2 compared to the control simulation. The maximum concentration of E2 increased 3.9 %, 4.5 %, 5.1 %, 5.6 %, and 6.0 % ng/ml in the ethyl acetate, hexane, PVPP ethanol, PVPP water and water only fractions of the secondary PPME, respectively.

Modeled cumulative vitellogenin was 459.4 mg/ml in the control after the simulation (Figure 6). Only the water only fraction from the primary PPME increased modeled cumulative

vitellogenin, which was 111.5 % of the control. The remaining fractions from the primary PPME reduced modeled cumulative vitellogenin, by 7.8 %, 11.9 %, 16.9 % and 90.1 % in the PVPP water, PPVP ethanol, ethyl acetate, and hexane fraction simulations, respectively (Figure 6A). There was a lesser effect on cumulative vitellogenin from the secondary PPME simulations. In comparison to the control simulation, the hexane and ethyl acetate fractions slightly increased cumulative vitellogenin by 1.2 % while the PVPP ethanol, PVPP water and water only fractions reduced cumulative vitellogenin by 1.7 %, 8.8 % and 16.9 %, respectively (Figure 6B).

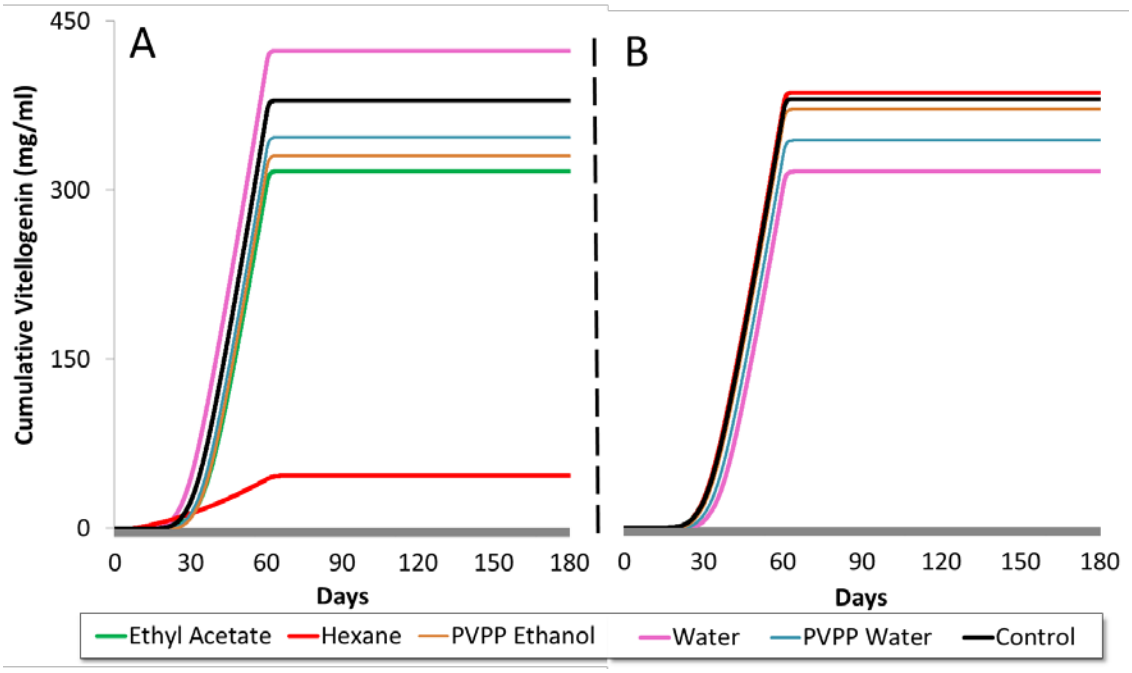

Figure 6: Simulated effects of primary (A) and secondary (B) pulp and paper mill effluent on modeled cumulative vitellogenin production in a generic female fish during vitellogenesis.

3.1.3 Relating Effects on Vitellogenin to Egg Production

If we assume that vitellogenin production is directly related to egg production as described in other studies (Miller at al. 2007, Murphy et al. 2009), we can convert the cumulative vitellogenin results into an estimated fecundity effect (Figure 7). Using the control simulation as our baseline, the model predicts a 111.5 % increase in fecundity in the water only fraction from

the primary PPME. The PVPP water, PVPP ethanol, ethyl acetate and hexane fractions each would reduce fecundity to 92.2 %, 88.1 %, 83.1 % and 9.9 %, respectively, of the control. The secondary PPME ethyl acetate and hexane fractions would slightly increase fecundity 101.9%, while the PVPP ethanol, PVPP water and water only fractions would reduce fecundity to 98.3 %, 91.2 % and 84.1 %, respectively, compared to the control. Additionally, assuming that the effects caused by individual fractions are additive to one another, we would expect that fecundity would be reduced by 92.6 and 6.9 % in the primary and secondary PPME, respectively, compared to the control.

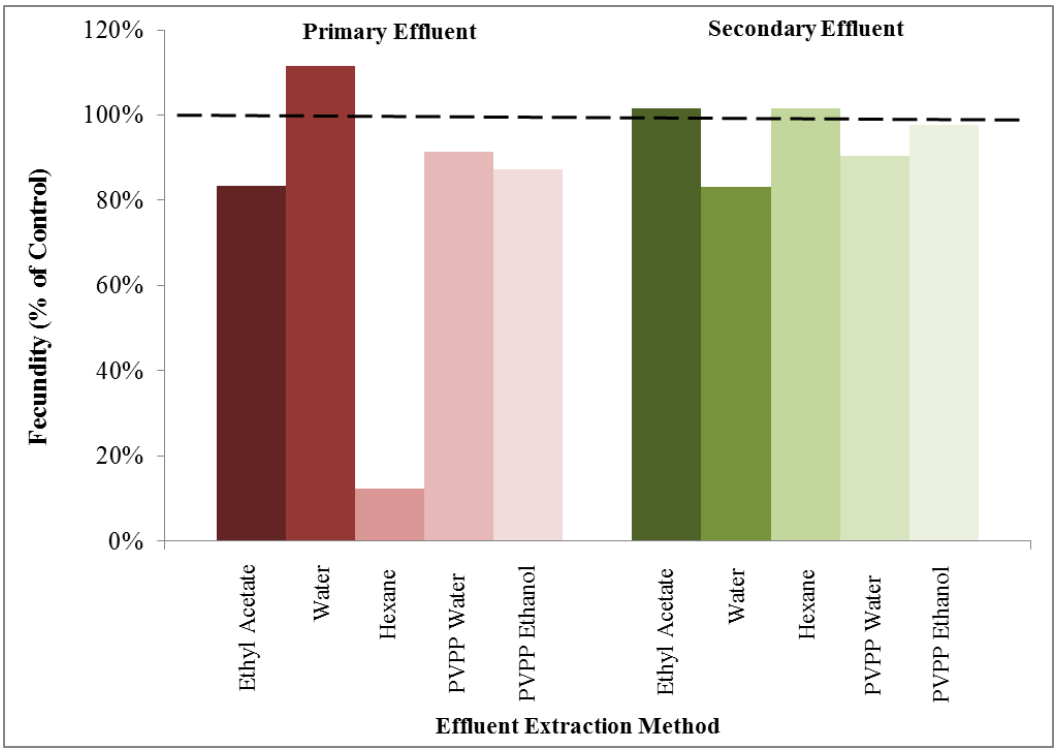

Figure 7: Extrapolating the effects of primary and secondary pulp and paper mill effluent on vitellogenin production to egg production in a generic female fish during vitellogenesis. Dashed line represents an unexposed female fish's egg production.

4.0 DISCUSSION

4.1 Comparison of Primary and Secondary PPME

Using a computational vitellogenesis model, we linked changes in neurochemical *in vitro* data for a complex mixture within PPME to adverse effects of vitellogenin production in an adult female fish to demonstrate how this could be done. While we don't have chemistry data to know the exact contaminants within the PPME - which may be over 250 different compounds (Ali & Sreekrishnan 2001), the *in vitro* work conducted by Basu et al. (2009) determined that at least 4 different molecular initiating events, changes to GABA and DA receptor binding and MAO and GABA-T enzyme activity, can occur following exposure. The model suggests that disrupted GABA and DA receptor binding and associated enzyme activity due to exposure to both primary and secondary treated PPME would reduce vitellogenin production, with the primary PPME having a more pronounced (13x) effect. Secondary treatment of the PPME reduced the modeled reproductive toxicity of the effluent, vitellogenin production increased 10x to and comparable to the level of the control (102 %).

Pulp and paper mill effluent can contain phytochemicals such as terpene, a product derived from conifer resin (Waye et al. 2014, Basu et al. 2009). Terpene is a non-polar lipophilic, organic chemical which can be extracted with hexane and other similar solvents (Basu et al. 2009). Terpenoids and other phytochemicals are hormonally active compounds present in bleached kraft pulp mill effluent (Belknap et al. 2006) which has been shown to reduce testosterone production in mummichog (Dube & MacLatchy 2000). The primary PPME hexane extract simulation resulted in a 90.1 % decrease in cumulative vitellogenin production in comparison to the control. The lack of vitellogenin inhibition (102 % of the control) during the

secondary PPME hexane extract simulation suggests that these substances may be removed during the secondary stage treatment process.

4.2 Future Model Development & Data Gaps

This model is still in the early stages of development and its intent is not to predict future population changes nor recommend any regulatory changes. Research needs to be conducted to test the validity of the assumptions made in this model, most importantly the Michaelis-Menten kinetic values for the neurotransmitters which were derived from the mammalian and avian literature. Additionally, the model was developed for a generic single batch synchronous spawning generic female fish and calibrated using sex steroid data collected from a percid laboratory study. The *in vitro* work conducted by Basu et al. (2009) used common goldfish as a model species, which is an asynchronous spawner capable of spawning many times over the course of their breeding season. My next chapter will focus on *in vitro* neurochemical data collected from a single batch synchronous spawning species, the yellow perch (Chapter 2: Dissertation).

The work by Basu et al. (2009) used pooled data from both male and female whole brains for their *in vitro* assays. Future work assessing the potential of PPME to affect GABA and DA dynamics and subsequent vitellogenin production should focus on only female brains, specifically the hypothalamus region, and preferably from individuals. To test the validity of the model, vitellogenin and egg production should be measured *in vivo* from female fish exposed to PPME in order to provide a population relevant 2nd anchor to the integrated AOP vitellogenesis model (Figure 8). These data would also allow us to test the assumption that reductions in vitellogenin directly relate to a reduction in egg production for fish exposed to PPME. Modeling

exercises such as this can greatly advance the environmental toxicology field by synthesizing available information and directing future research towards addressing data gaps.

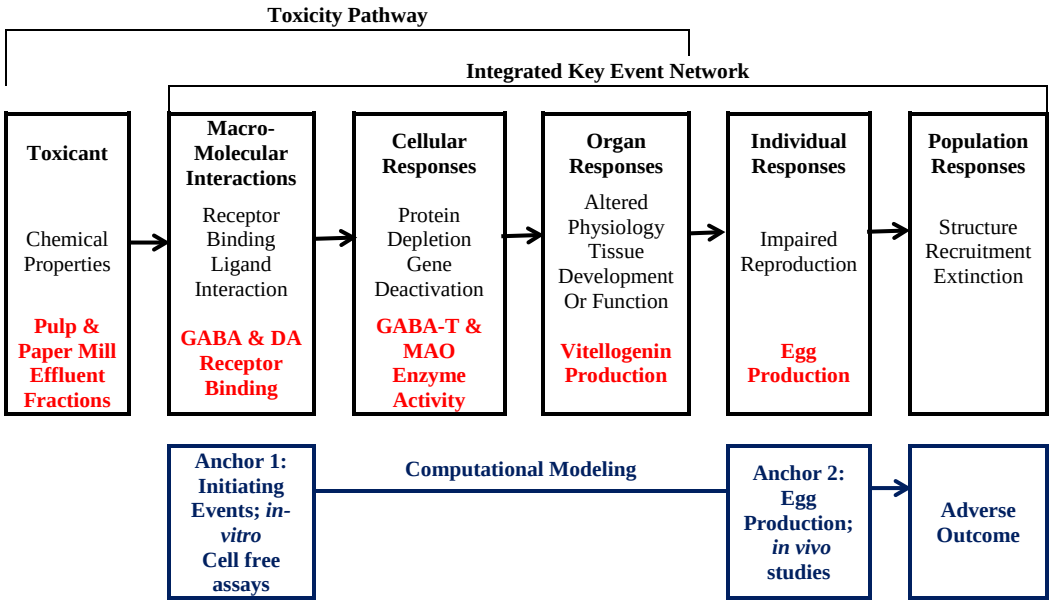

Figure 8: Future Integrated AOP and how computational modeling can be used to link *in vitro* data to estimate *in vivo* effects.

Future research should also look at testing *in vitro* effects of whole effluent on GABA and DA neurochemical processes. The Basu et al. (2009) paper fractionated the effluent into different chemical classes; however, it did not assess the effects of the whole effluent nor its predicted concentration in receiving waters. Without these data, we do not have a way to determine if these chemicals within the PPME are acting synergistically, antagonistically or additively to one another. Additional analysis of the specific chemical compounds found within the effluent fractions would also be beneficial in determining the active compounds of the effluent.

4.3 Proof of Principle and Future Intent

While not yet validated, these simulations demonstrate proof of principle for using computational modeling to link molecular effects of complex mixtures to adverse effects on fish populations. Once validated, this model can be used as a screening tool using *in vitro* data to help direct *in vivo* exposures towards potentially more harmful contaminants. The traditional fish short-term reproductive assay for assessing estrogenic chemical effects takes 35 days to conduct and is only capable of testing either just a few concentrations of a single contaminant or a single concentration of a mixture of just a couple of contaminants (Armstrong et al. 2015, Ankley et al. 2001). With over 85,000 registered chemicals on the U.S. Environmental Protection Agency's TSCA Chemical Substance Inventory (U.S. EPA 2015), it would be impractical to conduct *in vivo* methods on every chemical and even more impractical to test complex chemical mixtures. The effects of thousands of chemicals at varying concentrations and their mixtures can be collected in that same 35 day time span using *in vitro* methods. High-throughput screening can currently screen 100,000 compounds per day with the potential to test up to one million samples per day (Szymański et al. 2012). The data from these assays can be extremely variable and hard to relate to an *in vivo* response (Basu et al. 2009, Knudsen et al. 2011), however when coupled with a computational model using an AOP framework, quantifiable linkages can be made relating *in vitro* data to adverse *in vivo* effects.

Taking an Integrated AOP approach, we hypothetically linked together several molecular initiating events that may result in the same adverse outcome - impairment of vitellogenin production. Using a computational model to create quantitative linkages within the AOP framework, we extrapolated from *in vitro* neurochemical data to an adverse population outcome stemming from PPME exposure (Figure 9).

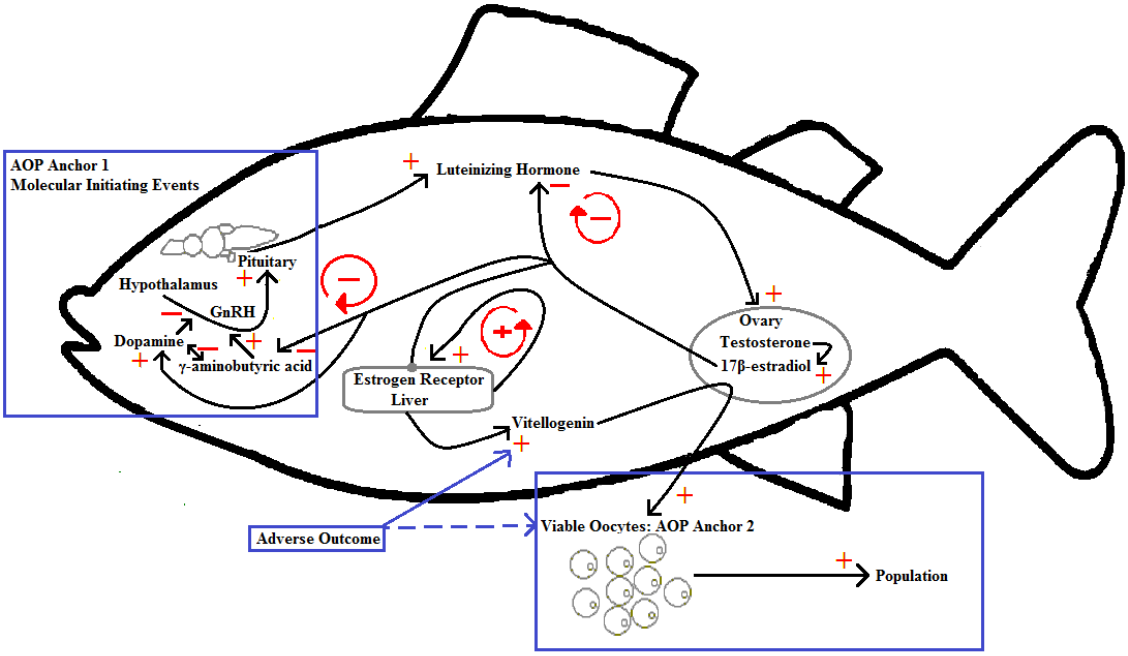

Figure 9: Conceptual vitellogenesis model of an integrated adverse outcome pathway framework to link multiple initiating events to adverse effects on egg production

It is likely that several AOPs will be activated due to exposure to complex mixtures. In order for computational models and AOPs to be used for risk assessment purposes they must undergo strict developmental guidelines which include testing for reliability and robustness (OECD 2013). Weight of evidence analyses then need to be conducted for each key element of the AOP(s) (Becker et al. 2015). These analyses can include a simple qualitative method by assigning a level of confidence (very strong, strong moderate, weak, very weak) to the amount of data available linking key events within an AOP to an apical endpoint (OECD 2013). Additionally, a quantitative weight of evidence approach can be applied where an expert panel uses specific criteria to apply weights and scores to individual lines of evidence for each key event within an AOP. This criterion would include mechanistic relationships between key events, evidence of a downstream key event being impaired if an upstream key event is blocked, and

consistency across a wide range of taxa and stressors for which the key event(s) occur. A mathematical or statistical model would then evaluate the weights and scores to determine an overall conclusion for support of the new AOP (Becker et al. 2015). The AOPs linked in this model are strictly hypothetical as none have been directly linked to vitellogenin production, nor has a weight of evidence approach been applied. Further research is needed to determine if GABA receptor antagonism, D2 receptor agonism, increased GABA-T activity and/or decreased MAO activity results in reduced vitellogenin production. As more single AOPs are tested and become available, future computational models could be updated to create a stronger integrated AOP framework.

With this research, we have a better understanding of how contaminant mixtures can affect fish populations, which is invaluable for developing guidelines for acceptable contaminant loads for healthy ecosystems. Once validated, we can use this approach in combination with the U.S. Environmental Agency's ToxCast™ program to help prioritize chemicals for further toxicological analyses. The ToxCast™ program consists of data collected from high-throughput screening assays and uses computational toxicology methods to predict toxicity of specific compounds (Knudsen et al. 2011).

CHAPTER 2

USING A VITELLOGENESIS MODEL TO LINK *IN VITRO* EFFECTS OF METHYLMERCURY TO ADVERSE REPRODUCTIVE OUTCOMES IN YELLOW PERCH

ABSTRACT

Yellow perch recruitment in Lake Michigan has declined since the 1990's which has been attributed to many factors such as increased predation and a reduced forage base. Exposure to contaminants may be an additional factor affecting yellow perch recruitment as several compounds have been found in adult yellow perch tissues collected from Lake Michigan and some of these, such as methylmercury (MeHg) can be a neurotoxin. Exposure to neurotoxic contaminants can impair neurochemical signaling within the brain and therefore may disrupt the reproductive hormonal cascade within the hypothalamic-pituitary-gonadal-liver (HPGL) axis. In some fish species, MeHg has been shown to adversely affect the HPGL axis by reducing sex steroid production and inhibiting gonadal formation and egg production. In yellow perch, MeHg disrupts neurotransmitter binding to receptors and alters enzyme activity within the yellow perch hypothalamus which may lead to the impairment of reproductive hormone release and vitellogenin production. Dopamine (DA) and γ-aminobutyric acid (GABA) are two neurotransmitters involved in fish reproduction. To assess whether disruption of GABA and DA signaling in the brain following MeHg exposure leads to a reduction in yellow perch vitellogenin production we calibrated the fish vitellogenesis model to simulate yellow perch sex steroid production. In our approach, we used data from a 20-week MeHg study which assessed *in vitro* changes in hypothalamic GABA and DA receptor binding, monoamine oxidase (MAO) enzyme activity and liver estrogen receptor β (ERβ) concentration in adult female yellow perch. In that study, MeHg exposure resulted in increased *in vitro* GABA and DA binding to their respective receptors, increased MAO activity and reduced ERβ concentrations. After incorporating these

effects into the vitellogenesis model, our model predicted that exposure to 0.5 ppm MeHg would increase cumulative vitellogenin production in female yellow perch by 4.8 % compared to the control. Exposure to 5.0 and 50.0 ppm MeHg resulted in a 13.7 and 11.8 % reduction in simulated cumulative vitellogenin production in female yellow perch, respectively. These results are not entirely supported by the MeHg laboratory study because ovary size, plasma sex steroid concentration and liver vitellogenin transcripts were unaffected by MeHg exposure. This suggests that our model is missing a key component related to vitellogenin production. Further model simulations suggest that MeHg exposure may affect GABA-transaminase activity and/or other liver estrogen receptor subtypes may compensate for the reduced ERβ and assist in vitellogenin production when yellow perch are exposed to MeHg. This study, and others like it, can direct future research to fill necessary data gaps to make these models predictive.

1.0 INTRODUCTION

Yellow perch populations in Lake Michigan declined in the late 1990's which was attributed to several environmental factors including heavy predation and low food supply (Dettmers et al. 2003, Clapp & Dettmers 2004, Santucci Jr et al. 2014). However, recent investigation of yellow perch tissues in Lake Michigan suggest exposure to several contaminants including dichlorodiphenyl dichloroethylene (DDE; up to 31.3 ppb), polychlorinated biphenyls (PCBs; up to 1076 ppb), and mercury (Hg; up to 440 ppb) (Brazner & DeVita 1998; Wiener et al. 2012). These contaminants have each been shown to reduce reproductive performance in fish raised in laboratory exposure settings (Macek 1968, Bengtsson 1980, Drevnick & Sandheinrich 2003) and contaminant exposure may be another reason leading to the yellow perch decline in Lake Michigan, but has not yet been explored.

Methylmercury (MeHg) is a common pollutant in aquatic environments that has been linked to neurotoxicity and reproductive impairment in many fish species (Crump & Trudeau 2009). As a neurotoxin, MeHg inhibits neurotransmitter release, reuptake and metabolism (Atchison & Hare 1994). For example, unsexed walking catfish (*Clarias batrachus*) exposed to 0.430 mg/L MeHg-chloride for 90 days experienced a decrease in brain monoamine oxidase (MAO) activity which correlated with an increase in brain DA levels (Kirubagaran & Joy 1990). Additionally, MeHg exposure can affect downstream processes in the fish hypothalamic-pituitary-gonadal-liver (HPGL) axis. For example, fathead minnow (*Pimephales promelas*) females fed a diet containing 870 ppb Hg for 250 days displayed significantly lower T and E2 concentrations which correlated with lower spawning success compared to a control group (Drevnick & Sandheinrich 2003). We hypothesize that disrupted neurotransmitter and neurochemical dynamics may be mechanisms for the reproductive impairment, specifically vitellogenin production, in fish exposed to MeHg.

Vertebrate reproduction is controlled by environmental factors, such as temperature and photoperiod, which stimulate the HPGL axis to release neurotransmitters (Van Der Kraak et al., 1998; Trudeau et al, 2000) which then bind to post synaptic terminal receptors (Treiman 2001). γ-aminobutyric acid (GABA) and dopamine (DA) are involved in the reproductive process in many fish species (Trudeau 1993, Trudeau 1997, Van Der Kraak 2009, Zohar et al. 2010). It was hypothesized that dopamine inhibition is an evolutionary mechanism to prevent spawning during periods of poor environmental conditions (Zohar et al., 2010). Dopamine inhibition of GnRH was found to be very high in cyprinids, however it was much less pronounced in salmonids and nearly absent in Atlantic croaker, (*Micropogonias undulates*; Van Der Kraak 2009) and percids

(Zakes & Demska-Zakes 2005, Dabrowski et al. 1994, Żarski et al. 2015), which suggests that DA involvement in fish reproduction may be species dependent (Levavi-Sivan et al. 2010).

Recently, a study investigated the *in vivo* and *in vitro* effects of MeHg on adult female yellow perch (Debofsky in review, Arini et al. 2016). The Arini et al. (2016) study concluded that the *in vitro* exposure to 0, 0.5, 5.0 and 50.0 ppm MeHg resulted in a dose dependent increase in hypothalamic DA and GABA receptor binding and MAO activity and a decrease in estrogen receptor β (ERβ) binding on the livers of female yellow perch. However, Debofsky et al. (in review) reported no adverse effects in the same set of fish on *in vivo* sex steroid production or fecundity following the twenty week exposure to 0.5, 5.0 or 50.0 ppm MeHg. The differences between these studies highlight the difficulty of solely using *in vitro* data to estimate an *in vivo* response.

Computational modeling has been used to create quantitative linkages between molecular-level data to an *in vivo* adverse response (Murphy et al. 2005, Watanabe et al. 2009, Li et al. 2011, Gillies et al. 2016). Some of these models have been developed to simulate the process of female fish vitellogenesis in order to understand how various stressors can affect fish reproduction (Murphy et al., 2005; Murphy et al, 2009; Li et al., 2011, Gillies et al. 2016). These models are driven by processes downstream of the hypothalamus and simulate the production of vitellogenin, which can be directly related to egg production in fish (Miller et al. 2007). We wished to further the development of these models by incorporating molecular initiation events that occur upstream in the hypothalamic-pituitary-gonadal-liver (HPGL) axis, such as disrupted neurochemical signaling, which may be responsible for disrupted vitellogenin production during exposure to neurotoxicants. For example, prochloraz is a fungicide that has been shown to reduce hypothalamic GnRH gene expression and subsequent egg production in Japanese medaka (Zhang

et al. 2008). Incorporating a hypothalamus compartment into the vitellogenesis model would allow for researchers to collect *in vitro* neurochemical data and, using the model, link to an *in vivo* response such as disrupted egg production. This would be a great benefit to researchers as cell free *in vitro* assays are easier to conduct in comparison to *in vivo* reproductive assays. Additionally, a model such as this may help in understanding the differences between the *in vitro* (Arini et al. 2016) and *in vivo* (Debofsky et al. in review) responses in yellow perch following MeHg exposure.

The goal of this study was to incorporate a neurochemical compartment to the existing fish vitellogenesis models, which would allow for the integration of *in vitro* data into the model to predict adverse *in vivo* effects on fish reproduction. We used the neurochemical data collected by Arini et al. (2016) following *in vitro* MeHg exposure of yellow perch hypothalamus into the vitellogenesis model and compared our results to the *in vivo* reproductive measurements reported by Debofsky et al (in review). Lastly, we used the model to highlight the importance of species differences, specifically between species with (for example cyprinids, catfishes and salmonids) and without DA (percids) control of GnRH production.

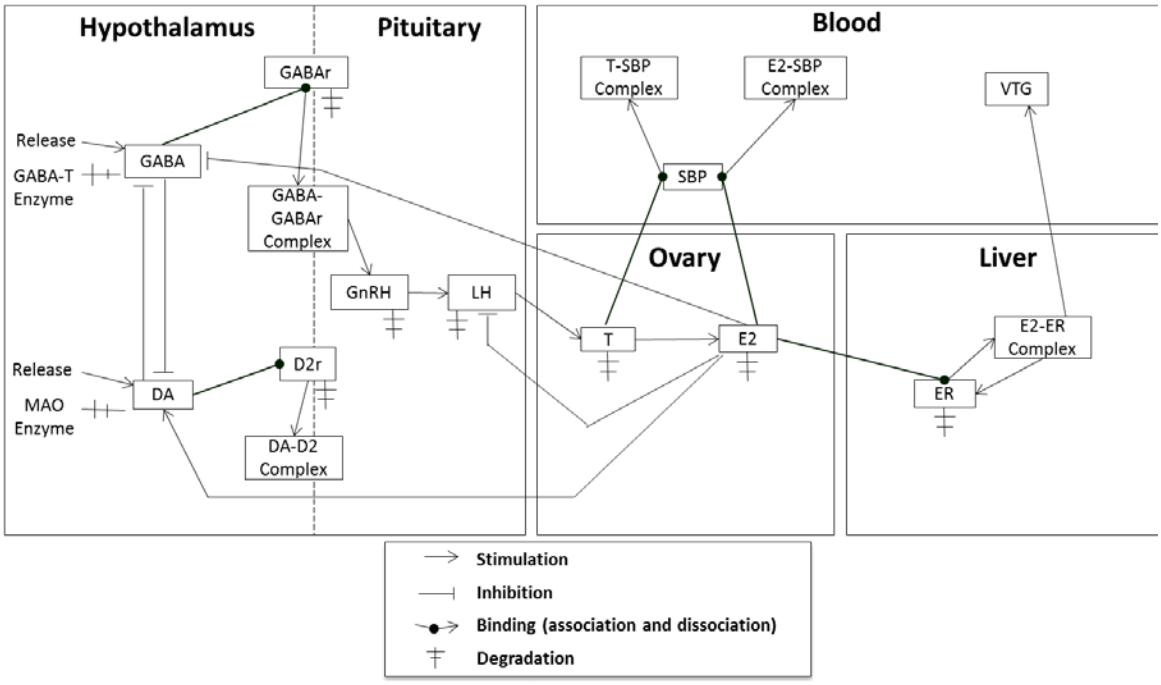

Figure 10: Conceptual diagram of the compartmentalized HPGL model for yellow perch vitellogenesis. Compartments include the hypothalamus, pituitary, ovary, liver and blood. Boxes indicate state variables within each compartment. Note: This figure differs from Chapter 1: Figure 3 as the dopamine inhibition of GnRH production has been removed.

2.0 METHODS

2.1 Model Purpose:

A physiological model which was built to simulate reproductive processes within the HPGL axis of a generic female fish (Chapter 1: Dissertation) was calibrated for a female yellow perch by removing the DA inhibition of GnRH production (Figure 10) and further described in Section 2.2. The objective was to incorporate the *in vitro* effects within the HPGL axis (Arini et al. 2016) and compare the model results to the *in vivo* yellow perch sex steroid concentration and vitellogenin expression (Debofsky et al. in review) following MeHg exposure.

2.2 Model Calibration

Neurotransmitters were released into the system for the first four months of the simulation to correspond to the period of gonadal recrudescence in yellow perch (Debofsky et al.

in review) which has been reported in a similar percid species, the Eurasian perch (Sulistyo et al. 1998). The neurotransmitter model parameters, $kelim_{GABA\text{-}A}$, $kelim_{D2}$, $kind_{GABA\text{-}A}$, $kind_{D2}$, inh_{GABA}, inh_{DA} (Table 9; Appendix) were incrementally adjusted to until the model roughly mimicked the measured estradiol concentrations in yellow perch from the laboratory exposure (Figure 11A). The simulations ran for six months beginning in September when yellow perch begin gonadal recrudescence (Debofsky et al. in review). Additionally, it has been shown that gonadotropin production in percid fish species lack a dopamine inhibition mechanism. Therefore the release of GnRH (*Syn[GnRH]*; Equation 13 [Chapter 1:Dissertation]) from the hypothalamus into the pituitary was only dependent upon GABA stimulation (Equation 14 Table 2; ng/ml).

2.3 Laboratory Derived MeHg Effects:

In the Arini et al. (2016) and Debofsky et al. (in review) studies, female yellow perch were raised to maturity in the aquaculture facility at the University of Wisconsin-Milwaukee School of Freshwater Sciences. Reproduction was initiated by simulating a natural photoperiod and gradual reduction in temperature. Prior to gonadal recrudescence, the fish were fed a concentration of MeHg (0.0, 0.5, 5.0 or 50.0 ppm) which was added to their diet (Finfish Perch 45-12 5.0 mm Slow Sinking Food [Ziegler Bros., Inc.; Gardners, PA]) using an ethanol vehicle. The exposure continued for twenty weeks. Four females were removed from the tanks every 30 days. The hypothalamus, pituitary, liver and blood samples were obtained from each fish for analysis of GABA and DA binding and enzyme activity, changes in LH transcripts, liver estrogen receptor binding and sex steroid concentration, respectively.

Table 2: Equations used in the female yellow perch vitellogenesis model

#	Equation
1.	$Syn[GABA] = \frac{500[1-1.0*\frac{\cos 2\pi(t-6.0)}{24.0}]}{1.0+[DA]*inh_{DA}+E2*inh_{E2GABA}}$
2.	$Syn[DA] = \frac{500[1-1.0*\frac{\cos 2\pi(t-6.0)}{24.0}*[E2]*Stim_{E2DA}]}{1.0+[GABA]*inh_{GABA}}$
3.	$\frac{dGABA}{dt} = Syn[GABA] - ka_{GABA}[GABA][GABA-A] + kd_{GABA}[GABA\_GABA-A] - Up_{GABA} - Deg_{GABA}$
4.	$\frac{dDA}{dt} = Syn[DA] - ka_{DA}[DA][D2] + kd_{DA}[DA_{D2}] - Up_{DA} - Deg_{DA}$
5.	$Deg_{GABA} = \frac{V_{GABAT}*[GABA]}{k_{GABAT}+[GABA]} * MultGABA - T$
6.	$Deg_{DA} = \frac{V_{MAO}*[DA]}{k_{MAO}+[DA]} * Mult_{MAO}$
7.	$Up_{GABA} = \frac{V_{GABA}*[GABA]}{k_{GABA}+[GABA]}$
8.	$Up_{DA} = \frac{V_{DA}*[DA]}{k_{DA}+[DA]}$
9.	$\frac{dGABA_{GABA-A}}{dt} = ka_{GABA}[GABA][GABA-A] - kd_{GABA}[GABA_{GABA}-A]$
10.	$\frac{dDA_{D2}}{dt} = ka_{DA}[DA][D2] - kd_{DA}[DA_{D2}]$
11.	$\frac{dGABA-A}{dt} = (kind_{GABA-A}[GABA-A] - ka_{GABA}[GABA][GABA-A] + kd_{GABA}[GABA_{GABA}-A] - kelim_{GABA-A}) * Mult_{GABA\text{-}A}$
12.	$\frac{dD2}{dt} = (kind_{D2}[D2] - ka_{DA}[DA][D2] + kd_{DA}[DA\_D2] - kelim_{D2}) * Mult_{D2R}$
13.	$Syn[GnRH] = GabaStim/DAInhib$
14.	$GABAStim = \frac{5*[GABA_{GABA}-BZ]^2}{2.0+[GABA_{GABA}-BZ]^2}$
15.	$\frac{dGnRH}{dt} = Syn[GnRH] - Syn[LH]$
16.	$GnRHStim = \frac{5*[GnRH]^2}{2.0+[GnRH]^2}$
17.	$Syn[LH] = \frac{GnRHStim}{1+\frac{[E2]}{10}}$
18.	$\frac{dLH}{dt} = Syn[LH] - Syn[T]$

Table 2 Continued:

#	Equation
19.	$Syn[T] = \frac{V_T * [LH]^{H_T}}{k_T{}^{H_T} + [LH]^{H_T}}$
20.	$\frac{dT}{dt} = Syn[T] - kdeg_T[T] + kd_T[SBP_T] - Syn[E2] - ka_T[T][SBP]$
21.	$Syn[E2] = \frac{V_{E2} * [T]^{H_{E2}}}{k_{E2}{}^{H_{E2}} + [T]^{H_{E2}}}$
22.	$\frac{dE2}{dt} = syn[E2] - kdeg_{E2}[E2] + k_{1[ER_{E2}]} + kd_{E2}[SBP_{E2}] - k1[E2][ER] - ka_{E2}[E2][SBP]$
23.	$\frac{dSBP}{dt} = kd_T[SBP_T] + kd_E[SBP_{E2}] - ka_T[T][SBP] - ka_E[E2][SBP]$
24.	$\frac{dSBP_T}{dt} = ka_T[SBP][T] - kd_T[SBP_T]$
25.	$\frac{dSBP_{E2}}{dt} = ka_{E2}[SBP][E2] - kd_{E2}[SBP_{E2}]$
26.	$\frac{dER}{dt} = 1.15 * k2[ER_{E2}] - kdegu[ER] + k\_1[ER\_E2] - k1[ER][E2]*Mult_{ER}$
27.	$\frac{dER_{E2}}{dt} = k1[E2][ER] - kdega[ER_{E2}] - k1[ER_{E2}] - k2[ER_{E2}]$
28.	$\frac{dVTG}{dt} = k3[ER_{E2}]$

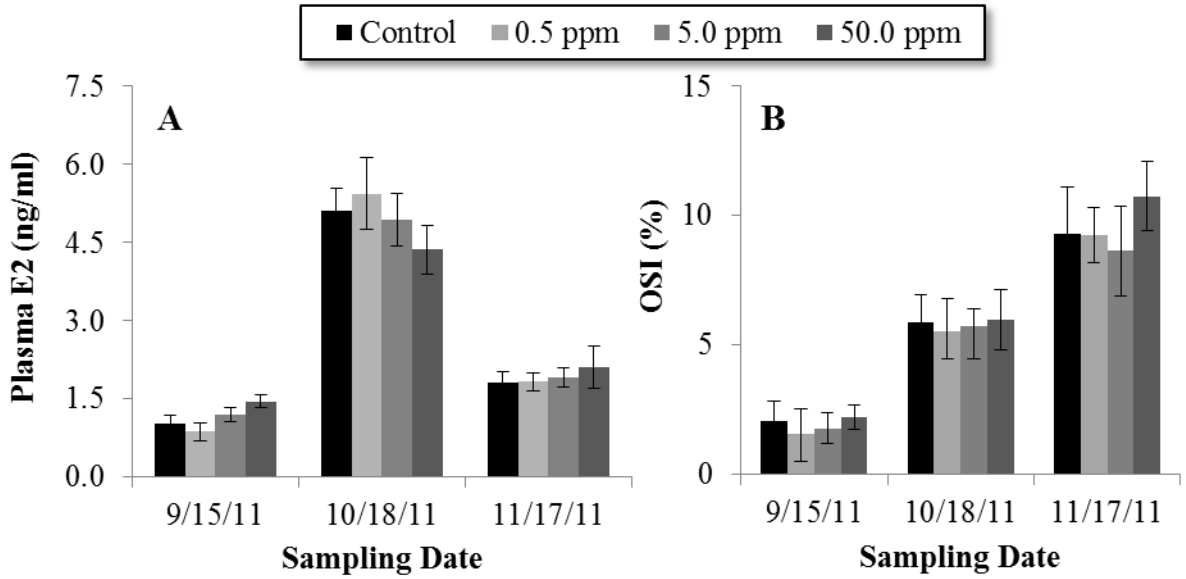

Figure 11: Effects of methylmercury (MeHg) on the female yellow perch 17β-estradiol (A) and ovarian somatic index (B). Adult female yellow perch (n = 12) were held in laboratory conditions during the period of gonadal recrudescence and exposed to MeHg for twenty weeks. Error bars indicate ±1 standard error. Data obtained from Debofsky et al. (in review).

Receptor binding assays were performed to determine hypothalamus $GABA_A$ and D2 receptor binding (Arini et al. 2016). MAO activity was determined using a neurochemical biomarker technique (Basu et al. 2007; Arini et al. 2016). Quantitative polymerase chain reactions (qPCR) were used to analyze LH-β transcript levels in the pituitary (Debofsky et al. in review). Plasma E2 and T concentrations were determined on a monthly basis from September through November using a previously described radioimmunoassay procedure (Jensen et al. 2001). Finally, estrogen receptor β (ERβ) concentration in the liver was quantified using an enzyme linked immunosorbent assay technique (Arini et al. 2016).

Arini et al. (2016) reported an *in vitro* increase in both D2 and $GABA_A$ binding and MAO activity within the hypothalamus for all MeHg treatments. Liver ERβ which is involved in

vitellogenin production (Leaños-Castañeda & Van Der Kraak, 2007, Nelson et al. 2013) was reduced by 65 and 64% compared to the control following exposure to 5 and 50 ppm MeHg.

Table 3: Multipliers (expressed as a % change from the control) for hypothalamic dopamine D2 and γ-aminobutyric acid (GABA) A receptors, liver estrogen receptor β, and hypothalamic monoamineoxidase (MAO) enzyme derived from Arini et al. (2016) *in vitro* study. Multipliers were incorporated into the yellow perch vitellogenesis model equations to simulate a MeHg exposure to 0.0, 0.5, 5.0 and 50.0 ppm MeHg exposure. * GABA transaminase (GABA-T) enzyme activity was not available therefore we assumed its activity was unaffected by MeHg exposure.

MeHg Conc (ppm)	Receptors			Enzymes	
	D2	$GABA_A$	ERβ	MAO	GABA-T*
0.0	1.00	1.00	1.00	1.00	1.00
0.5	3.93	1.47	0.92	3.73	1.00
5.0	6.06	1.65	0.35	2.26	1.00
50.0	2.84	1.81	0.36	1.41	1.00

In our simulations, multipliers were derived from the Arini et al. (2016) data for D2 ($Mult_{D2}$) and $GABA_A$ ($Mult_{GABA\text{-}A}$) receptor binding, MAO activity ($Mult_{MAO}$) and ERβ binding ($Mult_{ER}$). The multipliers were calculated based on a percent change from the control (Table 3) and applied to the model. Multipliers for $GABA_A$, D2 and liver ER binding were added to the state variable equations 2, 5, and 14, respectively. Additionally, multipliers for MAO enzyme activity were incorporated in the enzyme degradation equation 23. Arini et al. (2016) did not measure changes in GABA-T, therefore we made the assumption that GABA-T enzyme activity in yellow perch was unaffected by MeHg.

Despite these *in vitro* changes, Debofsky et al. (in review) determined that yellow perch reproduction is insensitive to a 20-week MeHg exposure up to 50.0 ppm. Sex steroid production (E2 and T) and ovarian somatic index, which is a ratio of the gonad size relative to the fish's total body weight, were unaffected *in vivo* following exposure to MeHg. Vitellogenin (VTG) and luteinizing hormone (LH) gene expression were also similar between the control and all three

MeHg treatments. We used the results from this study as a means to test how well our model characterized vitellogenin production in female yellow perch.

2.4 Sensitivity Analysis

For parameters that were added to or changed from the Murphy et al. (2009) vitellogenesis model, I conducted a one-factor-at-a-time (OFAT) sensitivity analysis (Broeke et al. 2016). Because many of the parameter values were obtained from the literature for many different animal species and sex (Table 9; Appendix), I used the OFAT analysis to provide insight on model robustness to small changes in parameter values. In the analysis, one parameter was varied over a wide range of values (Table 10; Appendix) while all other parameters were set equal to their nominal values. Additionally, the analysis allowed me to determine if any emergent patterns/relationships were apparent between the parameter and model output (cumulative vitellogenin).

3.0 RESULTS

3.1 Calibration

The model simulated E2 production similar to the mean control female yellow perch during the early gonadal recrudescence period of the laboratory raised fish (September through November; Figure 11). Maximum E2 production in our control simulation was 5.2 ng/ml which is similar to the laboratory measurement of 5.1 (+/- 1.4) ng/ml for adult yellow perch during the period of gonadal recrudescence (Figure 12). At the timing of the maximum E2 concentration, the modeled testosterone concentration was similar between our model control simulation, 2.1 ng/ml, and laboratory fish, 2.3 (+/- 1.2) ng/ml.

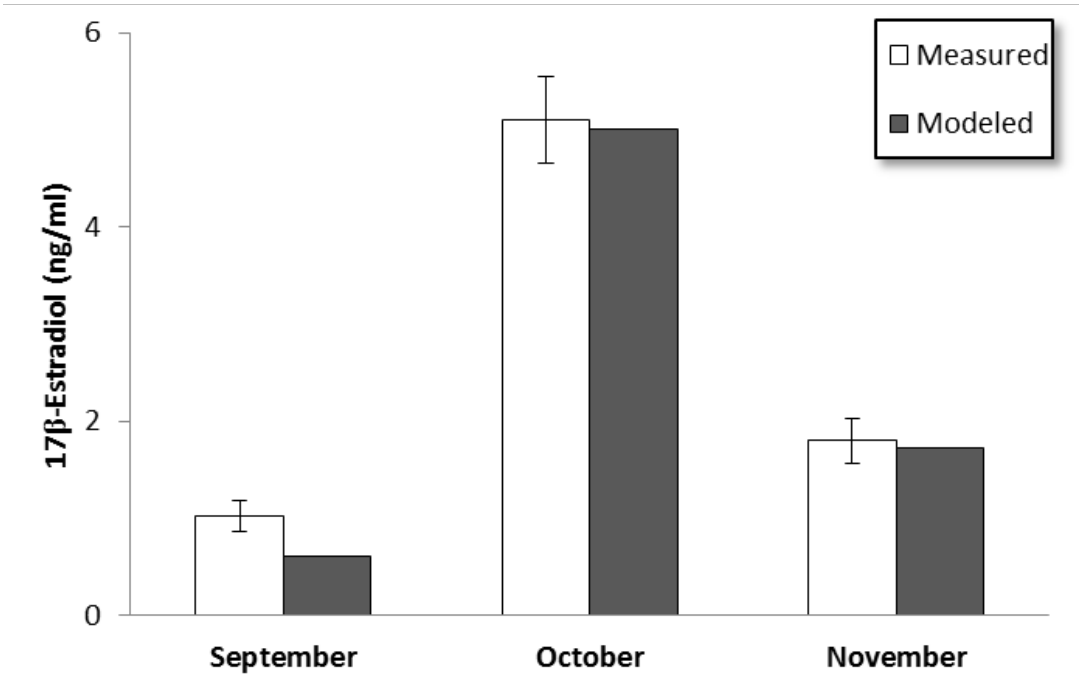

Figure 12: Comparison of measured vs simulated 17β-estradiol plasma concentrations in an adult female yellow perch. Laboratory measurements were obtained over a 3 month period during early vitellogenesis using a radioimmunoassay technique. Sexually mature female yellow perch (*Perca flavescens*) were raised in an indoor laboratory environment. Error bars +/- 1 standard error, N = 12. The yellow perch vitellogenesis model was then calibrated to roughly mimic the data.

3.2 Parameter Sensitivity

For the parameters in the hypothalamus and pituitary compartment, the sensitivity analysis revealed that thresholds exist for many parameters where vitellogenin is produced at very low (or high) levels throughout the simulation (Figure 31; Appendix). Once the threshold was reached, a similar asymptotic trend occurred for many of the hypothalamic parameters during which cumulative vitellogenin reached a maximum (or minimum) production point over a wide range of individual parameter values. Further analysis of the gonad compartment parameters for sex steroid production revealed a high sensitivity to the V_T (maximum production rate of testosterone) and H_E (hill coefficient for E2 production). Adjusting this parameter by 3x of its nominal value resulted in a 4.8x increase in cumulative vitellogenin production (Figure 31;

Appendix). The nominal values of these two parameters were derived from Murphy et al. (2009). In that study, V_T was adjusted during calibration to match laboratory derived sex hormone measurements.

3.3 Neurotransmitters and Neurohormones

Exposure to methylmercury resulted in a dose dependent decrease in the maximum free GABA concentrations in the hypothalamus (Figure 13A). In the model, a decrease in free neurotransmitter concentration can occur by increased binding to its receptor or increased degradation by its respective enzyme. Maximum Free GABA concentration was 2119.6, 1366.6, 1263.2, 1086.3 nmol/mg in the control, 0.05, 5.0 and 50.0 ppm MeHg treatment simulations, respectively. The total concentration of GABA bound to $GABA_A$ receptors was 25449, 28835, 24123 and 24042 nmol/mg in the control, 0.05, 5.0 and 50.0 ppm MeHg treatments simulations, respectively. Maximum free DA concentration was 127.1, 115.6, 121.6 and 125.5 nmol/mg in the control, 0.05, 5.0 and 50.0 ppm MeHg treatments simulations, respectively (Figure 13B). GnRH and LH concentrations were unaffected by MeHg exposure as all treatment simulations resulted in a maximum concentration of 1.8 and 1.5 ng/ml, respectively.

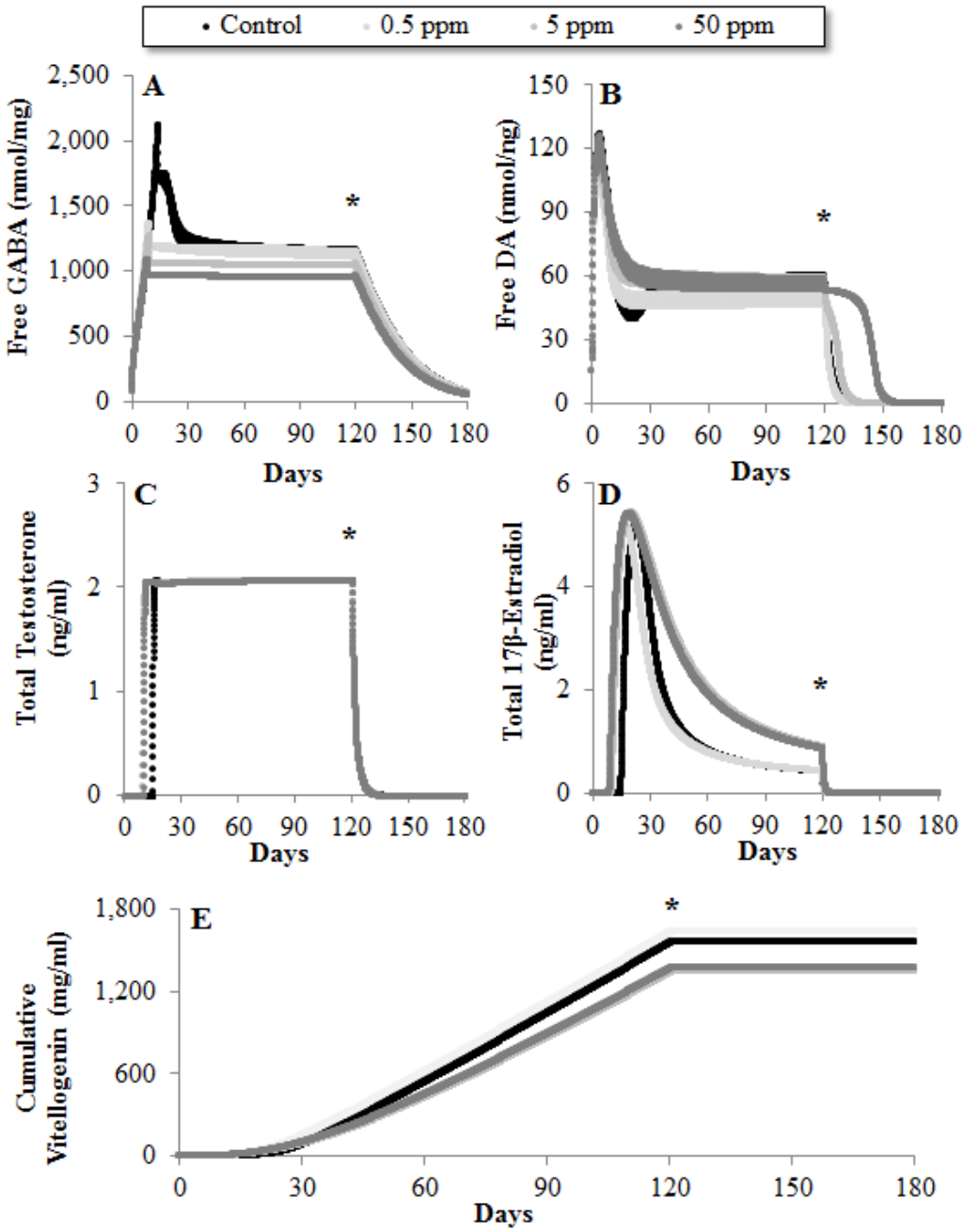

Figure 13: Simulated effects of 0.5, 5.0 and 50.0 ppm MeHg on hypothalamic γ-aminobutyric acid (A) and dopamine (B), sex steroids testosterone (C) and 17β-estradiol (D) and cumulative vitellogenin production (E) in a mature female yellow perch. Neurotransmitters were released during the first four months of the simulation which corresponds to yellow perch gonadal recrudescence period; (*) indicates when their release was turned off. MeHg exposure was simulated by incorporating *in vitro* changes of hypothalamic γ-

aminobutyric acid and dopamine receptor binding, monoamine oxidase activity and liver estrogen receptor β binding.

3.4 Plasma Sex Steroids

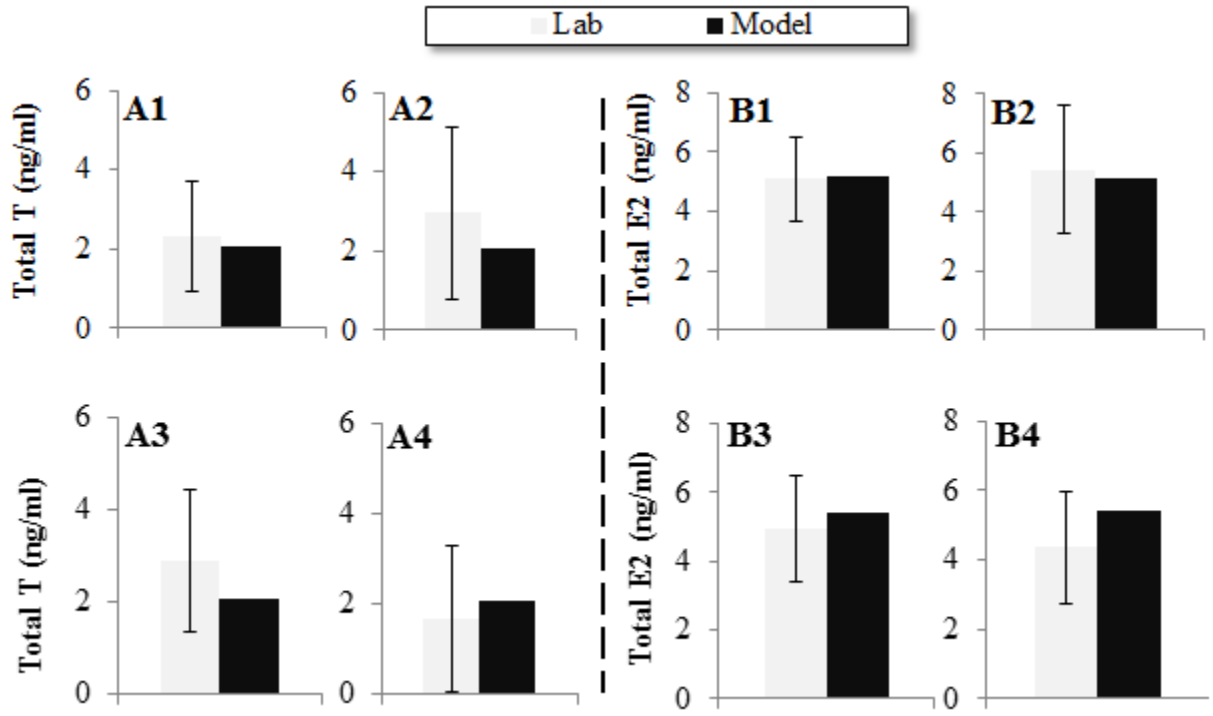

Figure 14: Comparison of laboratory measurement vs modeled total testosterone (A) and 17-β-estradiol (B) concentrations for the month of October in the adult female yellow perch plasma following exposure to methylmercury (MeHg). In the laboratory, adult female yellow perch were fed either a control (1), 0.5 ppm MeHg (2), 5.0 ppm MeHg (3) or 50.0 ppm MeHg (4) contaminated diet for twenty weeks. Radioimmunoassay was conducted for steroid measurement. Error bars indicate ±1 standard error (N = 12). MeHg exposure was simulated by incorporating *in vitro* changes of hypothalamic γ-aminobutyric acid and dopamine receptor binding, monoamine oxidase activity and liver estrogen receptor β binding.

Predicted testosterone in the control, 0.5, 5.0 and 50.0 ppm MeHg simulations reached a maximum concentration of 2.08, 2.07, 2.07 and 2.07 ng/ml, respectively (Figure 13C). The model slightly under predicted testosterone concentration in the 0.5 and 5.0 ppm MeHg treatments compared to the mean laboratory measurements during the month of October, 2.95 (+/- 1.49 S.D.) and 2.89 (+/- 1.49 S.D.) ng/ml, respectively. However, these modeled

concentrations were within one standard deviation of the mean laboratory measurements (Figure 14A).

Maximum E2 concentrations were similar between MeHg treatment simulations (Figure 13D). The E2 concentration reached a maximum concentration of 5.2, 5.2, 5.4 and 5.4 ng/ml in the control, 0.5, 5.0 and 50.0 ppm MeHg treatments, respectively. Modeled E2 concentrations for the month of October were within slightly higher in the 5.0 and 50.0 ppm MeHg treatments compared to the mean laboratory measurements, 4.9 and 4.4 ng/ml respectively, however were within one standard deviation (Figure 14B). The maximum concentration of E2 in all three MeHg treatment simulations was reached sooner compared to the control. Additionally, the 5.0 and 50.0 ppm MeHg simulations increased post-maximum concentration relative to the control (Figure 13D).

3.5 Vitellogenin and Egg Production

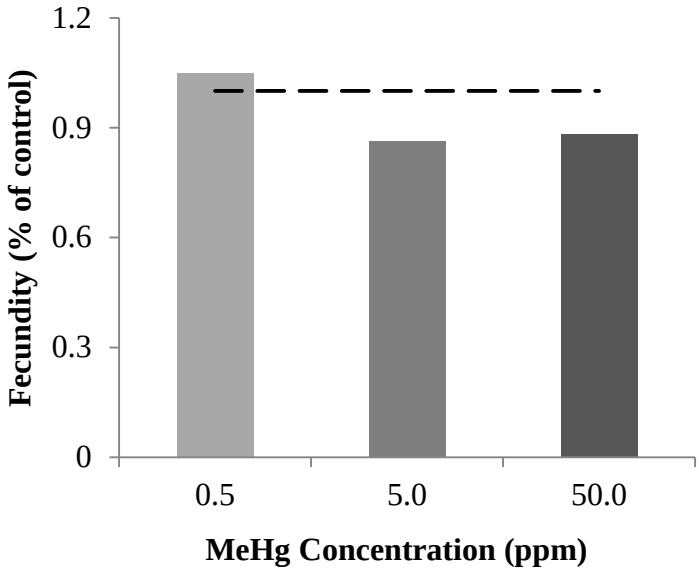

Figure 15: Estimated changes in yellow perch fecundity relative to control fish following MeHg exposure.

Predicted cumulative vitellogenin production in the control, 0.5, 5.0 and 50.0 ppm MeHg simulations was 1562.9, 1638.2, 1348.1 and 1377.7 mg/ml, respectively (Figure 13E). If we

assume that plasma vitellogenin measurements are a direct correlation of how much is produced on a given day, our modeled per day vitellogenin concentration (8.4 mg/ml) is similar to what has been reported in field collected yellow perch (3.9 to 21.6 mg/ml; Blazer et al. 2013). The earlier occurrence of the maximum E2 production resulted in a 4.8 % increase of vitellogenin production in the 0.5 ppm MeHg treatment. Relating predicted cumulative vitellogenin concentrations from each MeHg treatment as a proportion of the control fish, we are able to calculate predicted effects on yellow perch fecundity (Figure 15). The 0.5 ppm MeHg resulted in an estimated 4.8 % increase in fecundity while the 5 and 50.0 ppm treatments resulted in a 13.7 and 11.9 % reduction, respectively.

It is important to note that future use or development of this model must consider differences between fish species. It has been shown that dopamine inhibition is either weak or lacking in percid fish (Zarski et al. 2015) compared to other species such as cyprinids, catfishes and salmonids (Peter et al. 1986, Mylonas & Zohar 2007, Van Der Kraak 2009). Thus we did not incorporate the direct dopamine inhibition of GnRH release in our yellow perch simulations. For species under dopamine control of GnRH production, the full model for a generic fish (Chapter 1: Dissertation) should be used.

4.0 DISCUSSION

Our model suggests that exposure to 5.0 and 50.0 ppm MeHg would reduce yellow perch fecundity by just 13.7 and 11.9 %, respectively. These subtle findings are not supported by the *in vivo* laboratory study (Debofsky et al. in review) as sex steroid production, liver vitellogenin expression and ovarian somatic indices (OSI) were not statistically lower than the control in either MeHg treatment after 20 weeks of exposure. In that study, yellow perch OSI was significantly greater in the 50.0 ppm MeHg treatment and liver vitellogenin expression was

significantly higher in the 5.0 and 50.0 ppm MeHg exposed fish compared to the control fish. Similarly, in another fish species from the taxonomic order Perciformes, OSI was not significantly different between largemouth bass with high (5.42 ppm) and low (0.30 ppm) methylmercury content (Friedmann et al. 2002). In contrast, studies have shown that exposure to MeHg can significantly reduce reproduction in other fish taxonomic orders such as Cypriniformes (fathead minnows; Hammerschmidt et al. 2002), Siluriformes (walking catfish; Kirubagaran & Joy 1990), and Salmoniformes (rainbow trout; Birge et al. 1979). Overall, our model is close to mimicking the *in vivo* data and there are just a few key data gaps that should be addressed.

The increased GABA binding to the $GABA_A$ receptor sites as determined by Arini et al. (2016) *in vitro* resulted in a dose-dependent reduction in free GABA concentrations in each of our MeHg treatment simulations (Figure 13A). Vitellogenesis was initiated sooner due to the increased GABA binding in our model MeHg simulations compared to the control (Figure 13). For example, the maximum E2 production was reached 4.5, 4.8 and 6.3 days earlier in the 0.5, 5.0 and 50.0 ppm MeHg simulations, respectively when compared to the control (Figure 13D). Again, the *in vivo* E2 and OSI measurements do not support this finding (Figure 12).

Additionally, Arini et al. (2016) reported a significant decrease in *in vitro* liver ERβ binding in both the 5.0 and 50.0 ppm MeHg treatments. Incorporating the liver ER binding reductions into the HPGL model resulted in an increase in free E2 following its maximum production in both the 5.0 and 50.0 ppm MeHg simulations (Figure 13D). In these simulations cumulative vitellogenin production was reduced (Figure 13E). Again, these results are not supported by the laboratory measurements (Debofsky et al. in review; Figure 12). The Debofsky et al. (in review) laboratory post-maximum E2 concentration measurements were similar

between MeHg treatments at 1.8 (+/- 0.8), 1.8 (+/- 0.6), 1.9 (+/- 0.6) and 2.1 (+/- 1.2) ng/ml for the control, 0.5, 5.0 and 50.0 ppm MeHg treatments, respectively and vitellogenin expression was not significantly reduced in either MeHg treatment.

These findings suggest that we are missing an important step in yellow perch vitellogenesis. One missing parameter in our model is GABA-T activity because it was not measured in the Arini et al. (2016) study. Therefore, we made the assumption that MeHg does not affect the activity of GABA-T enzyme in yellow perch (Table 3). To test this assumption we incrementally increased (1.5, 2.0, 2.5 and 3.0x) the amount of GABA-T in the system for the 50.0 ppm MeHg simulation. Increased GABA-T correlated with a later vitellogenesis initiation date. In our baseline 50.0 ppm simulation, maximum E2 production occurred 6.3 days earlier than the control. When GABA-T was increased by 1.5 x, 2.0 x and 2.5 x in the 50.0 ppm MeHg simulation, maximum E2 production occurred 4.5, 2.6 and 0.5 days earlier than the control, respectively (Figure 32A; ; Appendix). The 3.0 x GABA-T simulation resulted in the maximum concentration being reached at 0.9 days later than the control. However, the increased GABA-T also resulted in a further reduction in cumulative vitellogenin production (Figure 32B; Appendix). In the 1.5x, 2.0x, 2.5x and 3.0x GABA-T multiplier simulations, cumulative VTG was reduced by 2.0, 4.0, 7.1 and 9.3 %, respectively, compared to the baseline 50.0 ppm MeHg simulation where the GABA-T multiplier was assumed to be unaffected by MeHg exposure. This finding suggests that MeHg may have an effect on GABA-T activity in the hypothalamus of yellow perch in order to compensate for the increased binding to $GABA_A$ receptors and negating the faster E2 production observed in our 5.0 and 50.0 ppm MeHg model simulations. However, the reduced vitellogenin production in our simulations suggests further mechanisms in our model are missing as Debofsky et al. (in review) did not observe a reduction in ovary size nor liver

vitellogenin mRNA transcripts. Therefore, we are assuming exposure to MeHg did not affect vitellogenin production of the laboratory exposed female yellow perch.

In order for vitellogenin to be produced, E2 must bind to an open estrogen receptor, which dimerizes and binds to an estrogen response element (ERE) to begin transcription of the vitellogenin gene. Arini et al. (2016) only measured ER-β concentrations *in vitro* from adult female yellow perch livers because ER-β has been shown to be the main receptor involved in vitellogenin production (Leaños-Castañeda & Van Der Kraak, 2007). Our model results indicate that our assumption that vitellogenin production is directly related to E2 binding to ER-β is either invalid or our model is missing a compensation mechanism occurring due to the reduced ERβ binding. In mice, two pathways of estradiol signaling can occur; 1: homodimer of a single ER subtype or 2: heterodimer consisting of two ER subtypes (Pettersson et al. 1997). Yellow perch have been shown to exhibit two estrogen receptor subtypes, α and β (Lynn et al. 2008, Goetz et al. 2009). One possibility is that when yellow perch are exposed to high concentrations of MeHg that reduce ERβ binding sites, the ERα subtype may compensate and assist in vitellogenin production. A similar compensatory mechanism was hypothesized to exist in mice as ovarian function was sustained in ERβ knockout mice (Enmark & Gustafsson 1999).

To test the assumption that ERα compensation occurs in yellow perch, we doubled the amount of ER in the model (Equation 27). We assumed that the two ERs are expressed in equal concentrations in yellow perch liver and MeHg has a similar effect on both subtypes. In this simulation, maximum E2 concentration was 5.2, 5.0, 5.2 and 5.2 in the control, 0.5, 5.0 and 50.0 ppm MeHg simulations (Figure 16A). Additionally, the delayed reduction in E2 following its maximum production was no longer present in our 5.0 and 50.0 ppm simulations. Cumulative vitellogenin concentration was 1563, 1753, 1569 and 1596 in the control, 0.5, 5.0 and 50.0 ppm

MeHg simulations (Figure 16B). The reduced effect on cumulative vitellogenin production in this simulation suggests that another ER subtype may be compensating for ERβ when yellow perch are exposed to high concentrations of MeHg.

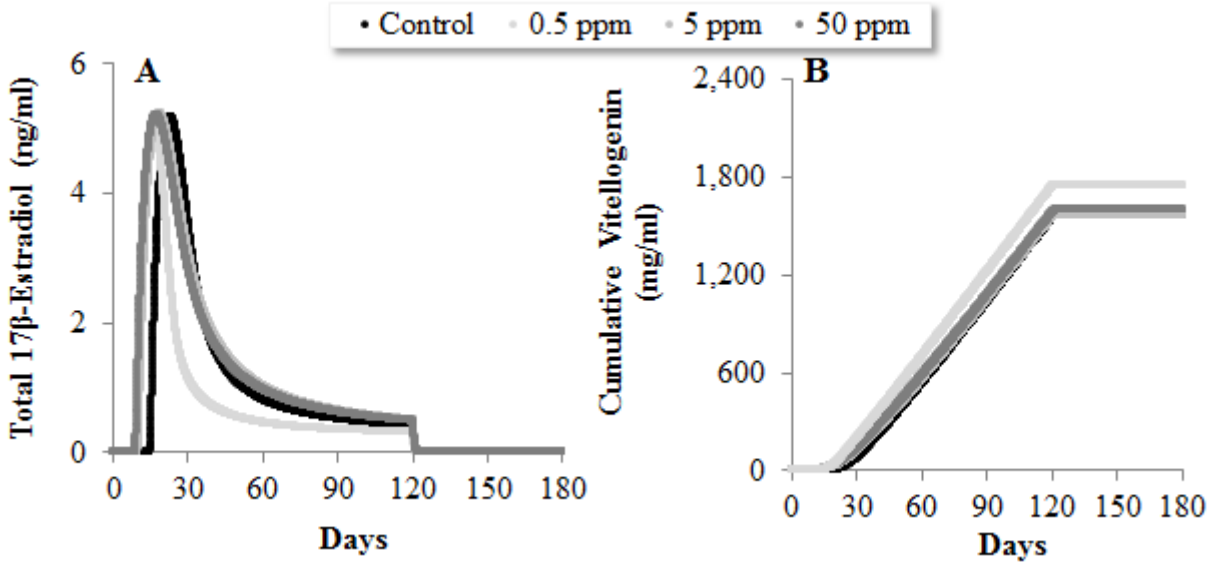

Figure 16: Simulations of a female yellow perch 17β-estradiol (A) and cumulative vitellogenin (B) concentration following exposure to MeHg, assuming both liver estrogen receptor α and β contribute equally to vitellogenin production during MeHg exposure. MeHg exposure was simulated by incorporating *in vitro* changes of hypothalamic γ-aminobutyric acid and dopamine receptor binding, monoamine oxidase activity and liver estrogen receptor β binding.

The addition of a DA inhibition of GnRH release in our model had a significant effect on cumulative vitellogenin production. When the HPGL axes was inhibited by DA, our simulations of the 5.0 and 50.0 ppm MeHg simulations experienced a 91% and 93% reduction in cumulative vitellogenin production, respectively, compared to the simulations absent of DA inhibition. Thus future studies that assess MeHg effects on fish reproduction should consider whether or not their model species reproduction is dependent upon hypothalamic dopamine. These differences in MeHg response for different fish species have been reported in the literature. For example, Debofsky et al. (in review) found no adverse effects on yellow perch reproduction following a 20

week exposure to MeHg up to 50.0 ppm. In contrast, female fathead minnows exposed to 3.93 ppm MeHg for 250 d exhibited decreased E2 levels (Drevnick & Sandheinrich 2003, Crump et al. 2009). Similarly, female largemouth bass (*Micropterus salmoides*) exposed to MeHg up to 6.25 ppm for 56 days displayed reduced E2 and VTG concentration (Fynn-Aikins et al. 1998, Crump et al. 2009).

Many assumptions were made while incorporating neurotransmitter dynamics into the model. Our model is similar to other fish vitellogenesis models which used either a generic estrogen receptor or assumed that the ERα subtype was solely involved in vitellogenin production (Murphy et al. 2005, Li et al. 2011, Sundling et al. 2014, Gillies et al. 2016). Additionally, because this is the first vitellogenesis model that incorporates a hypothalamic compartment with neurochemicals upstream of GnRH production, many data deficiencies exist for fish neurotransmission including neurotransmitter association and dissociation to the receptors and parameter values for reuptake and enzyme degradation. Many parameter values for the model were derived from the literature for other taxa, including amphibians, birds and mammals, in addition to both male and females. Therefore, future studies should focus on assessing these parameters in fish, specifically females, to address these data gaps.

Our sensitivity analysis (Figure 31; Appendix) revealed that the modeled cumulative vitellogenin was most sensitive to the sex steroid production parameters, with the maximum rate of testosterone (V_T) and estradiol production (V_E) being the most sensitive parameters. Very subtle changes to these parameters (+ 0.5 ng/ml/h) resulted in large fluctuations in modeled cumulative vitellogenin (+ 8931 mg/ml; - 2653 mg/ml, respectively). Many of the sex steroid production parameter values were originally used in the calibration process of Murphy et al. (2005). Additionally, there were thresholds for the neurochemical parameters for which

vitellogenin production was produced at very low levels for parameter values below (or above) these thresholds. Further research should aim to measure these parameters in fish which may improve the model's predictability.

Overall, incorporating the Arini et al. 2016 *in vitro* data for MeHg effects on yellow perch into the vitellogenesis model was close, but failed to mimic the *in vivo* responses reported by Debofsky et al. (in review). However, using the model to test various assumptions proved to be a useful exercise and we recommend an iterative approach that involves modeling to extrapolate *in vitro* data to *in vivo* results. Our simulation results highlighted a few key data gaps that need to be addressed in order to fully characterize yellow perch vitellogenesis and validate the model. These data gaps include the role of ERα in vitellogenin production when ERβ is reduced during contaminant exposure; the effect of MeHg on GABA-T; and neurotransmitter receptor binding and enzyme kinetics in fish. Once validated, the model can be used as a screening tool to link *in vitro* data to adverse effects on fish reproduction which would assist in assessing the adverse effects of the more than 85,000 registered chemicals (U.S. EPA 2015).

CHAPTER 3

YELLOW PERCH RECRUITMENT IN LAKE MICHIGAN I: EXPLORING THE IMPACTS OF METHYLMERCURY INDUCED BEHAVIORAL ALTERATIONS

ABSTRACT

Recently, consecutive year class failures have resulted in a decline of yellow perch populations in Lake Michigan. Poor recruitment of yellow perch has been associated with changes in trophic structure and adverse environmental conditions, but the potential effects of contaminants have not been explored fully either in isolation or in combination with other stressors. Methylmercury (MeHg), a persistent contaminant found in the Great Lakes, has been shown to alter foraging and predator avoidance behaviors of larval yellow perch, which could affect their recruitment in Lake Michigan. We adapted existing individual based models (IBMs) of larval fish (including perch species) to incorporate laboratory derived MeHg behavioral effects on a larval yellow perch cohort. Our model simulations suggest that exposure to neurotoxic contaminants such as MeHg could significantly reduce cohort survival. Effects on swimming speed and foraging efficiency simulated during a 0.03, 0.1 and 0.3 μM MeHg exposure resulted in a 19.7 %, 97.4 %, and 69.9 % decrease in survival relative to a MeHg absent simulation in larval yellow perch cohort, respectively. Additionally, the mean stage duration of the pelagic period of an individual larval yellow perch increased by 1.0, 3.8 and 2.2 days, respectively, in our simulations. While our experimental MeHg concentrations were higher those typically found in Lake Michigan, our findings suggest that contaminants could be an additional factor impacting recruitment of yellow perch in Lake Michigan, and that this deserves further exploration.

1.0 INTRODUCTION

Lake Michigan yellow perch (*Perca flavescens*) populations have declined since the early 1990's due to consecutive year-class failures (Dettmers et al. 2003, Clapp & Dettmers 2004, Santucci Jr et al. 2014). Several factors have been attributed to this decline including the invasion of exotic species such as the zebra mussel (Marsden & Robillard 2004) and alewife, *Alosa pseudoharengus*, (Shroyer & McComish 2000). Yellow perch recruitment in Lake Michigan has been adversely affected following these introductions due to an altered forage base and increased predation, which I explore further in Chapter 4. However, contaminants may be another factor contributing to the failure in larval yellow perch recruitment as larval fish behaviors specific to growth and survival can be affected following exposure (Mora et al. 2015).

Toxicants can cause adverse effects on behavior at lower exposure concentrations than those that induce mortality (Gerdhart 2007, Weis & Candelmo 2012). Effects on swimming performance, reproductive behaviors, and predator/prey interactions can all cause significant ecological consequences (Weis & Candelmo 2012). For example, reduced swimming ability and visual reactive distance can lead to increased predation and starvation rates within a simulated larval fish cohort which would lead to adverse population effects (Murphy et al. 2008).

Mercury (Hg) is a naturally occurring element, however its role in mining processes and industrial usage has caused it to become a global pollutant (Driscoll et al. 2013). Hg is transported in the atmosphere to aquatic and terrestrial ecosystems where it is converted to methylmercury (MeHg) (Depew et al. 2012, Driscoll et al. 2013). Once in the water, MeHg is concentrated (up to $>10^5$) by phytoplankton and then bioaccumulates and biomagnifies up the food chain (Chen et al. 2008) where MeHg accounts for more than 95 % of the total mercury in whole fish (Hammerschmidt et al. 1999, Wiener et al. 2012). For example, Mason & Sullivan

(1997) reported $3.2*10^{-4}$ parts per billion (ppb) and $1.3*10^{-5}$ ppb mean total Hg and MeHg concentrations for Lake Michigan, respectively. Zooplankton collected from Green Bay, Lake Michigan were found to have an average total mercury concentration of 7.82 ppb (Brazner & DeVita 1998). Wiener et al. (2012) reported a median Hg concentration of 88 ppb wet weight with a maximum of 430 ppb in whole yellow perch collected from Lake Michigan. Generally, Hg concentrations in fish collected from the Great Lakes have steadily declined since the late 1970's (Murphy et al. 2007, Bhavsar et al. 2010).

MeHg affects a variety of fish species and a dietary exposure can result in adverse effects on behaviors specific to spawning, predator response, motor functions and foraging in these species (Depew et al. 2012). For example, juvenile fathead minnows exhibited a dose-dependent delayed spawning, reduced spawning success and an overall decreased reproductive effort after being fed either 880, 4110 and 8460 ppb MeHg until sexual maturity (Hammerschmidt et al. 2002). Interestingly, mature female yellow perch fed up to 50,000 ppb MeHg for 20 weeks did not experience adverse reproductive effects (Debofsky et al in review), however newly hatched larval yellow perch exposed via water up to 0.03 μM MeHg for 25 days exhibited significantly reduced locomotor activity and foraging efficiency (Mora et al. 2015). Furthermore, adverse effects of maternally transferred MeHg (0.04 – 4.6 ppb) on larval Atlantic croaker survival skills were observed including lower swimming speed, reduced net-to-gross displacement ratio and total activity (Alvarez et al. 2006).

Changes in larval fish behavior due to contaminant exposure, such as reduced swimming speed and altered foraging success, can be incorporated into individual based models (IBMs) to predict adverse effects on populations (Murphy et al. 2008). IBMs are a valuable tool that incorporates natural individual variability to better predict changes in survival and growth

compared to aggregated modeling approaches. This variability in both extrinsic (the environment) and intrinsic (the individual) factors can have large influences on a population's growth and survival (Letcher et al. 1996). Another benefit of IBMs as opposed to more aggregated models is the inclusion of size-based behaviors such as swimming speed, foraging efficiency and predator avoidance. Previous IBMs have been developed for larval yellow perch in Lake Michigan (Fulford et al. 2006a, Fulford et al. 2006b, Beletsky et al. 2007) however they haven't been used to assess contaminant driven effects or to explore multiple abiotic and biotic stressors which may be contributing to the low recruitment of yellow perch in Lake Michigan.

Developing the IBMs to assess contaminant effects on fish populations will also help meet the U.S. National Research Council (NRC) goal that new, predictive approaches be developed to ease the demands of testing the environmental effects of the > 80,000 chemicals in use today on the hundreds of thousands of species (NRC, 2007). Therefore our goal was to construct an IBM for a newly hatched larval yellow perch cohort in Lake Michigan in order to assess whether sublethal behavioral effects of MeHg could be contributing to the recruitment loss of yellow perch in Lake Michigan. Specifically, our objective was to assess the impact of MeHg exposure on pelagic stage duration and survival of larval yellow perch in Lake Michigan. We hypothesized that the reduced foraging efficiency and swimming speeds following MeHg exposure would lead to increased predation and starvation mortality and lower growth rates of larval yellow perch.

2.0 METHODS

2.1 The Model

We adapted larval fish IBMs from previous models for larval yellow perch (Fulford et al. 2006a, Fulford et al. 2006b), Atlantic croaker (Murphy et al. 2008) and a generic marine larval

model (Letcher et al. 1996). The model is not spatially explicit and simulates a 1000 L cube of homogenous Lake Michigan water. The model was developed in FORTRAN 90 with the Lahey Fujitsu compiler (version 7.3) to perform simulation experiments. We followed the ODD (Overview, Design concepts, Details) protocol proposed by Grimm et al. (2006) for describing an IBM, and the required sections are described below.

2.2 Model purpose

The IBM was constructed to simulate a newly hatched larval yellow perch cohort, up to 30 mm in total length, in Lake Michigan to determine the effects of behavioral impairments, swimming speed and foraging efficiency, following continuous MeHg exposure on the cohort's growth and survival.

2.3 Entities, state variables and scales

Characteristics of each larval yellow perch individual were determined by eight state variables at each time step: total length (mm), mass (g), age (d), status [alive or dead], consumption variables [prey type proportion (%), total mass (g)], daily growth (g), and, if applicable, mortality type [starvation, predation].

The modeled lake environment was updated at each time step (described in Section 2.8) and had 7 state variables: daily lake temperature (ºC), prey type density (# individuals per mL), prey type length (mm) and mass (g), prey patch exhaustion time (d) and predator total length and mass (g). We assumed that six types of taxonomic prey items (copepods [identified to their taxonomic order Calanoida or Cyclopoida], copepod nauplii, the taxonomic phylum Rotifera and the genera *Bosmina* and *Daphnia*). Two species of predators (alewives and yellow perch) existed within the lake environment with randomly chosen body lengths (mm).

Model simulations for each individual larval yellow perch were conducted for 90 days or until the individual reached 30 mm, starved to death or was eaten by a predator. At 30 mm, the fish were assumed to become demersal and escape intense predation by leaving the upper water column and swimming down near the bottom of the lake (Janssen & Luebke 2004). Two sets of simulations were conducted. The first set of simulations included a baseline control for Lake Michigan absent of the MeHg effects on foraging efficiency and swimming speed. Simulations were then performed with the MeHg effects imposed on only the swimming speed or foraging efficiency of larval yellow perch. The objective of these simulations was to determine which individual MeHg effect had the largest impact on larval yellow perch survival and growth. The second set of simulations included both MeHg effects on swimming speed and foraging efficiency to determine the overall impact on larval yellow perch survival and growth.

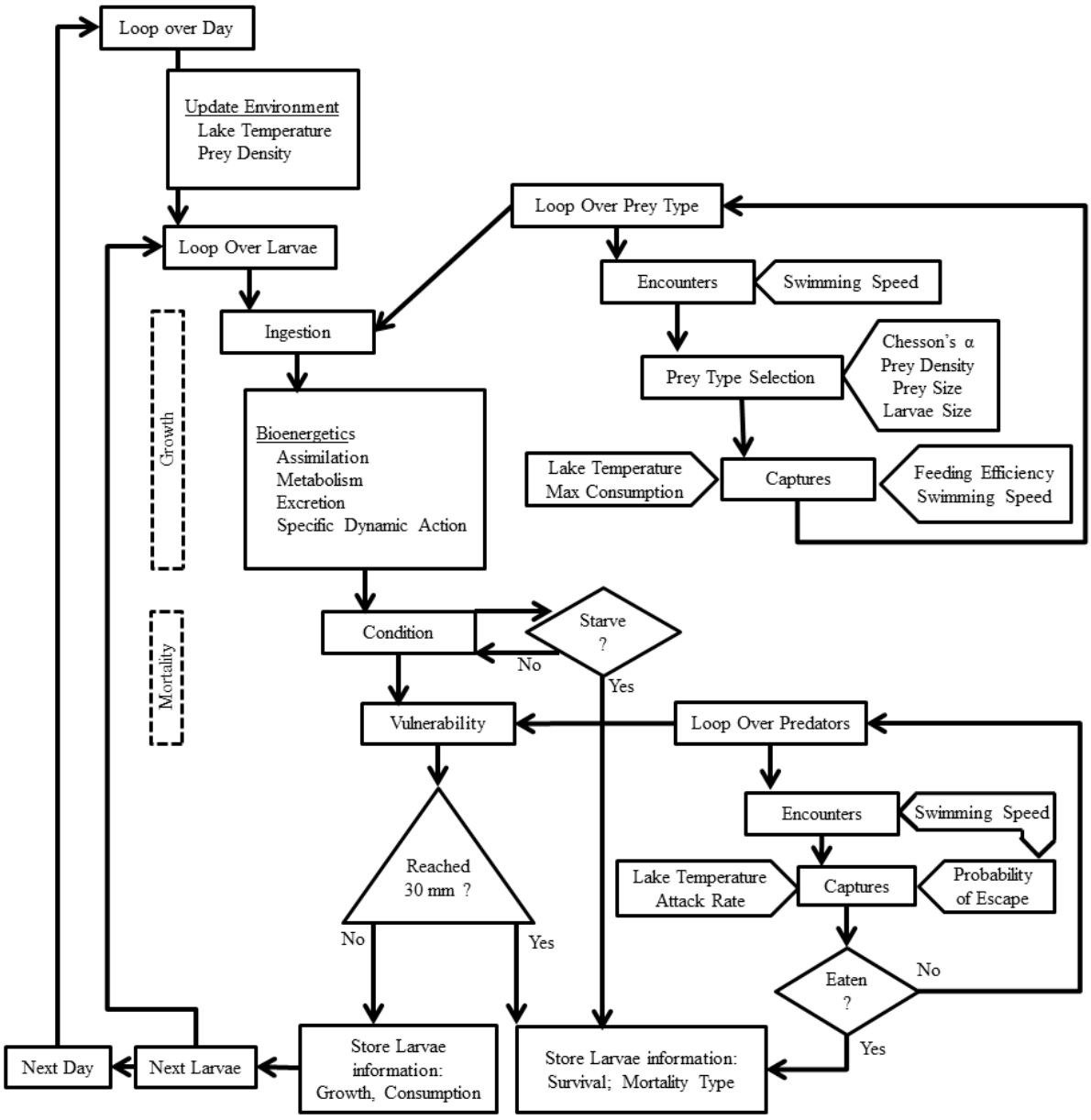

Figure 17: Flow chart of the Individual Based Model simulating a larval yellow perch cohort for Lake Michigan.

2.4 Process overview and scheduling

Each day, the model updated the state variables within the lake environment for each larval fish. On a given day, all simulated larval yellow perch were subject to the same lake temperature; however, each fish was provided a randomly chosen prey density (Figure 17;

further details in section 2.8). Prey density for each larval yellow perch was dependent upon its previous day's density and patch exhaustion status, which were randomly determined at the first day of feeding. We assumed that the first four days of life post-hatch the individuals would be strictly undergoing endogenous (egg yolk) feeding and on day 5 they would switch to exogenous (zooplankton) feeding. Prey patches were assumed to exhaust between 3 and 14 days (Folt et al. 1993). Therefore, a patch exhaustion day was randomly chosen using a uniform distribution (U~3,14). Once a patch was exhausted, a new prey density and patch exhaustion day for that individual larval yellow perch were randomly selected. After the habitat conditions were determined for an individual on a given day, the foraging, bioenergetics and predation submodels were run sequentially. During a foraging event, an individual would encounter, select and attempt to capture prey items. The number of encounters and selectivity parameters for each prey type were updated each day for each larval fish (described in section 2.8.3). Consumption of each prey type for each larval fish was determined based on the number of successful encounters and time spent foraging and the total consumption for the day was bound to a maximum consumption rate based on the size of the individual (Letcher et al. 1996, Fulford et al. 2006b, Murphy et al. 2008). The total biomass consumed on a daily basis was input into a bioenergetics submodel which calculated the amount of energy used towards daily growth (g). If negative growth occurred, the starvation submodel was implemented. Concurrently, each day the individuals were vulnerable to predation by predatory fish based on the size of both the individual and encountered predators as well as the distance the individual swam that day. Surviving individuals graduated from the model once they reached 30 mm in length.

2.5 Design Concepts

2.5.1 Stochasticity

The length of each individual larval fish at time of hatch (day 1) was randomly selected from a normal distribution using hatch length mean (5.3 mm) and standard deviation (0.43 mm); the length data were estimated from field collections of < 1 d old larval perch in Lake Michigan (Granet 2000, McNaught 2002, Edwards 2010). Within the foraging submodel, prey type densities for each larval fish were determined from a negative binomial distribution (described in section 2.8.2). Prey densities remained constant between days until the patch was exhausted. While the mean number of successful encounters by an individual larval fish for a given prey type was determined from a binomial deviate of the capture success and number of encounters for that prey type (Letcher et al. 1996, Murphy et al. 2008), the number of realized encounters was randomly chosen from a Poisson distribution to account for small scale patchiness (Letcher et al. 1996, Murphy et al. 2008). Within the predator submodel, predation occurred if a random number drawn from a uniform distribution (0 – 1) was less than the predation vulnerability (Fulford et al. 2006a), further described in Section 2.8.5.

2.5.2 Emergence

Larval yellow perch diet was dependent upon the individual's prey preference for the various types of prey available in the environment which included a prey item selectivity index (Chesson's α; Fulford et al. 2006b). This index ranked selection for encountered prey items according to their presence in field diet data (described in section 2.8.3). Size based prey dynamics and density (# / mL) in the surrounding environment were incorporated into the prey selection process. The foraging activity by an individual then influenced its daily growth rate (g).

2.5.3 Observation

After every time step the model stored detailed information about the lake environment, which included lake temperature (ºC), prey type density (# / ml) and prey type mass (g) and length (mm). Additionally, information was stored for each individual larval fish including survival (or mortality type), current day weight (g) and total length (mm), and diet [total ingestion rate (g); prey type proportion (%)].

2.5.4 MeHg Effects

A recent study investigated the effects of MeHg on larval yellow perch behavior (Mora et al. 2015). In that study, 300 recently hatched larval yellow perch were exposed via water to 0, 0.03, 0.10 or 0.30 μM MeHg for 25 days. Following exposure, swimming speed was measured for 120 individual larval fish within each MeHg treatment for 30 seconds. Feeding efficiency was estimated using a brine shrimp, *Artemia* spp., feeding trial. Thirty larval yellow perch (four replicates per treatment) were placed in a 10 cm diameter petri dish. One hundred *Artemia* were introduced into the dish and the larval fish were allowed to forage for 10 minutes following which the number of eaten prey was recorded. Overall, exposure to MeHg reduced larval yellow perch swimming speed and forage efficiency (Figure 18).

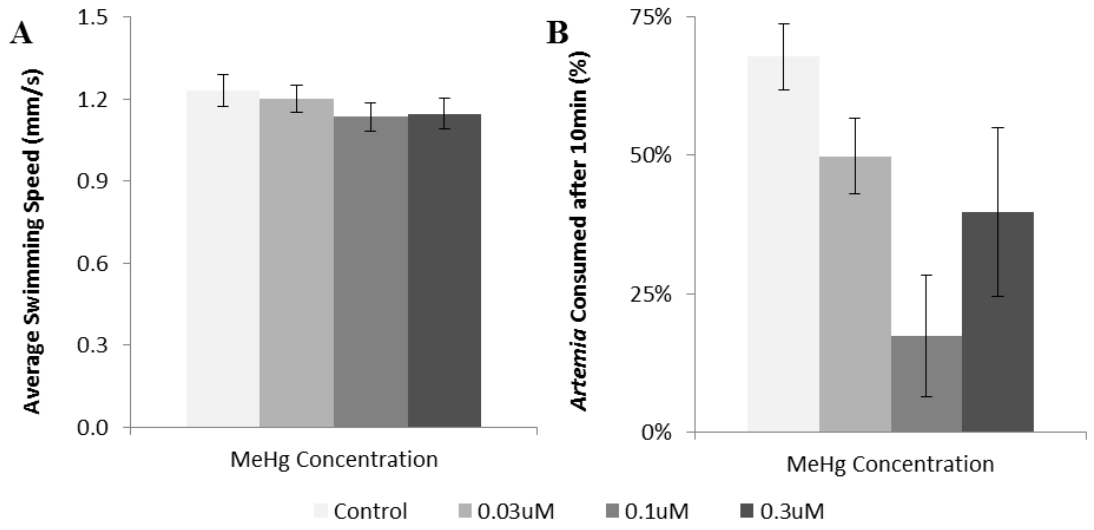

Figure 18: Effects of MeHg waterborne exposure on larval yellow perch swimming speed (A) and feeding efficiency (B). 300 newly hatched yellow perch were exposed for 25 days to 0.03, 0.1 and 0.3 µM MeHg or a water only control. Swimming speed was individually measured for 120 individuals per MeHg treatment. For the feeding efficiency trial, four replicates, each containing 30 larval yellow perch, were allowed to feed on 100 *Artemia* for 10 minutes following exposure to MeHg. Data obtained from Mora et al. (2015). Error bars are ± 1. Standard error.

Table 4.1: Swimming speed multipliers used in a pelagic larval yellow perch individual based model. Multipliers were derived from Mora et al. (2015)

MeHg Treatment	Average (%)	StDev (%)	Max (%)	Min (%)
Control	100	49	240	24
0.03 µM	97	43	239	19
0.10 µM	92	46	248	19
0.30 µM	93	49	266	14

Table 4.2: Capture success multipliers used in a pelagic larval yellow perch individual based model. Multipliers were derived from Mora et al. (2015)

MeHg Treatment	Average (%)	StDev (%)	Max (%)	Min (%)
Control	96	6	100	84
0.03 µM	73	12	97	55
0.10 µM	28	18	74	6
0.30 µM	58	27	100	2

The individual based data from Mora et al. (2015) was incorporated into the IBM model and expressed as multipliers. Swimming speed multipliers (Table 4.1) were calculated for all 120 larval fish within a treatment from the Mora et al. (2015) swimming speed study by dividing an individual's swimming speed by the mean control swimming speed (1.23 mm/sec, figure 18A). In the IBM model, a swimming speed multiplier (SSMult) was randomly selected from a fish in the laboratory exposure, which was drawn from a uniform distribution, and applied to a modeled individual's swimming speed (Equation 3) similar to the method used by Murphy et al. (2008). Once a swimming speed multiplier was chosen for an individual, it remained for the entire simulation. This process was repeated for all 10,000 individuals in the IBM at the beginning of each simulation. We assumed these effects would not be reduced during the simulation as previous studies have shown that adult fish exposed to MeHg (up to 0.3 μM) as embryos still suffered from abnormal behaviors (Smith et al. 2010, Xu et al. 2012).

Prey capture success multipliers (Table 4.2) were calculated from the Mora et al. (2015) feeding efficiency study by dividing a treatment's feeding efficiency by the average control feeding efficiency (67.83%; Figure 18B). A capture success multiplier (FeedMult) was then randomly chosen based on a normal distribution given the mean and standard deviation multiplier of that treatment from the laboratory exposure and applied to an individual's prey capture success in the simulation (Equation 8). We chose a normal distribution rather than a uniform distribution because the feeding efficiency study by Mora et al. (2015) was conducted on a group of larval fish (N = 30, Replicates = 4) rather than on individuals. Once a capture success multiplier was chosen for an individual it remained constant throughout the simulation. This process was repeated for all 10,000 individuals in the IBM at the beginning of each simulation. Capture success multipliers were upper bound to 100 %. Five simulations were

conducted for each MeHg treatment including a baseline MeHg absent control to allow for the built in stochasticity, further described in Section 2.5.1.

2.6 Initialization

Each simulation started with 10,000 larval yellow perch in a 1000 L volume of Lake Michigan water. This density was equivalent to the larval yellow perch density estimate of 1 x 10^{-5} fish/mL reported for Southern Lake Michigan (Fulford et al. 2006a).

2.6.1 Hatch Characteristics

Initial hatch length (L, mm) for each larval fish was calculated based on a random number generator with mean = 5.3, standard deviation of 0.43 (Granet 2000, McNaught 2002, Edwards 2010). Larval fish weight (Equation 1; W, g) was then calculated based on larval fish length (Mills & Forney 1981, Fulford et al. 2006b).

$$W = 5.19E - 07 * L^{3.293} \quad (1)$$

During the 1st four days of each model simulation, the fish were considered yolk sac larval fish. Over this period, the larval fish grew at a standard rate of 0.032g/g/day (Granet 2000, McNaught 2002, Edwards 2010) and were not subject to starvation (Gordon 1982, Manning et al. 2014).

2.7 Inputs

Model inputs included a daily water temperature function (ºC) and prey and predator length (mm) and density (# individuals / mL) which is further described in Section 2.8: Submodels.

2.8 Submodels

2.8.1 Lake Temperature

The temperature (Equation 2; T, ºC) of Lake Michigan was calculated for each day beginning June 1st based on average surface temperatures collected from 1992 to 2013 by the Great Lakes Surface Environmental Analysis (Great Lakes CoastWatch 2014). All individuals were subjected to the same lake temperature on a given day.

$$T = 9.86\text{e} - 06 * day^3 - 8.74\text{e} - 03 * day^2 + 2.42 * day - 192.77 \quad (2)$$

where day corresponds to the corresponding day number (January 1 = 1, June 1 = 151).

2.8.2 Prey Community

Calanoid and cyclopoid copepods, nauplii, rotifers, *Bosmina*, and *Daphnia* densities in Lake Michigan near Frankford, MI were obtained from field data (Granet 2000, McNaught 2002, Edwards 2010). The field sampling was conducted by duplicate zooplankton tows at 3, 6 and 9m below surface in June, July and August from 1998 to 2002. The resulting zooplankton density data from the field collection was highly variable, perhaps because zooplankton populations tend to distribute into highly dense patches (Young et al. 2009). Zooplankton patches were reported to be up to 1000 times greater in density than mean sample densities (Folt et al 1993; Omori & Hamner 1982, Mackas et al. 1985). Therefore, to accommodate patchiness, we included a patchy distribution of prey items by fitting a negative binomial probability distribution (Young et al. 2009) to zooplankton density data collected from Lake Michigan (Granet 2000, McNaught 2002, Edwards 2010). Parameters for the distribution of each prey type (Table 5) were determined using a maximum likelihood estimator and the solver function in Microsoft Excel®.

On Day 5, the first day of feeding, the larval fish were assigned a zooplankton density using a random negative binomial number generator. Once the patch exhaustion time was

reached, each larval fish was randomly assigned new prey densities drawn from the negative binomial distributions and a new patch exhaustion time was assigned.

Table 5: Fitted parameters for a negative binomial prey density probability distribution and associated log likelihoods

	Parameter		Log
Prey Item	p	s	Likelihood
Calanoid	0.17	1.00	-271.48
Cyclopoid	0.24	1.00	-234.37
Daphnia	0.25	1.00	-228.48
Bosmina	0.09	1.00	-335.251
Nauplii	0.08	1.00	-357.264
Rotifer	0.01	1.00	-551.16

Prey length (PreyLen, mm) encountered by each larval fish was randomly chosen from a normal distribution using mean and standard deviations obtained from Fulford et al. (2006b). Prey mass (PreyW, g) was calculated based on PreyLen and also derived from length weight relationships from Fulford et al. (2006b). Energy for all prey items was assumed to be equal to 400 calories / g (Beletsky et al. 2007).

2.8.3 Foraging

Larval fish swimming speed (Equation 3; SS_{larval}, mm/sec) was derived from a yellow perch laboratory experiment (Houde et al. 1969) and based on larval yellow perch length. SSMult was a multiplier used to incorporate swimming speed effects following MeHg exposure, further detailed in Section 2.5.4: MeHg effects.

$$SS_{larvae} = (54.534 * \ln L - 95.441)\text{*SSMult} \quad (3)$$

Larval fish reactive distance (Equation 4; RD_{larval}, mm) to its prey was a function of the prey's length (Breck & Gitter 1983), which was then used to calculate reactive area (Equation 5; RA_{larval}, mm^2; Letcher et al. 1996, Murphy et al. 2008). Search volume (Equation 6; SV,

mm^3/day) was a function of both swimming speed and reactive area (Letcher et al. 1996, Murphy et al. 2008).

$$RD_{larvae} = Preylen_i/(2 * \text{TAN}\frac{\alpha}{2}) \quad (4)$$

where

$$\alpha = \frac{e^{(9.14-2.4*\ln L+0.229*\ln L^2)*2\pi}}{(360*60)}$$

$$RA_{larvae} = RD_{larval}{}^2 * \pi * 0.5 \quad (5)$$

$$SV_{larvae} = SS_{larval} * RA_{larval} \quad (6)$$

Mean daily encounter rate (Equation 7; ERmean, #/ml) of larval fish to prey was a function of search volume and prey density (Letcher et al. 1996, Murphy et al. 2008). Realized encounter rate (ER_i) was calculated based on a Poisson distribution of the mean encounter rate.

$$ERmean_i = \frac{SV_{larvae}*Preyden_i}{1000} \quad (7)$$

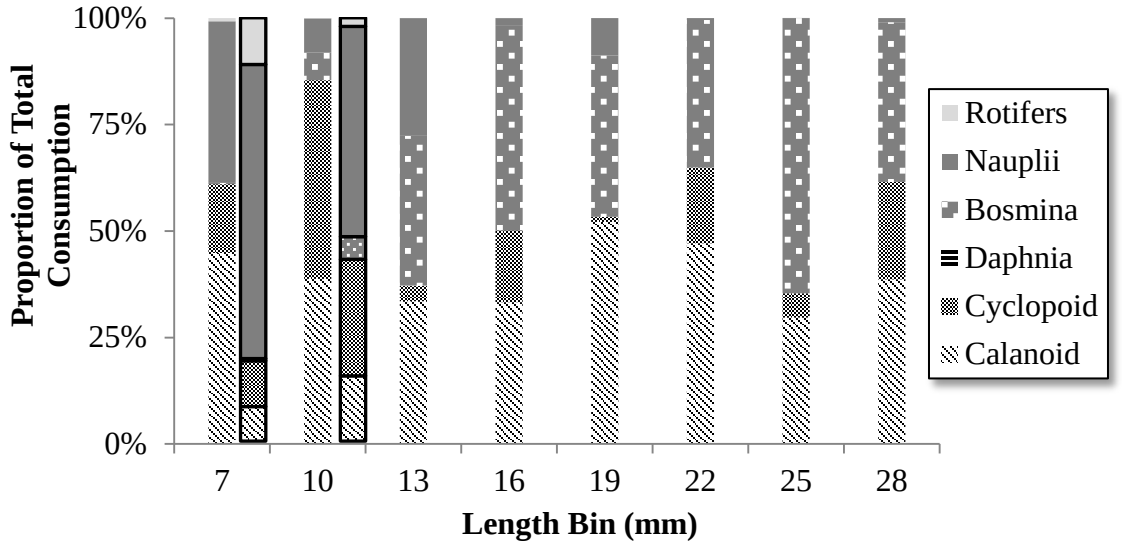

Figure 19: Proportion of prey items in larval yellow perch diets by length following an individual based model simulation for Lake Michigan and comparison to data (highlighted in black) collected from Lake Michigan from 1998 to 2002. Field data from Granet 2000, McNaught 2002 & Edwards 2010.

Prey item selectivity's (Chesson's α) for a given larval fish length were obtained from Fulford et al. (2006b) and slightly modified. In their study, they did not observe a size dependent selectivity for nauplii and therefore set Chesson's α for nauplii constant at 0.07. Using the Chesson's α for nauplii from Fulford et al. (2006b), our modeled diet did not match the observed diet from the field data (Granet 2000, McNaught 2002, Edwards 2010) for larval yellow perch in Lake Michigan as newly hatched fish < 7mm in our simulations ate primarily rotifers (49% of the diet) and only 1% of the diet consisted of nauplii (Figure 34; Appendix). In comparison, there was a strong preference for nauplii (70% of the diet) by newly hatched larval fish up to about 10 mm in length and rotifers only consisted of 11 % of the diet in the field data (Figure 19). Therefore, we adjusted the Chesson's α parameter values for nauplii and rotifers (Equation 8 and 9, respectively; Figure 34; Appendix). Using these new Chesson's α for nauplii and rotifers, the modeled newly hatched larval fish ate more nauplii (38% of diet) than rotifers (1% of diet).

$$\text{Chesson } \alpha_{\text{Nauplii}} = 1300 * \text{L}^{-4.5} \quad (8)$$

$$\text{Chesson } \alpha_{\text{Rotifers}} = 3870 * \text{L}^{-7.64} \quad (9)$$

Probability of attack and capture (Equation 10; $Pcap_i$) for each prey type was dependent upon selectivity and prey density where i = prey item number and n = total number of prey items (Letcher et al. 1996, Murphy et al. 2008). FeedMult was a multiplier used to incorporate laboratory derived effects of foraging efficiency following MeHg exposure (detailed in Section 2.5.4: MeHg Effects).

$$Pcap_i = \left(\frac{\frac{Chesson's\ \alpha_i}{PreyDen_i}}{\sum Chesson's\ \alpha_{i,n}}\right)\text{*FeedMult} \quad (10)$$

Handling time of each captured prey type (Equation 11; HT_i, sec) was a function of both prey length and larval fish length (Letcher et al. 1996, Murphy et al. 2008).

$$HT_i = e^{0.264*10^{7.0151*\frac{Preylen_i}{L}}} \quad (11)$$

The total number of successful encounters within a prey type ($SucEnc_i$) was calculated as a binomial deviate similar to previous IBMs (Letcher et al. 1996, Murphy et al. 2008) with probability = capture success and trials = encounter rate . Total time spent foraging (Equation 12; $Forage_{Time}$, sec) was a function of encounter rate, capture success and handling time where *Active* was the number of hours (12, Fulford et al. 2006b) larval yellow perch are active throughout a 24 h period.

$$Forage_{Time} = \sum(\frac{ER_i}{60*60*Active} * Pcap_i * HT_i) \quad (12)$$

The actual number of prey eaten within a prey type (Equation 13; $ActualEat_i$) depended on the number of successful encounters and total time spent foraging (Letcher et al. 1996, Murphy et al. 2008). Daily consumption (Equation 14; Consum, g) was then calculated based on the total number of prey eaten and prey weight (Letcher et al 1996, Murphy et al. 2008).

$$ActualEat_i = \frac{SucEnc_i}{Forage_{Time}} \quad (13)$$

$$Consum = \sum(ActualEat_i * PreyW_i) \quad (14)$$

Larval fish consumption was bound by a maximum consumption rate (Equation 15; Cmax, g). Post (1990) reported maximum consumption values parameter values for young-of-the-year (YOY) and adult yellow perch. We had trouble matching our growth data using the Cmax parameter values reported for YOY yellow perch (Post 1990). Beletsky et al. (2007) had similar issues and reported a better fit using the adult parameter values for larval perch in Lake Michigan. Therefore, we adapted the parameters to fit our observed growth data, further described in Section 2.9: Calibration. The parameter, p, was the observed consumption rate as a proportion of maximum consumption rate and was dependent upon prey biomass (mg/L; Post

1990). Additionally, maximum consumption was a dependent upon larval fish weight and lake temperature (Kitchell & Stewart 1977) where $F(T)_{C,warm}$ (Equation 1; Appendix) was a temperature dependent function for larval yellow perch consumption (Hanson et al. 1997).

$$Cmax = 0.25 * W^{-0.42} * p * W * F(T)_{C,warm} \quad (15)$$

Where:

$$p = 0.679 * Prey\ Biomass^{0.278}$$

2.8.4 Bioenergetics

A bioenergetics model was incorporated into the IBM and was modified from previous models for yellow perch (Kitchell & Stewart 1977, Fulford et al. 2006a, Fulford et al. 2006b), Atlantic croaker (Murphy et al. 2008) and a generic ocean larval fish (Letcher et al 1996). Standard metabolic rate (Equation 16; SMR, g/d) was calculated based on the larval fish weight (Fulford et al. 2006a).

$$SMR = 0.0065 * W^{-0.2} \quad (16)$$

Total respiration (Equation 17; RM, g/d) was then determined from the standard metabolic rate and lake temperature (Fulford et al. 2006b) where $F(T)_R$ (Equation 2; Appendix) was a function for temperature dependence for larval yellow perch respiration (Hanson et al. 1997).

$$RM = SMR * W * F(T)_R \quad (17)$$

Active metabolism (Equation 18; ActMetab, g/24) was calculated based on total respiration and proportion of the day spent active (Fulford et al. 2006a). Assimilation efficiency (Equation 19; AE) was a function of larval fish weight (g) and bound to > 0.5 (Letcher et al 1996, Murphy et al. 2008).

$$ActMetab = (4.4 - 1.0) * Active_H * \text{RM} \quad (18)$$

Where $Active_H$ was the number of hours (12)

the larval fish are active divided by a 24 hour period

$$AE = 0.8 * (1 - \left(0.25 * \left(e^{-0.002*(W-0.00001)}\right)\right)) \quad (19)$$

Total daily ingestion (Ingest, g) was calculated by multiplying total consumption and assimilation efficiency (AE) similar to previous larval fish IBMs (Letcher et al. 1996, Murphy et al. 2008). Combined specific dynamic action and excretion costs were assumed to be equal to 30% of ingestion similar to previous IBMs (Letcher et al. 1996, Murphy et al. 2008). Total daily cost (TC, g) was a sum of total respiration, active metabolism and specific dynamic action and excretion. Daily weight change was then calculated by subtracting total costs from total ingestion and multiplying the energy ratio of prey (400 calories/g; Beletsky et al. 2007) to larval yellow perch energy density (600 Cal/g; Fulford et al. 2006a).

Maintenance (Equation 20; Maint, g), the amount of consumption required for weight change to be 0, was calculated based on total respiration, active metabolism and assimilation efficiency (Letcher et al 1996, Murphy et al. 2008). Weight loss (W_{Loss}) occurred if Consumption was less than Maintenance. If weight loss occurred, the actual weight loss was calculated by subtracting submaintanence (Equation 21; Submaint) from ingestion (Murphy et al. 2008) and multiplying by the energy ratio of the prey to larval yellow perch (Beletsky et al. 2007). We implemented a 75% starvation threshold similar to other larval fish IBMs (Letcher et al. 1996, Murphy et al. 2008). A larval fish starved to death if its body weight was less than the starvation threshold multiplied by the fish's maximum body weight. *M50* was defined as the shape of the 50% mortality function (Letcher et al. 1996).

$$Maint = \frac{RM + ActMetab}{1 - 0.30 * AE} \quad (20)$$

$$Submaint = W_{Loss} + TC * (1 - e^{(-(-Maint * \ln\frac{W_{Loss}}{Maint}) * \frac{Consum}{TC}))}) \quad (21)$$

Where:

$$W_{Loss} = (1 - \beta) * W$$

$$\beta = (1 - 0.75)^{\frac{1}{M50}}$$

$$M50 = 1.30 * L$$

2.8.5 Predation

The main predator for larval yellow perch in Lake Michigan is the alewife (Santucci Jr et al. 2014). Additionally, yellow perch have been shown to be cannibalistic (Tarby et al. 1974, Braband 1995). Braband (1995) reported that cannibalism may contribute to the high fry mortality in perch populations. Therefore, this model assumes that these two species are the only predators contributing to predation loss of larval yellow perch within Lake Michigan. Total predator density in Lake Michigan was reported to be 0.045 predators / m^3 (Fabrizio et al. 1997, Fulford et al. 2006a). Therefore, we assumed that alewives are the major predators in the lake and set alewife and yellow perch density to 40 and 5 in the $1000m^3$ volume of water, respectively. These densities were chosen as it allowed our baseline model to achieve a pelagic phase larval yellow perch survival rate between 1 and 2 % (Fulford et al. 2006a). Predator lengths (PredLen, mm) were randomly drawn from a normal distribution with mean = 145 and 150, standard deviation = 10.0 and 5.0 and constrained between 113 – 180 mm and 144 – 157 mm for alewife (Brandt et al. 1987) and yellow perch (Fulford et al. 2006a), respectively. Predator swimming speed (SS_{pred}, mm/sec) was a function of 3 times the predator length (PredLen, mm). Reactive radius of the larval fish encountering the predator (Equation 22; $Rrad_{larval}$, mm) and reactive radius of the predator (Equation 23; $Rrad_{pred}$, mm) were functions of the predator and larval fish length, respectively (Fulford et al. 2006a).

$$Rrad_{larvae} = \frac{2*L}{\pi^2} \quad (22)$$

$$Rrad_{pred} = 0.8 * PredLen \quad (23)$$

Capture probability (Pcap) of larval perch by alewife and yellow perch was derived from the Miller model formula (Fulford et al. 2006a). Mean number of encounters between larval yellow perch and predators (Equation 24; Z, #) was a function of swimming speed and reactive radius of both predator and prey and predator activity where $Active_S$ was number of seconds predators are active in a 24 hour period, 43200, and volume was the modeled water volume (mL).

$$Z = \left(\pi * \left(\frac{Rrad_{Pred}}{Rrad_{Larvae}}\right)^2\right) * \left(\frac{\left(SS_{larvae}{}^2 + 3.0 * SS_{pred}{}^2\right)}{3 * SS_{pred}} * \frac{1e-09}{Volume} * Active_S\right) \quad (24)$$

Realized number of encounters (ZZ) was then calculated based on a Poisson distribution with mean = Z. Predator attack rate (Equation 25) was a function of predator and prey size ratio and lake temperature (Fulford et al. 2006a) where F(T) was derived from temperature dependent parameters for yellow perch and juvenile alewife consumption (Appendix Equation 1 or 3, respectively; Hanson et al. 1997).

$$Alewife\ Attack\ Rate = 0.33 * (-1.2 * \frac{PredLen}{L} + 33.2) * F(T)_{C,cold} \quad (25a)$$

$$Yellow\ Perch\ Attack\ Rate = 0.5 * F(T)_{C,warm} \quad (25b)$$

Probability of attack and capture (Pattack) was equivalent to capture probability multiplied by attack rate. Vulnerability (Equation 26) was a function of probability of attack and capture. The larval fish was then eaten by the predator if a uniform random number (0 – 1) was less than vulnerability (Fulford et al. 2006a).

$$Vulnerability = 1 - (1 - Pattack)^{ZZ} \quad (26)$$

2.8.6 Temperature Effects

Larval yellow perch consumption and respiration rates depended upon the temperature of the water. As a warm water species, yellow perch consumption function $F(T)_{C,warm}$ (Equation 1;

Appendix) was described by Hanson et al. (1997) which defined *CTO* as the optimal water temperature for consumption; *CTM* as the maximum water temperature for which consumption will occur; and *CQ* which approximates a rate at which $F(T)_{C,warm}$ increases over relatively low water temperatures. The temperature dependent respiration function $F(T)_R$ (Equation 2; Appendix) was also obtained from Hanson et al. (1997). *RTM*, *RTO,* and *RQ* held similar definitions as *CTM, CTO and CQ* from the consumption function however were specific to larval yellow perch respiration.

Additionally, we assumed that temperature of the water would also affect predator rates of attack on larval yellow perch. Because alewives are a cold water species, their temperature function [$F(T)_{C,cold;}$ Equation 3; Appendix] differed from yellow perch [$F(T)_{C,warm}$] (Hanson et al. 1997). Additional parameters were needed for the cold-water species temperature function. CQ is the coldest water at which the temperature dependence is a small fraction (CK1) of the maximum consumption rate (Hanson et al. 1997). CTO is the water temperature which corresponds 98 % of the maximum consumption rate (Hanson et al. 1997). CTM is the upper water temperature threshold above CTO at which temperature dependence remains at 98 % of maximum consumption (Hanson et al. 1997). CTL is the temperature above CTM that results in a reduced fraction (CK4) of the maximum consumption rate (Hanson et al. 1997).

2.9 Calibration

The model was calibrated to simulate larval yellow perch growth observed in Lake Michigan (Granet 2000, McNaught 2002, Edwards 2010) so that the mean larval fish reached 30 mm and completed the pelagic phase around 50 days (Beletsky et al. 2007). We calibrated growth rate of the cohort (mm/d) by adjusting the maximum consumption (Cmax; g) for individual larval yellow perch. Using the Cmax parameters reported by Post (1990) for YOY or

adult yellow perch our modeled individuals grew too fast or slow to match our observed data, respectively. Therefore, we incorporated parameters from both Cmax functions in order to fit our observed data (Figure 32; Appendix).

2.10 Validation

In our validation process, we used data collected from Crystal Lake (Benzie County, MI) which included predator type (*Osmerus mordax*) temperature dependence parameters, larval yellow perch prey type densities and lake temperature (Granet 2000, McNaught 2002, Edwards 2010). Once the data was incorporated into the IBM, baseline simulations for Crystal Lake were compared against the yellow perch growth data collected from the lake from 1998 to 2002 (Granet 2000, McNaught 2002, Edwards 2010). Similar to the Lake Michigan data, only comparisons of yellow perch smaller than 20 mm were possible. In the field, a 19 day old larval yellow perch averaged 13.4 mm (0.73 S.D.) in total length which was similar to our modeled 13.2 mm (0.03 S.D.). For further details of the validation results, see Chapter 4 (Dissertation).

3.0 RESULTS

3.1 Baseline Control Simulations:

Shape parameters for the prey density probability distribution (*p* and *s*, Table 5) were obtained using a maximum likelihood estimator and the solver function in Microsoft Excel®. The modeled prey density probability distributions were similar to observed Lake Michigan distributions (Figure 35; Appendix). Modeled mean calanoid copepod density (individuals / L) was 4.84 (± 5.24 S.D.) in comparison to the observed mean density of 4.37 (± 7.37 S.D.). Mean cyclopoid density in the model was 3.36 (± 3.68 S.D.) whereas the observed density was 2.69 (± 3.54 S.D.). Mean *Bosmina* densities were 9.47 (± 9.99 S.D.) and 9.05 (± 15.54 S.D.) in the model and observed, respectively. Modeled mean nauplii density was 11.21 (± 11.89 S.D.)

compared to the observed mean of 11.57 (± 12.55 S.D.). Rotifer mean density in the model was 80.68 (± 82.09 S.D.) and the observed mean density was 84.30 (± 103.55 S.D.). Lastly, *Daphnia* mean densities were 0.03 (± 0.03 S.D.) and 0.02 (± 0.09 S.D.) in the model and observed, respectively.

There was not a statistical difference between observed and modeled diet prey fractions for larval yellow perch total length ranging from hatch to 7 mm or 7 to 10 mm (χ^2 = 1.945 and 0.754, degrees of freedom (df) = 4, p = 0.75 and 0.94, respectively.). Once the larval fish began exogenous feeding on day 5, their simulated diet consisted of 45 % calanoid copepods, 38 % copepod nauplii, 16 % cyclopoid copepods and 1 % rotifers (Figure 19). In Lake Michigan, newly hatched larval perch have been shown to feed predominately on nauplii (69 %), cyclopoid copepods (11 %), calanoid (8 %) and rotifers (11 %) (Figure 19; [Granet 2000, McNaught 2002, Edwards 2010]). By the time they reach 10 mm they switch to a calanoid (50 %), cyclopoid (43 %) and nauplii (7 %) diet. As the larval fish grew in our simulations, they began replacing nauplii with *Bosmina* and by the time they reached 30 mm, the majority (99 %) of their diet was *Bosmina*, cyclopoid and calanoid copepods. A comparison of our model diet results for larval fish larger than 10 mm was not possible as they were not collected in the Lake Michigan survey (Granet 2000, McNaught 2002, Edwards 2010).

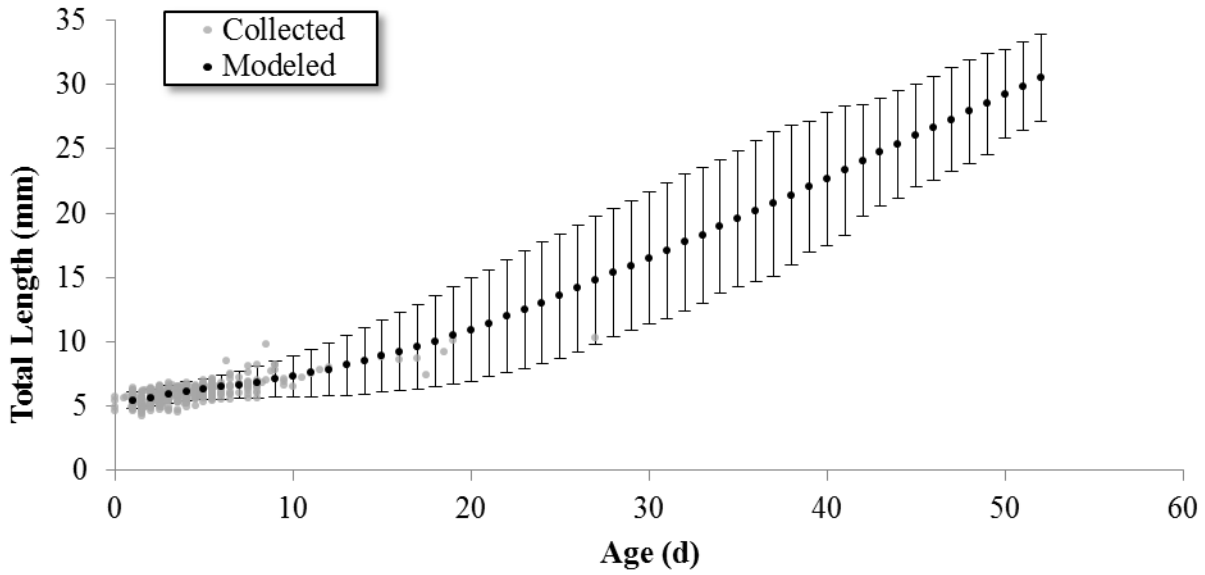

Figure 20: Variability of larval yellow perch growth from a single individual based model simulation and comparison to individual yellow perch collected from Lake Michigan from 1998 to 2002. Simulation started with 10,000 individuals and was absent of MeHg effects. Data shown is mean length for a given day. Error bars are ± 2 standard deviations.

Simulated mean growth rate of larval yellow perch rapidly increased soon after the onset of exogenous feeding, reaching an asymptotic growth rate of 0.65 mm/day by 17 mm of length. Overall, the growth of modeled larval yellow perch was similar to field collected data (Granet 2000, McNaught 2002, Edwards 2010). The growth range of individuals collected from Lake Michigan, with exception to a few individuals, fell within 2 standard deviations of mean growth rate of the 10,000 modeled individuals in a single baseline simulation (Figure 20). On average, it took a larval yellow perch 54.07 days (± 1.15 S.D.) to reach 30 mm with an average growth rate of 0.464 mm/d (± 0.174 S.D.). This mean growth rate was similar to field collections of offshore pelagic larval yellow perch in Lake Michigan (0.36 – 0.52 mm/day; Weber et al. 2011). By Day 19, the average length of a simulated larval yellow perch was 10.0 mm (± 1.71 S.D.) in comparison to the 10.1 mm 19 day old larval fish in Lake Michigan (Granet 2000, McNaught

2002, Edwards 2010). Comparisons to larger yellow perch could not be made as they were not collected in the Lake Michigan survey (Granet 2000, McNaught 2002, Edwards 2010).

The baseline model predicted that 1.46 % (± 0.07 S.D.) of the yellow perch cohort would survive the pelagic stage and transition to the demersal stage. This estimate was similar a previous estimate for the yellow perch pelagic stage (1-2%; Fulford et al. 2006a). Alewife and yellow perch predation contributed to 68.45 % (± 0.47 S.D.) and 8.39 % (± 0.23 S.D.) of the mortality, respectively, for a total predation mortality of 76.85 % (± 0.70 S.D.). Predation by alewife contributed to the greatest decline in number of surviving larval yellow perch followed by starvation and yellow perch predation (Figure 21). Starvation contributed to an additional 21.69 % (± 0.38 S.D.) of total mortality rate.

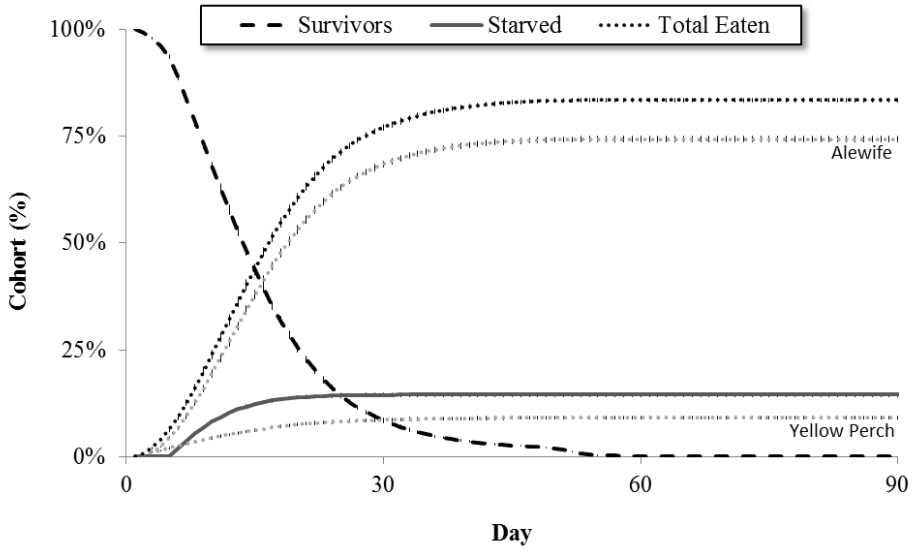

Figure 21: Average cumulative percent of the larval yellow perch cohort surviving, being consumed by a predator (alewife or yellow perch) or starving following individual based model simulations for Lake Michigan; absent of the effects of MeHg. Error bars represent ± 1 standard deviation between five simulation means.

3.2 Effects of MeHg: Swimming Speed

Overall, our model suggests that the reduced swimming speed as a result of MeHg exposure would have minimal effect on larval yellow perch growth rate and subsequent pelagic

phase duration. Simulated average growth rates in the MeHg simulations were similar to the control (0.464 mm/d) when the swimming speed multipliers (absent of the prey capture efficiency multipliers) were incorporated into the model: 0.464 (± 0.002 S.D.), 0.462 (± 0.002 S.D.) and 0.464 (± 0.001 S.D.) mm/d following a simulated exposure to 0.03, 0.10 and 0.30 μM MeHg, respectively (Figure 22A). Additionally, pelagic phase duration was similar to the control: 54.08 (± 0.35 S.D.), 54.44 (± 0.21 S.D.), and 54.09 (± 0.10 S.D.) days for the larval fish to reach 30 mm following exposure to 0.03, 0.1 and 0.3 μM MeHg, respectively (Figure 22B).

Our simulations suggest that the reduced swimming speed would slightly decrease survival compared to the control (1.46%) to 1.39 % (± 0.14 S.D.), 1.35 % (± 0.13 S.D.) and 1.32 % (± 0.11 S.D.) following exposure to 0.03, 0.10, and 0.30 μM MeHg, respectively (Figure 22C). Average simulated starvation rate was reduced in the 0.03 μM MeHg treatment from 21.69 % to 20.17 % (± 0.72 S.D.) and increased to 23.64 % (± 0.44 S.D.) and 23.88 % (± 0.44 S.D.) in the 0.10 and 0.30 μM MeHg treatments, respectively (Figure 22D).

Simulated total predation was increased in the 0.03 μM MeHg treatment from 76.85 % to 78.44 % (± 0.96 S.D.) and decreased to 75.02 % (± 0.66 S.D.) and 74.80 % (± 0.82 S.D.) in the 0.10 and 0.30 μM MeHg treatments, respectively, compared to the control (Figure 22E). Alewife consumed 70.23 % (± 0.62 S.D.), 66.98 % (± 0.36 S.D.) and 66.84 % (± 0.47 S.D.) of the larval yellow perch in the 0.03, 0.1 and 0.3 μM treatments, respectively. Additionally, 8.21 % (± 0.34 S.D.), 8.03 % (± 0.30 S.D.) and 7.96 % (± 0.35 S.D.) of the larval yellow perch were consumed by cannibalistic yellow perch.

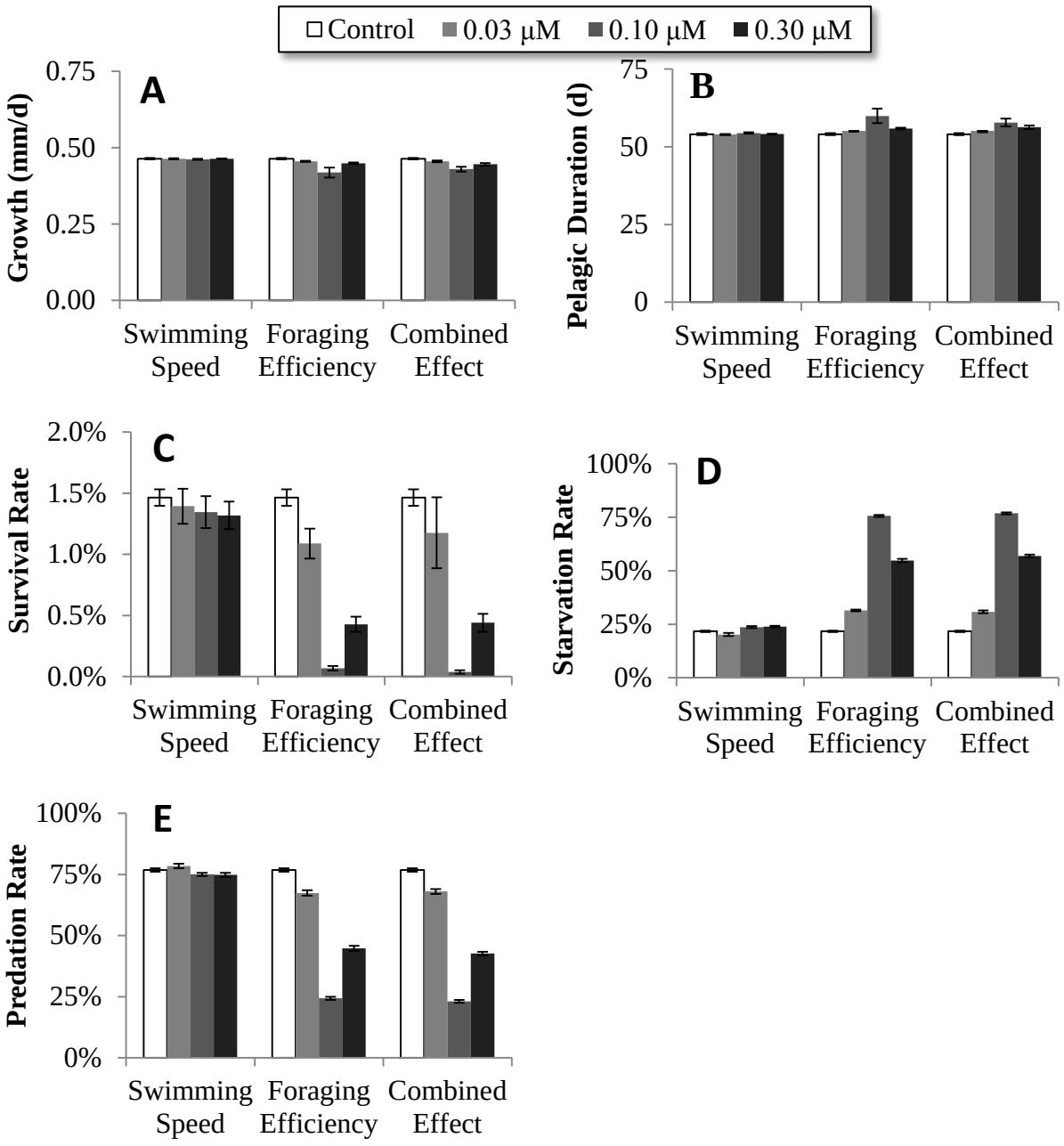

Figure 22. Simulated effects of methylmercury (MeHg) on larval yellow perch mean growth rate (A), pelagic phase duration (B), survival rate (C), starvation rate (D) and predation rate (E). An individual based model was used to incorporate the behavior effects of MeHg derived from a laboratory exposure study (Mora et al. 2015). In that study, newly hatched fish were fed food containing one of four MeHg treatments (A water only control, 0.03, 0.10 and 0.30 µM) for 25 days. After the exposure, swimming speed and foraging efficiencies were measured. Separate simulations were performed looking at the individual effects of swimming speed impairment and foraging efficiency in addition to a combined effect simulation. Five

simulations were conducted. Error bars are presented as ± 1 standard deviation between simulations.

3.3 Effects of MeHg: Feeding Efficiency

Our model suggests reduced feeding ability would have a larger effect on larval growth rate and subsequent pelagic phase duration compared to the reduced swimming speeds. Simulated average growth rates were reduced when feeding multipliers were incorporated (absent of swimming speed multipliers) compared to the control (0.464 mm/d) to 0.455 (± 0.002 S.D.), 0.419 (± 0.016 S.D.) and 0.449 (± 0.002 S.D.) mm/d following an exposure to 0.03, 0.10 and 0.30 μM MeHg, respectively (Figure 22A). On average, our simulations took an additional 1.05 (± 0.22 S.D.), 5.86 (± 2.31 S.D.), and 1.76 (± 0.28 S.D.) days for the larval fish to reach 30 mm following exposure to 0.03, 0.1 and 0.3 μM MeHg, respectively (Figure 22B).

Our simulations suggest that the reduced foraging ability would reduce survival compared to the control from 1.46% to 1.09 % (± 0.12 S.D.), 0.07 % (± 0.02 S.D.) and 0.43 % (± 0.06 S.D.) following exposure to 0.03, 0.10, and 0.30 μM MeHg, respectively (Figure 22C). Average simulated starvation rate was increased from 21.69 % in the control to 31.49 % (± 0.43 S.D.), 75.59 % (± 0.53 S.D.) and 54.77 % (± 0.79 S.D.) in the 0.03, 0.10 and 0.30 μM MeHg treatments, respectively (Figure 22D).

Due to the higher starvation rates, simulated total predation was reduced from 76.85 % in the control to 67.42 % (± 1.06 S.D.), 24.34 % (± 0.69 S.D.) and 44.80 % (± 1.04 S.D.) in the 0.03, 0.10 and 0.30 μM MeHg treatments, respectively (Figure 22E). Alewife consumed 59.99 % (± 0.56 S.D.), 20.45 % (± 0.44 S.D.) and 39.06 % (± 0.79 S.D.) of the larval yellow perch in the 0.03, 0.1 and 0.3 μM treatments, respectively. Additionally, 7.43 % (± 0.51 S.D.), 3.88 % (± 0.25 S.D.) and 5.74 % (± 0.25 S.D.) of the larval yellow perch were consumed by larger yellow perch.

3.4 Effects of MeHg: Combined Effects

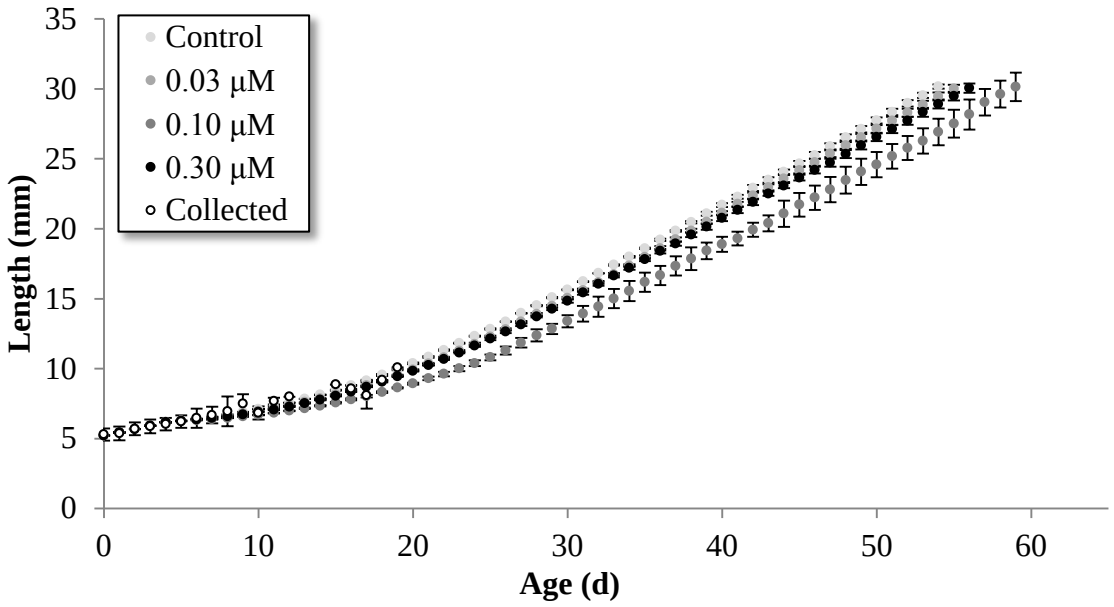

Figure 23: Predicted effects MeHg exposure on mean larval yellow perch growth and comparison to field data from Lake Michigan obtained from Granet 2000, McNaught 2002 & Edwards 2010. Error bars represent ± 1 standard deviation between the mean of 5 IBM simulations.

Overall, simulated average growth rates were reduced when both swimming speed and feeding multipliers were incorporated into the model from 0.464 mm/d of the control to 0.455 (± 0.003 S.D.), 0.430 (± 0.008 S.D.) and 0.446 (± 0.004 S.D.) mm/d following an exposure to 0.03, 0.10 and 0.30 µM MeHg, respectively (Figure 22A). On average our simulations took an additional 1.03 (± 0.42 S.D.), 3.76 (± 1.25 S.D.), and 2.21 (± 0.58 S.D.) days for the larval fish to reach 30 mm following exposure to 0.03, 0.1 and 0.3 µM MeHg, respectively (Figure 23).

Our simulations suggest that the reduced foraging ability and swimming ability would reduce the 1.46% control survival rate to 1.18 % (± 0.18 S.D.), 0.04 % (± 0.01 S.D.) and 0.44 % (± 0.07 S.D.) following exposure to 0.03, 0.10, and 0.30 µM MeHg, respectively (Figure 22C). Average simulated starvation rate was increased from 21.69 % in the control to 30.80 % (± 0.70

S.D.), 76.83 % (± 0.49 S.D.) and 56.90 % (± 0.59 S.D.) in the 0.03, 0.10 and 0.30 μM MeHg treatments, respectively (Figure 22D).

The reduced feeding efficiency and swimming speed resulted in a simulated total predation reduction from 76.85 % in the control to 68.03 % (± 0.99 S.D.), 23.13 % (± 0.60 S.D.) and 42.66 % (± 0.78 S.D.) in the 0.03, 0.10 and 0.30 μM MeHg treatments, respectively (Figure 22E). Alewife consumed 60.48 % (± 0.63 S.D.), 19.21 % (± 0.40 S.D.) and 37.19 % (± 0.58 S.D.) of the larval yellow perch in the 0.03, 0.1 and 0.3 μM treatments, respectively. An additional 7.55 % (± 0.35 S.D.), 3.93 % (± 0.20 S.D.) and 5.47 % (± 0.20 S.D.) of the larval yellow perch were consumed by larger yellow perch, respectively.

4.0 DISCUSSION

Yellow perch populations within Lake Michigan have experienced poor recruitment due to an inadequate food supply, predation by alewife and other limiting environmental factors (Dettmers et al. 2003, Clapp & Dettmers 2004, Santucci Jr et al. 2014) including suboptimal water temperatures for larval yellow perch consumption (Hanson et al. 1997, Great Lakes Coastwatch 2014). Coupling these known stressors with exposure to MeHg, our model suggests that contaminant impairment of larval fish behavior may be another factor contributing to failed recruitment of yellow perch populations in systems with high MeHg exposure. The results from our model suggest that exposure to high concentrations of MeHg may reduce larval fish growth and cohort survival through impaired swimming and foraging. When accounting for reduced swimming speed and foraging efficiency, exposure to the 0.1 μM MeHg treatment resulted in a near collapse of the larval yellow perch cohort with an average of only 4.0 (± 1.5 S.D.) of the initial 10,000 fish surviving to the demersal larval stage.

Interestingly, the 0.3 μM MeHg treated larval yellow perch in the Mora et al. (2015) study exhibited a higher foraging efficiency and swimming speed than the 0.1 μM MeHg treated fish. This U-shaped dose response curve was also found in several genes that were measured as a part of the study (Mora et al. 2015) including genes specific to circadian clock timing (*cry1a*, *per3*), solute carriers (*slc1a2a*), ATP binding (*prkacbb*) and photoreceptor function (*opn1lw1*). Additionally, Mora et al. (2015) revealed an inverted U-shaped dose response in zebrafish feeding efficiency and swimming speed and the expression of the genes previously mentioned following exposure to lower concentrations of MeHg. Therefore, it is possible that compensatory mechanisms are activated during the 0.3 μM MeHg exposure in yellow perch.

Growth depends on a variety of factors occurring at the level of the individual including prey encounters, swimming speed and environmental stressors (i.e. contaminant exposure). With reduced prey densities in Lake Michigan due to invasive species such as the zebra mussel and alewife (Shroyer & McComish 2000, Marsden & Robillard 2004), exposure to contaminants that impair foraging ability may lead to significant losses of individuals in the population through starvation. Even small reductions in mean growth rate of individuals within a cohort can lead to significantly lower survival (Rice et al. 1993) due to a prolonged pelagic phase and increased predation and/or starvation rates (Rice et al. 1993, Fulford et al. 2006a). Additionally, lower growth rates may reduce the energy supply needed to trigger the switch from pelagic to demersal stage thereby extending the pelagic planktonic phase of larval fish (Searcy & Sponaugle 2000). Our simulations suggest that 0.03, 0.10 and 0.30 μM MeHg exposure would reduce larval perch growth rate by only 0.01, 0.03, and 0.02 mm/d, respectively (Figure 22B). If we assume the pelagic phase ends when the larval fish reaches 30 mm, our simulations suggest the 0.03, 0.10 and 0.30 μM MeHg exposure would extend the larval yellow perch pelagic phase by 1.03, 3.76,

and 2.21 days, respectively, thus prolonging susceptibility to pelagic predation and starvation (Figure 22).

Variability in behavior at the level of the individual can be important in driving overall system dynamics and would be overlooked using more traditional aggregated population models. IBM's can incorporate individual variability making them a useful tool for estimating sublethal effects of contaminants on populations (Harvey & Railsback 2007, Murphy et al. 2008). For example, the foraging efficiency replicate data (Figure 18B) in the 0.10 μM MeHg treatment ranged from 0.06% to 74% in comparison to the average control treatment (Mora et al. 2015). Incorporating this variability into the model, our results suggest that a 0.10 μM MeHg exposure would only slightly reduce growth rate (- 0.03 mm/d) yet lead to a high starvation rate (+ 55.1 %) compared to the control. The larval fish that fed at a high foraging efficiency continued to grow similar to that of the controls and avoided starvation where individuals who experienced reduced foraging efficiency starved early in the simulation (Figure 21).

The increased starvation rate of pelagic larval yellow perch in our MeHg simulations resulted in a reduced total predation rate (Figures 22C and 22D). Our simulations suggest that exposure to 0.03, 0.10 and 0.30 μM MeHg would reduce the total predation rate of pelagic larval yellow perch by 11.6, 70.0 and 44.5 %, respectively, relative to the control. Fleeger et al. (2003) suggested that changes in predator-prey relationships are a common indirect effect of contaminant exposure. As an important component to the trophic cascade in the pelagic community, decreases in larval fish density may lead to changes in other parts of the trophic cascade (Fleeger et al. 2003). For example, if larval fish density decreased as a food source due to MeHg exposure, pelagic predators, such as alewives, may shift their diet to include more zooplankton potentially increasing the food limitations on any surviving larval fish.

Our study explored concentrations of MeHg higher than is typical for Lake Michigan. Previous studies reported Lake Michigan mean total Hg values for zooplankton with 54.3 ppb (11 to 376 ppb; McCarty et al. 2004), YOY yellow perch with 11.3 ppb (9.4 to 31 ppb; Brazner & DeVita 1998) and adult yellow perch fillets with 110 ppb (49 to 440 ppb; Wiener et al. 2012). The larval fish from the lowest treatment in the Mora et al. (2015) study averaged 208 (± 190 S.D.) ppb, nearly 7 times higher than the maximum Hg concentration for YOY yellow perch and similar to adult yellow perch tissues in Lake Michigan. However, the Hg in replicates from the Mora et al. (2015) low MeHg treatment ranged from 70 to 424 ppb and was environmentally relevant for other areas within the Great Lakes region. For example, YOY yellow perch from the Ottawa River (Canada) were predicted to have a mean Hg concentration of 82 ppb (Trudel & Rasmussen 2001). Emissions of Hg are expected to increase due to the expansion of coal-fired electricity generation in developing countries, unless emission controls are adopted (Driscoll et al. 2013). Therefore, we suggest that continued monitoring of both adult and larval fish tissue Hg concentrations is needed to determine if their tissues are approaching MeHg concentrations similar to those tested in this study found to impair larval yellow perch behavior which may lead to reduced cohort survival in Lake Michigan.

It is possible that larval yellow perch in Lake Michigan are experiencing adverse behavior effects following low MeHg exposure, below the concentrations tested by Mora et al. (2015) and used in this study. For example, larval Mummichog (*Fundulus heteroclitus*) exposed to 10 ppb MeHg for 14 days post hatch (dph) experienced reduced prey capture efficiency (Zhou et al. 2001). Additionally, prey capture efficiency was reduced in mummichog following exposure to 5 ppb MeHg as embryos and for 14 dph. A future study should be conducted to determine effects of a low (ppb) MeHg exposure on larval yellow perch behaviors.

Often, environmental systems experience a multitude of stressors, both from natural and anthropogenic sources, and the cumulative effects of these stressors may contribute to significant outcomes for those populations inhabiting these systems. Larval fish in Lake Michigan are exposed to other contaminants in addition to MeHg. For example, Brazner & DeVita (1998) reported that yellow perch collected from Green Bay, Lake Michigan had tissue contaminant concentrations of total Hg (up to 80 ppb), polychlorinated biphenyls (PCBs; from 6 to 1076 ppb) and dichlorodiphenyl dichloroethylene (DDE; from 1.5 to 31.3 ppb). Injections of a PCB congener (100 ppb) was reported to reduce swimming performance of adult rainbow trout after 9 days post injection (Bellehumeur 2010). Similarly, exposure to 1 ppb DDT, the parent compound of DDE, for 7 days altered schooling behaviors and reduces predator avoidance in goldfish (Weis & Weis 1974). Our study only incorporated the effects of a single contaminant on larval fish behavior and how these effects transition to the population. Further investigation should be conducted to determine how mixtures of these contaminants at environmentally relevant concentrations alter larval yellow perch behaviors. Our model could then incorporate these mixture effects and determine how these contaminants within Lake Michigan are affecting survival and growth of larval yellow perch.

Overall the simulated the growth rate was similar to field data (Granet 2000, McNaught 2002 & Edwards 2010) and a previous IBM (Fulford et al. 2006b) for pelagic larval yellow perch. We had to adjust the Chesson's α selection indices for nauplii and rotifers in order to force the newly hatched fish to consume nauplii and match the field data. If some prey types, such as soft-bodied rotifers, are digested faster than others, field measured diets based on gut analyses may be biased (Fulford et al. 2006b). Comparison of diets for fish greater than 10 mm was not possible as they were absent in the field data. Future work should aim to characterize the diets of

larger pelagic yellow perch in order to validate our model's diet results. The model could then be used to track how changes in prey community density may impact the foraging behaviors of larval yellow perch.

Several assumptions were made in this model. For example, we assumed that the energy density is equal between all prey types and size ranges (Beletsky et al. 2007). Future work should aim to characterize the energy density for each specific prey type which would increase the model's utility to determine potential impacts of prey community shifts. Additionally, we assumed prey patches containing a higher density of prey would exhaust similar to less dense patches. It has been hypothesized that larval fish rely on finding dense patches of prey in order to grow and survive (Young et al. 2009). If prey patch exhaustion is positively correlated with the density of the prey items, our model may over estimate starvation rates. Lastly, total predator density was set equal to the 45 individuals per 1000 L density reported by Fulford et al. (2006a) however we assumed that alewives are found in much higher density (40 individuals per 1000 L) over yellow perch (5 / 1000 L). Abundance of age 3 + alewife peaked in 2002 but steadily declined afterwards (Tsehaye et al. 2014) and remained low through 2011. If predator densities are lower than the estimate we used in the model we would expect larval yellow perch survival to increase. Future studies should focus on testing these predator-prey assumptions and their validity.

We used data obtained from Mora et al. (2015) who assessed the effects of MeHg on larval yellow perch feeding efficiency and swimming speed. In that study, the authors evaluated swimming speed effects on the individual but, due to feasibility, evaluated feeding efficiency effects on replicates containing thirty larval fish. Ideally, it would be best to evaluate effects on the individual, which would allow our IBM to incorporate natural variability to more accurately

scale these effects from the individual to the population. Additionally, this IBM did not consider learning ability associated with prey and predator interactions. The inclusion of a learning mechanism is important as it is likely that these processes are developed through cognition and not strictly a size-specific or density recognition process (Dill 1983) as we assumed using the Chesson's α prey selectively. Additionally, prenatal MeHg exposure has been shown to reduce cognitive performance in children (Grandjean et al. 1998). This may be another mechanism contributing to failed recruitment in larval fish populations exposed to MeHg, specifically if a larval fish is unable to determine that a particular prey item is too big to eat and wastes time and energy trying to capture these items. Incorporating these variables may help the IBM predict population effects of neurotoxic contaminants more accurately.

Our model incorporated sublethal effects of MeHg on larval fish swimming and foraging behavior into an IBM and scaled these effects to the population. Our results suggest impairment of these behaviors can lead to recruitment effects yellow perch in Lake Michigan. Our next step (Chapter 4: Dissertation) is to assess multiple stressors including both biotic and abiotic factors (Lake temperature, predation, low forage base) to determine which factors are specifically leading to the estimated low survival rates (< 2 %) of pelagic phase larval yellow perch in Lake Michigan.

CHAPTER 4

YELLOW PERCH RECRUITMENT IN LAKE MICHIGAN II: EXPLORING IMPACTS OF HABITAT ON PELAGIC LARVAL FISH GROWTH AND SURVIVAL

ABSTRACT

The low recruitment of yellow perch in Lake Michigan has been attributed to several components, some that include a declining prey base, intense predation by the exotic alewife and sub-optimal water temperature. In other similar aquatic systems that are free of alewife predation and also have a higher quality zooplankton community, such as Crystal Lake (Benzie County, MI), larval yellow perch experience faster growth rates and maintain higher densities. Other components contributing to differences observed between the systems could include temperature as the cold water temperatures of Lake Michigan may hinder the growth process of warm water species, such as the yellow perch, compared to warmer waters often found in inland lakes. To explore which ecological component(s) may be contributing to the low yellow perch recruitment in Lake Michigan, we used an individual based model (IBM) specific to pelagic phase larval yellow perch. The model was calibrated to simulate real-life conditions in Lake Michigan and nearby Crystal Lake. Overall, our model suggested that suboptimal water temperatures were the main component driving slow growth rates of larval yellow perch whereas alewife predation contributed to low survival rates. The reduced forage base did not have a major effect on either growth rate or survival of larval yellow perch in our simulations. Each individual component only explained a small portion of the overall lower growth and survival rates experienced by larval yellow perch in Lake Michigan compared to Crystal Lake. Our simulations highlighted a synergistic effect between warmer water temperatures and predatory temperature thresholds which created a refuge in Crystal Lake. This predation free refuge resulted in a more stable yellow perch population in Crystal Lake compared to Lake Michigan. When these biotic and

abiotic stressors were coupled with a contaminant stressor, methylmercury, the larval yellow perch cohort experienced reduced growth and higher mortality, but were more likely to survive the exposure in Crystal Lake compared to Lake Michigan. These IBM simulations highlight the importance of evaluating the effects of complex mixtures of stressors from a variety of abiotic and biotic sources in aquatic systems.

1.0 INTRODUCTION

Yellow perch, *Perca flavescens*, are native to the Great Lakes region (Fuller & Neilson 2015) and are ecologically and economically important in Lake Michigan (Wells & McLain 1972, Santucci Jr et al. 2014). They are a highly prized sport fish and historically supported a commercial fishery throughout the lake (Wells & McLain 1972, Clapp & Dettmers 2004, Santucci Jr et al. 2014). Yellow perch play an integral role in the lake by linking the nearshore and pelagic food webs (Clapp & Dettmers 2004) and serving as an important prey item for piscivorous fish and wildlife (Wiener et al. 2012).

Historically, yellow perch were abundant throughout the shallow areas of Lake Michigan (Wells & McLain 1972); however their populations declined in the early 1990's (Clapp & Dettmers 2004, Santucci Jr et al. 2014) due to consecutive year-class failures (Dettmers et al. 2003, Clapp & Dettmers 2004, Santucci Jr et al. 2014). These failures may be attributed to low larval fish food availability (Dettmers et al. 2003) as recent sampling of the zooplankton community within Lake Michigan has shown very low abundances of preferred yellow perch prey items and higher abundances of less preferred prey (Granet 2000, McNaught 2002, Edwards 2010). Other factors that may be responsible for the yellow perch decline include food web alterations following the introduction of the zebra mussel (Wells & McLain 1972, Marsden & Robillard 2004), increased predation following the introduction of the alewife (Shroyer &

McComish 2000), and other abiotic and biotic factors (Clapp & Dettmers 2004). Additionally, growth and survival rates of larval fish can be affected by their environment including sub-optimal water temperatures (Kitchell & Stewart 1977, Wang & Eckmann 1994) and, as I explored in Chapter 3, exposure to contaminants.

Exotic introductions of predators have also had drastic effects on the pelagic communities in the Great Lakes region (Crowder 1980, Mercado-Silva et al. 2006, Creque & Czesny 2012). Rainbow smelt (*Osmerus mordax*) were one of the first exotic invasions in Lake Michigan (Crowder 1980). They were originally stocked in Crystal Lake (Benzie County, MI) in 1912 and then became established in Lake Michigan by the early 1920's (Van Oosten 1937, Crowder 1980). Rainbow smelt have been known to out-compete native species for similar food resources such as zooplankton (Hrabik et al. 1998). Predation of native larval fish by the exotic rainbow smelt has been linked to native species extirpation in other systems (Hrabik et al. 1998).

Alewife (*Alosa pseudoharengus*) invaded Lake Michigan in the early 1950's (Miller 1957, Crowder et al. 1980). In the late 1980's, alewife abundance in Lake Michigan increased from a low catch-per-unit-effort (CPUE) of 11.6 individuals per hour in 1988 and reaching a peak CPUE in 1996 of 156.1 individuals per hour (Shroyer & McComish 2000). Recently, Warner et al. (2014) sampled the pelagic prey community of Lake Michigan and reported that alewives were over 4 times more abundant than rainbow smelt. Similar to rainbow smelt, alewives compete with native fish for resources and their predation on larval stages of native fish can be attributed to population declines (Crowder 1980, Creque & Czesny 2012).

Around the same time of the alewife abundance increase in Lake Michigan, mean zooplankton density and larval yellow perch abundances declined. In 1988, southern Lake Michigan was observed to have a mean zooplankton density of over 600 individuals per L and by

1996 the density was less than 10 individuals per L (Dettmers et al. 2003). Similarly, two year old yellow perch recruitment was highest in 1984 with a mean CPUE of 919 individuals per hour but declined to a low CPUE of 1.2 individuals in 1992 (Shroyer & McComish 2000). Alewives are the primary predator of pelagic zone larval yellow perch in Lake Michigan (Crowder 1980, Shroyer and McComish 2000, Fulford et al. 2006a) and it has been suggested that predation of yellow perch is the main driving force behind yellow perch year-class strength (Dettmers et al. 2005)..

Comparisons between neighboring systems have been previously used to highlight habitat influences on important population metrics such as species abundance and diversity and individual age composition, growth, and fecundity (Fritz & Garside 1975, Stone et al. 1979, Parker et al. 2009, Froehlich & Kline 2015). For example, Granet (2000), McNaught (2002) and Edwards (2010) evaluated prey community density and temperature differences between Lake Michigan and nearby Crystal Lake (Benzie County, MI) and how individual habitat components may have influenced diet and growth in larval yellow perch. They found that larval yellow perch in Crystal Lake had a higher abundance of prey items in their guts which correlated with the higher density of preferred prey in the lake. Additionally, larval yellow perch in Crystal Lake were observed to have a faster growth rate than those sampled from Lake Michigan. From these studies, it was concluded that the higher density of more preferred prey types and warmer water temperature lead to improved yellow perch recruitment in Crystal Lake compared to Lake Michigan.

Collecting and comparing data from two similar but separate systems can help highlight correlations between individual habitat components and population metrics. However, to achieve a more mechanistic understanding, the data could also be incorporated into a calibrated model to

determine which component(s) are most influential and how several habitat components may interact with one another to affect a cohort's survival and growth. Individual-based models (IBMs) are a useful tool to conduct these types of comparisons as they can create plausible mechanistic links between the lake environment and larval fish survival by sequentially adding in potentially important components to the model (Fulford 2003). For example, Fulford et al. (2006b) used an IBM to compare yellow perch populations between Lake Michigan and Green Bay and concluded that the prey community composition differences between the two systems affected larval yellow perch diet, growth and survival. In our approach, we wanted to add more complexity to a larval model and to be able to draw comparisons of lake temperature, predation and prey density between two populations of larval yellow perch. We chose to compare Lake Michigan and nearby Crystal Lake (Benzie County, MI) yellow perch populations using the large data set obtained from Granet (2000), McNaught (2002), and Edwards (2010).

Crystal Lake (Benzie County, MI) is a large (4000 hectares), deep (maximum depth of 50m) inland lake (Tonello 2015). It supports a more abundant yellow perch population than Lake Michigan. On average, from 1998 to 2002, larval yellow perch were nearly 5 times more dense in Crystal Lake (0.55 fish / m^3 ± 0.46 S.D.) than Lake Michigan (0.12 fish / m^3 ± 0.24 S.D) (Granet 2000, McNaught 2002, & Edwards 2010). Additionally, the yellow perch in Crystal Lake were observed to grow at a faster rate (0.40 mm / day) than those in Lake Michigan (0.21 mm / day) (Granet 2000, McNaught 2002, Edwards 2010). Survival rates for pelagic larval yellow perch in Lake Michigan have been estimated between 1 – 2 % (Fulford et al. 2006a) where survival in smaller inland lakes have been reported to be as high as 26 % (Dahlberg 1979).

Table 6: Comparison of mean surface water temperature and yellow perch prey type densities between Lake Michigan and Crystal Lake (Benzie County, MI). Numbers in parentheses indicate standard deviation of the mean. Data obtained from Granet 2000, McNaught 2002, Edwards 2010, Great Lakes Coastwatch 2014.

Ecological Component	Lake	
	Michigan	Crystal
Mean Temperature (^{o}C)	17.84 (3.59)	21.07 (2.54)
Total Prey Density (#/L)	114.16 (138.93)	85.68 (111.91)
Daphnia	0.02 (0.09)	0.97 (3.74)
Calanoid	4.37 (7.37)	9.61 (12.54)
Cyclopoid	2.69 (3.54)	6.53 (8.43)
Bosmina	11.21 (11.88)	2.29 (3.36)
Nauplii	11.57 (12.55)	13.90 (16.10)
Rotifer	84.3 (103.5)	52.38 (67.74)

Differences in ecological components such as prey composition, predator type and lake temperature may be contributing to the lower growth rate and survival of yellow perch in Lake Michigan relative to Crystal Lake (Tables 6 and 7). Being a smaller lake, Crystal Lake has a warmer mean surface water temperature than Lake Michigan throughout the larval pelagic period of yellow perch (Granet 2000, McNaught 2002, Edwards 2010, Great Lakes Coastwatch 2014). Because yellow perch are a warm water species, the warmer water temperatures in Crystal Lake likely contribute to faster growth rates than Lake Michigan due to temperature dependence on consumption (Hanson et al. 1997). Additionally, Crystal Lake supports a higher density of larger, more preferred prey items, such as *Daphnia*, *Bosmina*, and calanoid copepods, than Lake Michigan (Granet 2000, McNaught 2002, Edwards 2010). In comparison, Lake Michigan has a higher density of smaller, less preferred prey such as cyclopoid copepods and rotifers. Finally, alewives have yet to invade Crystal Lake (Tonello 2015). The main predator of larval yellow perch in Crystal Lake is the exotic rainbow smelt (Granet 2000, McNaught 2002, Edwards

2010). Rainbow smelt have a narrower temperature threshold for consumption of prey items, including larval fish, as they do not feed at temperatures above 18 °C, in comparison to 25 °C for alewives (Hanson et al. 1997). Crystal Lake's yellow perch population may be under less predation constraint than those populations in colder Lake Michigan as a result of its higher temperatures. We used an IBM for pelagic larval yellow perch detailed in Chapter 3 (Dissertation) to explore the contributions of water temperature, predator type or prey composition and composition components to larval yellow perch survival and growth.

Additionally, contaminants could play a role in larval yellow perch recruitment as discussed in Chapter 3 (Dissertation); exposure to high concentrations of methylmercury (MeHg) were shown to adversely affect larval yellow perch swimming speed and foraging efficiency (Mora et al. 2015). Suboptimal habitat conditions have been shown to reduce tolerances of macroinvertebrates to various contaminant exposures (Thrush et al. 2008). Adult yellow perch collected from Crystal Lake had similar total Hg concentrations in their fillets (0.12 to 0.24 ppm) as those collected in Lake Michigan (Grand Haven, MI: 0.12 to 0.25 ppm) (MDEQ 2013). As an additional stressor, I used the IBM to determine if the differences in habitat between Lake Michigan and Crystal Lake could have an effect on growth and survival of larval yellow perch exposed to similar MeHg concentrations.

Table 7: Parameter values for main predator of larval yellow perch in either Lake Michigan (A) or Crystal Lake, MI (B). Where CTO is the optimal water temperature for the predator species. CTM, CTL, CQ, CK1 and CK4 are shape parameters of the temperature dependence function for cool water species. Swimming speed was assumed to be three times the predator length (Letcher et al. 1996, Murphy et al. 2005). Temperature parameters were obtained from Hanson et al. (1997). Predator length data was obtained from Fulford et al. 2006a and Tonello 2015.

	Predator	Parameter		Value
A	Alewife *Alosa pseudoharengus*	Length (mm)	Avg	145
			S.D.	10
		Temperature Dependent Consumption	CTO	16
			CTM	18
			CTL	25
			CQ	3
			CK1	0.17
			CK4	0.01
		Swimming Speed (mm/sec)		3*Len
		Density (#/m^3)		0.04
B	Rainbow Smelt *Osmerus mordax*	Length (mm)	Avg	141
			S.D.	10
		Temperature Dependent Consumption	CTO	14
			CTM	16
			CTL	18
			CQ	3
			CK1	0.4
			CK4	0.01
		Swimming Speed (mm/sec)		3*Len
		Density (#/m^3)		0.04

2.0 METHODS

2.1 Yellow perch life history

Yellow perch are relatively short-lived, typically living 7 years, and they reach sexual maturity by 3 years (Wydoski & Whitney 2003). Adult yellow perch migrate to the shallow nearshore zones of Lake Michigan to spawn (Miehls & Dettmers 2011) with a preference towards rocky substrates (Goodyear et al. 1982, Beletsky et al. 2007). Spawning usually begins in mid-May when lake temperatures reach 9.5 °C (Goodyear et al. 1982). An average female lays around 50,000, but may lay up to 158,000 eggs (Brazo et al. 1975).

Following successful fertilization, yellow perch eggs hatch within 10-20 days with the larvae measuring around 5 mm in total length (Granet 2000, McNaught 2002, Fulford 2006a, Edwards 2010). After hatching, the larval fish are transferred in water currents to the limnetic zone (Dettmers et al. 2005) and this transport is believed to help the fish escape intense littoral zone predation (Whiteside et al. 1985). The pelagic phase lasts 30 – 40 days, but can be up to 75 days in larger lakes, such as Lake Michigan (Dettmers et al. 2005, Beletsky et al. 2007). The pelage phase concludes with fish measuring, on average, 30mm in total length, but can be up to 70 mm (Dettmers et al. 2005).

After transport, the pelagic larval fish must locate dense patches of prey in order to survive (Santucci Jr et al. 2014). Zooplankton density within these patches may be up to 100 times the median density of the water column (Megard et al 1997). Larval yellow perch are known to feed on a variety of organisms including small cladocerans, copepods, planktonic crustaceans and rotifers (Fulford et al. 2006a, Fulford et al. 2006b, Miehls & Dettmers 2011). Selectivity for prey items is dependent on fish size with smaller larval yellow perch preferring

rotifers and cyclopoid copepods and larger individuals preferring calanoid copepods, and cladocerans (Fulford et al. 2006b). Once they transition to demersal larvae, they shift their diet towards benthic invertebrates (Forney 1971).

2.2 The Model

A complete model description is provided in Chapter 3. (Dissertation) and followed the overview, design concepts, details protocol for describing individual based models (Grimm et al. 2006, Grimm et al. 2010). Briefly, the non-spatially IBM simulated the growth and survival of a larval yellow perch cohort consisting of 10,000 newly hatched individuals. The model tracked two entities at each time step (1 day): the environmental conditions [water temperature (ºC), prey type density (# individuals per mL), prey type length (mm) and mass (g), prey patch exhaustion time (d), and predator total length (mm) and mass (g)] and larval perch characteristics [total length (mm), mass (g), age (d), alive or mortality type (starvation, predation), prey consumption proportion (%) and prey consumption mass (g)]. Simulations were conducted for 90 days or until all 10,000 individuals experienced a mortality event or completed the pelagic phase by reaching 30 mm in total length. Five replicate simulations were performed to allow for the variation of the model's stochastic parameters, further detailed in Chapter 3 (Dissertation).

2.3 Model Purpose

We used the IBM to investigate how changes in environmental components may contribute to differences in larval yellow perch growth and survival between two systems: Lake Michigan and Crystal Lake (Benzie County, MI). First we ran separate baseline simulations for Crystal Lake and compared to the baseline simulations for Lake Michigan. The baseline simulations were conducted using the lake's corresponding prey composition and water temperature (Granet 2000, McNaught 2002, Edwards 2010) and temperature thresholds for the

lakes predator species (Hanson et al. 1997). Fulford et al. (2006b) presented the utility of an IBM to predict differences in diets and growth of a larval fish cohort between two systems by accounting for differences in a single component, prey composition. We wished to explore this further by comparing several habitat components between Lake Michigan and Crystal Lake systems to see which component had the largest overall effect on larval yellow perch growth and survival. In our approach, we substituted an individual component (prey community density, predator type or lake temperature) from one system into the baseline model for the other system to see how that component affected larval yellow perch survival and growth. Additionally, previous studies have indicated that interactions between habitat conditions and contaminants are likely to occur (Forbes et al. 2003, Lenihan et al. 2003, Thrush et al. 2008) with suboptimal habitats generally leading to a lower contaminant tolerance (Thrush et al. 2008). Therefore, we investigated how multiple biotic and abiotic environmental stressors may affect a larval yellow perch population when an additional stressor, methylmercury (MeHg) is present.

2.4 Crystal Lake Simulation

2.4.1 Temperature

Crystal Lake water temperature (Equation 1; T, ºC) was calculated for each day beginning June 1st based on average surface temperatures collected from 1998 to 2002 (Granet 2000, McNaught 2002, Edwards 2010).

$$T = 9.0\text{e}-06 * day^3 - 8.0\text{e}-03 * day^2 + 2.17 * day - 164.03 \quad (1)$$

where day corresponds to the corresponding day number (January 1 = 1, June 1 = 151).

2.4.2 Crystal Lake Prey Community

Prey densities for Crystal Lake were obtained from Granet (2000), McNaught (2002), and Edwards (2010) which surveyed the lake from 1998 – 2002. The data included zooplankton tows

during the months of June, July and August for each year conducted at 3, 6 and 9 m below surface. Similar to Chapter 3 (Dissertation), patchy distribution of prey items were incorporated into the model by fitting a negative binomial probability distribution. Similar to our Lake Michigan simulations, we assumed patches exhausted between 3 and 14 days (Folt et al. 1993). Maximum likelihood estimate and solver functions in Microsoft Excel ® were used to obtain the distributions parameters for each prey type (Table 8).

Table 8: Fitted parameters for a negative binomial prey density probability distribution and associated log likelihoods

	Parameter		
Prey Item	p	s	Log Likelihood
Calanoid	0.09	1.00	-281.7
Cyclopoid	0.12	1.00	-252.9
Daphnia	0.02	1.00	-390.1
Bosmina	0.25	1.00	-185.0
Nauplii	0.06	1.00	-310.2
Rotifer	0.02	1.00	-417.3

2.4.3 Crystal Lake Predators

Rainbow smelt are the primary pelagic predator of larval yellow perch in Crystal Lake and, to date, alewives have not been introduced in Crystal Lake. The dynamics of rainbow smelt predation are similar to those of alewives detailed in Chapter 3. (Dissertation), however they have different a body size range (Rainbow Smelt [110 to 172 mm], Tonello 2015]; Alewives [113 to 180 mm, Fulford et al. 2006a]) and different temperature threshold for consumption (Hanson et al. 1997; Table 7). Density data for rainbow smelt in Crystal Lake could not be obtained; therefore we assumed that their density is similar to the estimated alewife density for Lake Michigan (0.040 predators / m^3). Assuming equal density allowed us to estimate the effects of predator type (alewife) in Lake Michigan rather than comparing differences of predator density differences between the two lakes. We also assumed that cannibalism from larger yellow

perch exists in Crystal Lake equal to the rate as Lake Michigan and, therefore, set the total predator density to 0.045 predators / m^3 in our simulations (Fulford et al. 2006b). Finally, we assumed the predator speed regardless of predator type was three times its total body length which is an assumption used in other IBMs (Letcher et al. 1996, Fulford 2003, Murphy et al. 2008). Richardson (2004) summarized the literature regarding species specific swimming speeds and similar speeds were reported for alewife (42.6 to 53.5 cm/s) and rainbow smelt (39 – 59 cm/s).

2.5 Determining Habitat Component Influence

Five baseline simulations for Crystal Lake were conducted and compared to the five baseline Lake Michigan simulations (Chapter 3 Dissertation). Next, an individual Crystal Lake habitat component [1. Daily lake temperature; 2. Prey types densities and 3. Predator type and respective consumption based temperature parameters] was substituted for the corresponding Lake Michigan component into the baseline Lake Michigan model. Finally, an individual Lake Michigan habitat component [1. Daily lake temperature; 2. Prey type densities and 3. Predator type and respective consumption based temperature parameters] was substituted for the corresponding Crystal Lake habitat component into the baseline Crystal Lake Model. Five simulations were performed for each substituted habitat component with a different random number seed. Comparisons were made to determine which component(s) had the greatest influence on mean larval yellow perch pelagic phase duration, growth, starvation, predation and survival rates in Lake Michigan and Crystal Lake. Additionally, temperature plays an indirect role in predation as predators are subjected to a temperature dependent attack rate in our model. Therefore, we turned off the temperature dependence on predation [F(T); Equation 25 Chapter 3 Dissertation] to see how the model responded as a means of quantifying potential synergistic

effects between predator type and temperature on larval yellow perch survival. Finally, to help tease out these potential synergistic effects we applied two Crystal Lake variables to the Lake Michigan baseline model. This allowed us to determine if the habitat components may act synergistically or antagonistically to one another.

2.6 MeHg Effects

Similar to Chapter 3 (Dissertation), behavior effect data from a larval yellow perch MeHg exposure study (Mora et al. 2015) were incorporated into the model to estimate the effects of MeHg on a Crystal Lake larval yellow perch cohort. Swimming speed and feeding efficiency multipliers were randomly chosen (further described in Chapter 3 Dissertation) and applied to the 10,000 larval fish in each simulation. Five separate simulations were performed for each MeHg treatment (0.03, 0.10 and 0.30 μM) including a water only negative control.

3.0 RESULTS

3.1 Crystal Lake Baseline Simulations

3.1.1 Diet

Prey density probability distribution shape parameters (*p* and *s*, Table 8) were obtained using a maximum likelihood estimator and the solver function in Microsoft Excel®. The modeled prey density probability distributions were similar to observed Crystal Lake distributions (Figure 36A; Appendix). Simulated mean calanoid copepod, cyclopoid copepod, *Bosmina*, nauplii, rotifer and *Daphnia* density (# individuals / L) was 10.07 (± 10.60 S.D.), 7.02 (± 7.53 S.D.), 2.87 (± 3.29 S.D.), 14.52 (± 15.03 S.D.), 52.80 (± 52.95 S.D.) and 0.04 (± 0.04 S.D.), respectively (Figure 37; Appendix). In comparison, mean densities collected from samples in Crystal Lake were 9.61 (± 12.54 S.D.), 6.53 (± 8.43 S.D.), 2.29 (± 3.36 S.D.), 13.90 (± 16.10 S.D.), 52.38 (± 67.74 S.D.) and 0.97 (± 3.74 S.D.), respectively (Figure 37; Appendix).

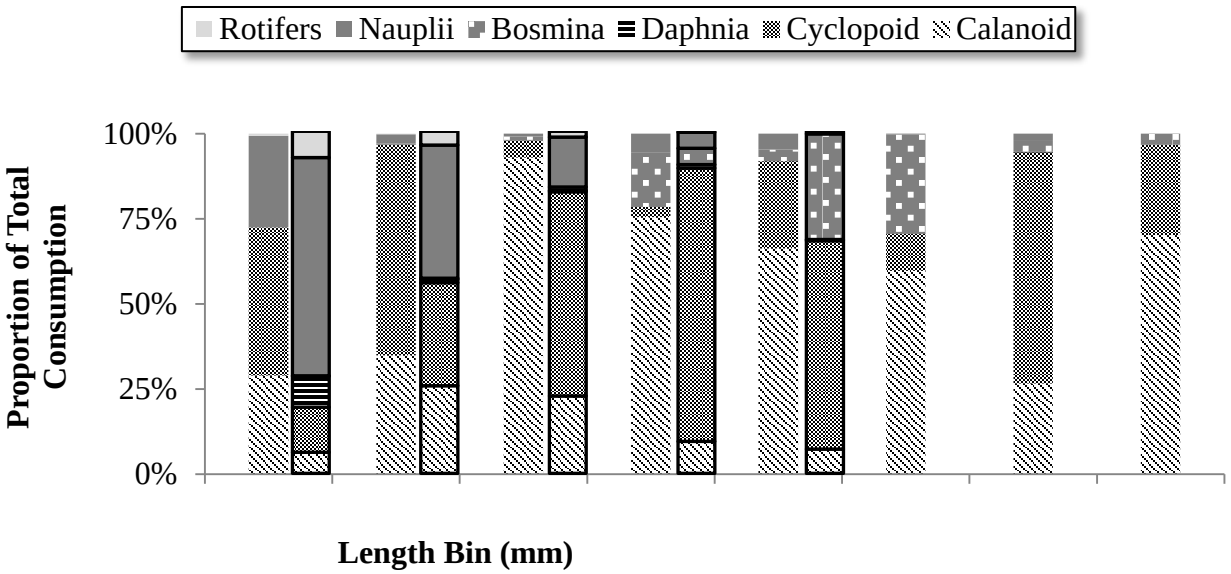

Figure 24: Proportion of prey items consumed by pelagic larval yellow perch during an individual based model simulation for Crystal Lake (Benzie County, MI) and comparison to field diet data collected from Crystal lake from 1998 to 2002 (Granet 2000, McNaught 2002, Edwards 2010) [represented in black highlighted bars].

There was not a statistical difference between observed and modeled diet prey fractions for larval yellow perch total length ranging from hatch to 7 mm ($\chi^2 = 1.91$, degrees of freedom (df) = 5, p = 0.86), 7 to 10 mm ($\chi^2 = 0.75$, df = 5, p = 0.98), 10 to 13 mm ($\chi^2 = 2.84$, df = 5, p = 73), 13 to 16 mm ($\chi^2 = 5.73$, df = 5, p = 0.33), or 16 to 19 mm ($\chi^2 = 5.62$, df = 4, p = 0.23). Once the fish began exogenous feeding on day 5 in our simulations, cyclopoids comprised the majority of the fish's diet (43.5 %). Calanoid copepods (29.0 %), nauplii copepods (26.8 %) and rotifers (0.7 %) were the remaining proportions of their diet (Figure 24). As fish grew, they began eating more calanoid and cyclopoid copepods. By the time larvae reached 30 mm, the majority (96.6 %) of their diet was calanoid and cyclopoid copepods. In comparison, diet analysis of larval yellow perch in Crystal Lake determined that newly hatched larval perch feed predominately on nauplii (63.8 %), with cyclopoid copepods (13.1 %), *Daphnia* (9.1 %), rotifers (7.7 %) and calanoid (6.2 %) comprising the remainder of the diet (Figure 24, Granet 2000, McNaught 2002, Edwards 2010). By the time they reach 19 mm they switch to a cyclopoid copepod (60.9 %), *Bosmina*

(30.8 %), calanoid copepod (7.1 %) and rotifer/*Daphnia*/nauplii (< 2 %) diet. A comparison of our model diet results for larger fish was not possible as they were not collected in the Granet (2000), McNaught (2002) and Edwards (2010) diet studies.

3.1.2 Growth

The average growth rate for the Crystal Lake simulations was 0.58 mm/d (± 0.01 S.D.) and the mean pelagic phase duration was 43.8 days (± 0.04 S.D.). This is in comparison to the Lake Michigan simulations where the mean growth rate was 0.46 mm/d and subsequent pelagic phase duration was 54.1 days (Figure 25). Generally, the model simulations encompassed the growth variability for larval yellow perch collected in Crystal Lake up to 19 mm in total length, however a few individuals grew faster or slower than 2 standard deviations of the mean modeled growth rate (Figure 26).

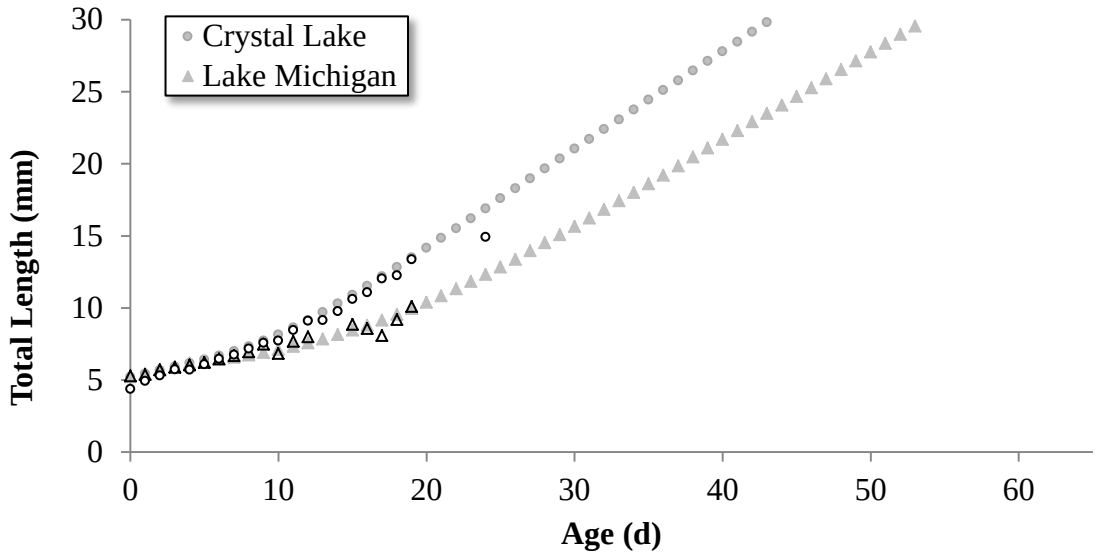

Figure 25: Comparison of the simulated mean larval yellow perch growth and pelagic phase duration between two systems, Lake Michigan and Crystal Lake (Benzie County, MI), using an individual-based model. Five simulations were performed; each starting with 10,000 newly hatched individuals. Pelagic phase duration was assumed to end once an individual reached 30 mm. Open circles (Crystal Lake) and triangles (Lake Michigan) are the mean total length (mm) at age (d) data collected from the two systems from 1998 to 2002 (Granet 2000, McNaught 2002, Edwards 2010).

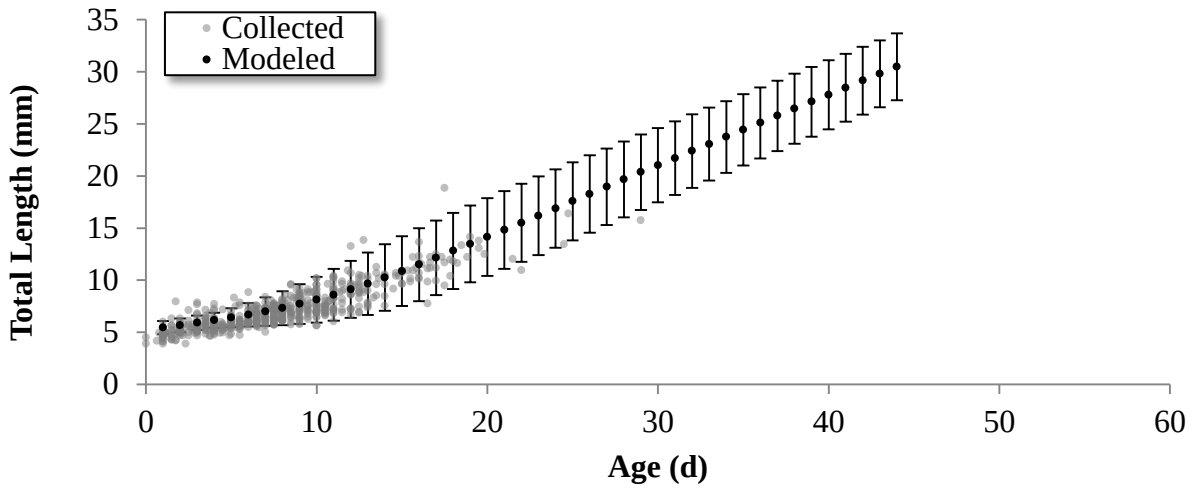

Figure 26: Variability of larval yellow perch growth from a single individual based model simulation and comparison to individual yellow perch collected from Crystal Lake from 1998 to 2002 (Granet 2000, McNaught 2002, Edwards 2010). Error bars are ± 2 standard deviations. Simulation started with 10,000 individuals.

3.1.3 Survival

The model predicted that 26.8 % (± 1.3 S.D.) of the 10,000 larvae in Crystal Lake would reach 30 mm in total length and survive the pelagic phase. On average, rainbow smelt and yellow perch consumed 46.8 % (± 0.82 S.D.) and 14.8 % (± 0.58 S.D.) of the cohort, respectively. The remaining 11.7 % (± 0.49 S.D.) of the cohort in Crystal Lake starved during the simulations (Figure 27).

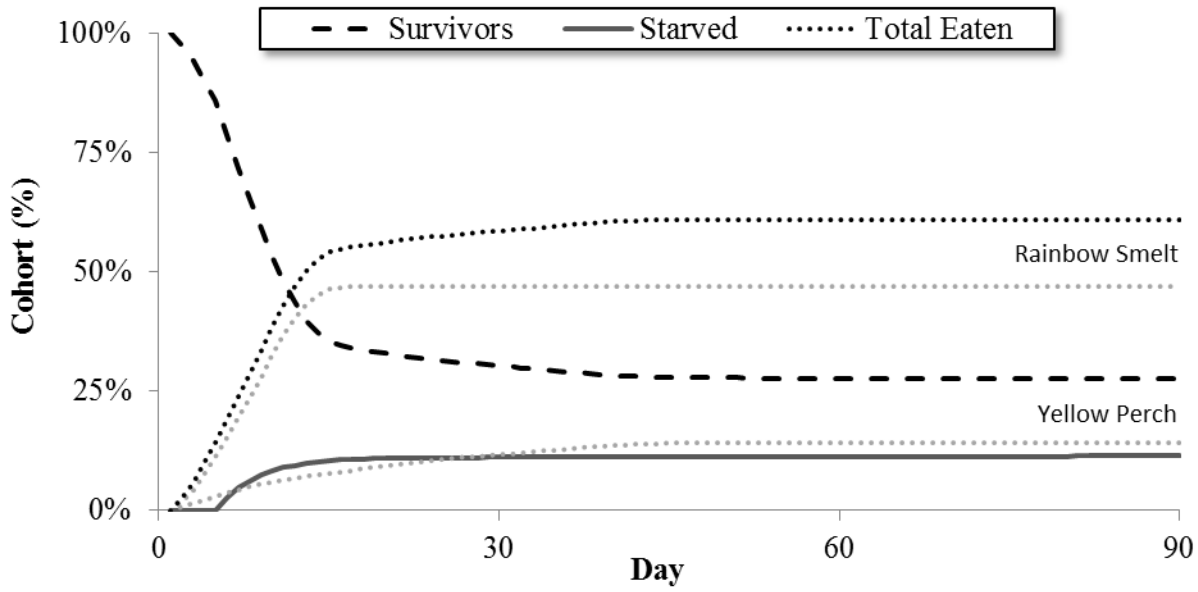

Figure 27: **Cumulative percent of a larval yellow perch cohort surviving, being consumed by a predator (rainbow smelt or yellow perch) or starving following an individual based model simulation for Crystal Lake (Benzie County, MI).** Simulation started with 10,000 individuals.

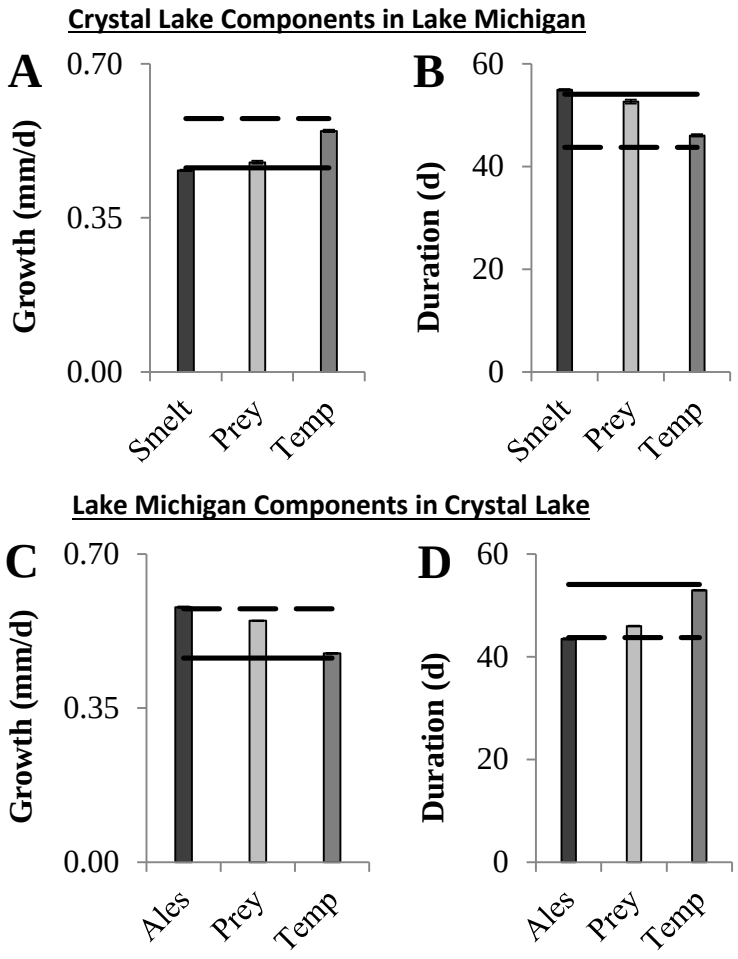

Figure 28: Simulated mean growth rate (A; mm/d) and pelagic larval phase duration (B; d) in two systems. Lake Michigan (———) and Crystal Lake (– –). Baseline simulations (represented by lines) were conducted for a cohort consisting of 10,000 newly hatched yellow perch. Habitat components from one system (represented by bars) were then individually substituted into the other system in order to determine which component was most influential on larval yellow perch growth and survival. Components included (predator type [Smelt or Alewife (Ales)], prey density and composition [Prey] and lake temperature [Temp]). Larval yellow perch survived the simulation by reaching 30 mm in length and transforming to the demersal larval stage. Error bars are ± 1 standard deviation of five simulations.

3.2 Environmental Impacts on Growth

Temperature had the largest influence on larval yellow perch growth rate among all other tested components (Figure 28). If Lake Michigan surface water temperatures were to increase to those of Crystal Lake, our model suggests that mean growth rates of larval yellow perch would increase from 0.46 mm/d (Chapter 3 Dissertation) to 0.548 mm/d (± 0.003 S.D.) (Figure 28A)

thus reducing the pelagic phase by an average of 8.0 days (Figure 28B). Similarly, after applying a Lake Michigan temperature component to the Crystal Lake model, mean growth rates of larval yellow perch decreased from 0.576 mm/d to 0.474 mm/d (± 0.001 S.D.; Figure 28C) and the pelagic phase was increased by an average of 9.2 days (Figure 28D).

Prey density and composition had the next highest influence on larval yellow perch growth rate and pelagic phase duration (Figure 28). Adjusting the zooplankton prey densities in our Lake Michigan model to those found in Crystal Lake resulted in a mean growth rate of 0.476 mm/d (± 0.003 S.D.) (Figure 28A), decreasing the mean pelagic phase duration by only 1.4 days compared to our baseline Lake Michigan simulations (Figure 28B). Similarly, switching the zooplankton prey composition to that found in Lake Michigan, our Crystal Lake model suggests mean larval yellow perch growth rate would be reduced to 0.55 mm/d (± 0.001 S.D.; Figure 28C) and the mean pelagic phase would increase by just 2.2 days compared to the baseline Crystal Lake simulations (Figure 28D).

Predator type had minimal influence on yellow perch growth rate and pelagic phase duration in either of our lake simulations (Figure 28). Replacing alewives with rainbow smelt in our Lake Michigan model resulted in a 0.458 mm/d (± 0.001 S.D.) mean growth rate (Figure 28A) and pelagic phase duration slightly increased by an average of 0.9 days compared to our baseline Lake Michigan simulations (Figure 28B). Similarly, replacing rainbow smelt with alewives in the Crystal Lake simulations resulted in a mean growth rate of 0.58 mm / day (Figure 5C) and a 0.3 day decrease in mean pelagic phase duration (Figure 28D) compared to the baseline Crystal Lake simulations.

3.3 Environmental Impacts on Survival

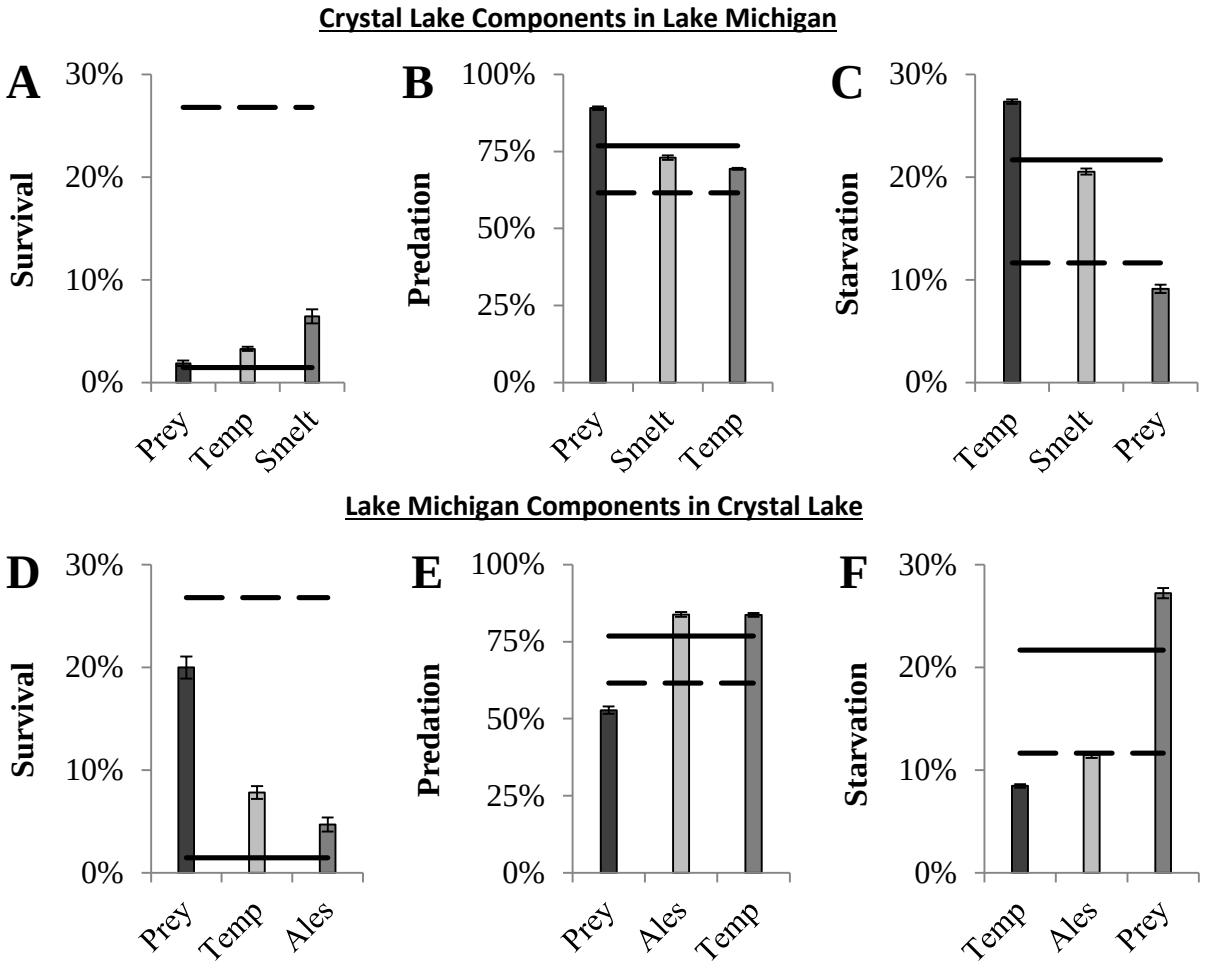

Figure 29: Simulated mean survival rate (A; %), total predation rate (B; %), and starvation rate (C; %) of a yellow perch cohort in two systems. Lake Michigan (——) and Crystal Lake (– –). Baseline simulations (represented by lines) were conducted for a cohort consisting of 10,000 newly hatched yellow perch. Habitat components from one system (represented by bars) were then individually substituted into the other system in order to determine which component was most influential on larval yellow perch growth and survival. Components included (predator type [Smelt or Alewife (Ales)], prey density and composition [Prey] and lake temperature [Temp]). Larval yellow perch survived the simulation by reaching 30 mm in length and transforming to the demersal larval stage. Error bars are ± 1 standard deviation of five simulations.

Predator type had the largest influence on survival rates of larval yellow perch in both of our lake simulations (Figure 29). If alewives were to become extinct in Lake Michigan and rainbow smelt were to take over as the main predator of larval yellow perch, our model suggests

that larval yellow perch survival would increase from 1.46 % (Chapter 3 Dissertation) to 6.45 % (± 0.68 S.D.) assuming that the total predator density would remain the same (Figure 29A). Rainbow smelt and larger yellow perch predation would contribute to 64.3 % (± 0.6 S.D.) and 8.7 % (± 0.3 S.D.) of larval yellow perch mortality, respectively, for a total predation rate of 73% (Figure 29B). This is in comparison to the simulated 68.5 % and 8.4 % predation rate by alewives and larger yellow perch in our baseline Lake Michigan model (Chapter 3 Dissertation). Starvation rate (Figure 29C) would slightly reduce from 21.7 % (± 0.4 S.D.) to 20.5 % (± 0.3 S.D.). While not as drastic of a change in the Lake Michigan simulations, if alewives were to invade Crystal Lake and replace rainbow smelt as the top predator our model suggests that survival of larval yellow perch would decrease from 26.8 % to 4.7 % (± 0.7 S.D.; Figure 29D). The total predation rate of larval yellow perch would increase from 61.5 % (± 0.8 S.D.) to 83.8 % (± 0.9 S.D.) (Figure 29E), with alewives contributing 73.1 % (± 0.6 S.D.) of the predation mortality. Starvation rate would remain low at 11.5 % (± 0.3 S.D.; Figure 29F).

Lake temperature had a significant effect on larval yellow perch survival but was not as large as predator type (Figure 29). When we increased the water temperature in Lake Michigan to that of Crystal Lake, larval yellow perch survival increased to 3.35 % (± 0.71 S.D.) from 1.46 % in our baseline Lake Michigan simulations (Figure 29A). Alewife predation was reduced from 68.5 % to 59.1 % (± 0.3 S.D.) while larger yellow perch predation increased from 8.4 % to 10.3 % (± 0.5 S.D.). Starvation rates (Figure 29C) of larval yellow perch increased to 27.3 % (± 0.2 S.D.). When we reduced the temperature in our Crystal Lake model to that of Lake Michigan, survival decreased from 26.80 % to 7.82 % (± 0.62 S.D.; Figure 29D) which again wasn't as a drastic of a change in our Lake Michigan temperature simulation. Total predation remained similar at 83.7 % (± 0.6 S.D.; Figure 29E) with rainbow smelt contributing 74.7 % (± 0.7 S.D.)

to the total predation rate. Incorporating the lower temperature into the Crystal Lake model resulted in a lower starvation rate of 8.46 % (± 0.16 S.D.; Figure 29F).

Prey composition differences between the two systems had the smallest influence on pelagic larval yellow perch survival (Figure 29). Our simulations suggest that if the larval yellow perch prey items in Lake Michigan increased to a density and composition observed in Crystal Lake, larval yellow perch survival rates would only increase from 1.46 % (Chapter 3 Dissertation) to 1.87 % (± 0.3 S.D.) (Figure 29A). Predation of larval yellow perch by alewives would increase from 68.5 % (± 0.7 S.D.) to 80.5 % (± 0.5 S.D.) with larger yellow perch contributing to an additional 8.5 % (± 0.5 S.D.) of the larval yellow perch predation rate (Figure 29B). Starvation of larval yellow perch in Lake Michigan would decrease from 21.7 % (± 0.4 S.D.) to 9.12 % (± 0.2 S.D.; Figure 29C). Similarly, changing the prey composition in our Crystal Lake model to that found in Lake Michigan resulted in a decrease in larval yellow perch survival to 19.99 % (± 1.07 S.D.; Figure 29D). Total predation rate was reduced to 52.8 % (Figure 29E) with rainbow smelt contributing 39.3 % (± 1.1 S.D.) of the total predation mortality. The changed prey composition in Crystal Lake caused an increase in starvation rate from 11.7 % in the baseline model to 27.7 % (± 0.51 S.D.; Figure 29F).

When the attack rate of pelagic predators was independent of lake temperature the growth rate of larval yellow perch was unaffected by predator type and was similar to the respective lake baseline simulation (Figure 38A; Appendix). Larval yellow perch survival was decreased in both lakes in comparison to the baseline simulations with Crystal Lake exhibiting a larger reduction (Figure 38A; Appendix). In Crystal Lake, there was a 92.0 % and 90.6 % reduction in larval yellow perch survival when alewives or rainbow smelt were in the system compared to the baseline simulation, respectively (Figure 38B; Appendix). In comparison, survival of larval

yellow perch in Lake Michigan was reduced by 62.3 % and 37.0 %, respectively. Total predation rates in both lakes increased compared to their respective baseline simulations (Figure 38C; Appendix). Crystal Lake predation increased by 41.5 % when the primary predator was alewife or rainbow smelt (Figure 38C; Appendix). In Lake Michigan, when alewives or rainbow smelt were the primary predator in the lake total predation increased by only 5.9 % and 6.1 %, respectively. Starvation rate was reduced by 17.1 % and 16.7 % in Lake Michigan and Crystal Lake, respectively and was independent of predator type (Figure 38D; Appendix).

The synergistic simulations, where two Crystal Lake parameters were applied to the Lake Michigan baseline model, all had a greater effect on larval yellow perch survival to 30 mm than the individual component applications: Temperature plus prey composition increased survival of larval yellow perch in Lake Michigan by 3.2 % compared to the baseline simulation. Prey composition plus predator type increased survival by 6.4 % and temperature plus predator type resulted in an 18.5 % survival increase in comparison to the baseline simulations.

3.4 Methylmercury in Crystal Lake

Incorporating the 0.03, 0.10 and 0.30 μM MeHg swimming speed and foraging efficiency multipliers (Chapter 3 Dissertation) into the baseline Crystal Lake model simulations reduced larval yellow perch mean growth rate from 0.58 mm/d to 0.57, 0.52 and 0.56 mm/d, respectively (Figure 30A). Mean pelagic phase duration increased to 44.4 (± 0.07 S.D.), 48.0 (± 0.14 S.D.) and 45.4 (± 0.05 S.D.) days, respectively, compared to the 43.8 (± 0.03 S.D.) days in the Crystal Lake baseline control simulations. Larval yellow perch survival decreased from 26.8 % (± 1.3 S.D.) to 24.8 % (± 1.0 S.D.), 5.2 % (± 0.3 S.D.), and 13.6 % (± 0.1 S.D.), respectively (Figure 30B). Total predation rate of the cohort decreased from 61.5 % (± 0.8 S.D.) to 58.2 % (± 1.1 S.D.), 34.9 % (± 1.0 S.D.), and 47.1 % (± 1.0 S.D.), respectively. Starvation rate increased from

11.7 % (± 0.5 S.D.) to 17.1 % (± 0.2 S.D.), 59.9 % (± 0.8 S.D.), and 39.3 % (± 0.9 S.D.), respectively.

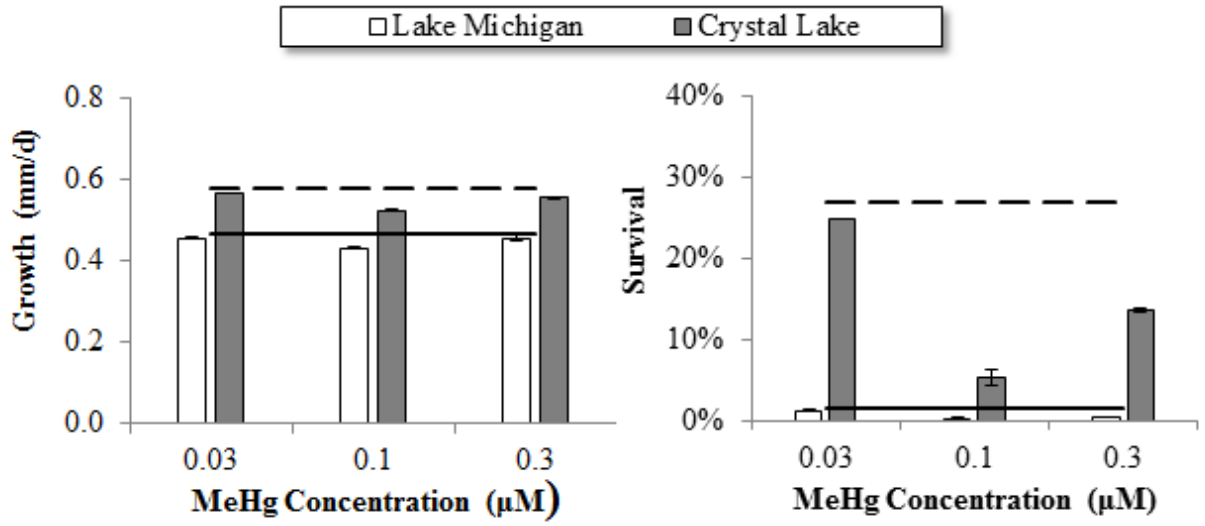

Figure 30: Simulated mean growth rate (A) and survival rate (B) of a yellow perch cohort in Lake Michigan or Crystal Lake, MI exposed to methylmercury (MeHg). Five simulations were conducted for a cohort consisting of 10,000 newly hatched yellow perch exposed 0.03, 0.10 or 0.30µM MeHg and compared to baseline simulations for Lake Michigan (——) and Crystal Lake (– –). MeHg simulations included laboratory effects of MeHg on larval yellow perch swimming speed and feeding efficiency (Mora et al. 2015). In that study, newly hatched fish were fed food containing one of four MeHg treatments (A water only control, 0.03, 0.10 and 0.30 µM) for 25 days. After the exposure, swimming speed and foraging efficiencies were measured. Error bars are ± 1 standard deviation of five simulations.

4.0 DISCUSSION

Overall, our baseline model simulation growth of pelagic larval yellow perch was comparable to field collected measurements from 1998 to 2002 in Crystal Lake (Figure 25). The simulated mean growth rate of larval yellow perch, aged up to 24 d, was 0.49 mm/d (± 0.18 S.D) in comparison to the field measurement of 0.47 mm/d (± 0.29 S.D). A comparison of survival rate of pelagic larval yellow perch between Crystal Lake and our model simulations could not be obtained. However, our estimate of a 26.1 % survival rate in Crystal Lake is similar to what has

been reported in other systems. For example, Dahlberg (1979) reported a 26 % survival rate from yolk sac absorption to 30 days of age in larval yellow perch from Oneida Lake (New York).

The component that had the highest impact on survival rates of pelagic larval yellow perch in our model was alewife predation. When alewives were replaced with rainbow smelt in our Lake Michigan simulations, mean survival rate of the yellow perch cohort increased nearly 4.5x that of our baseline Lake Michigan simulations (Figure 29A). Similarly, when rainbow smelt were replaced with alewives, larval yellow perch survival to 30 mm decreased nearly 6x compared to our baseline Crystal Lake simulation (Figure 29D). These simulation results are consistent with the hypothesis that yellow perch recruitment strength is highly tied to alewife predation (Brandt et al. 1987, Shroyer & McComish 2000) and also highlight the importance of reducing the devastating effects of invasive species and preventing their further spread into nearby systems.

Differences in optimal thermal preferences between alewife and rainbow smelt are a potential reason for the observed change in larval yellow perch survival in our simulations. Rainbow smelt have a lower upper thermal tolerance than alewives (Hanson et al. 1997). During periods of warm temperatures, rainbow smelt migrate toward the colder temperatures near the bottom on the lake. For example, the highest densities of rainbow smelt in Lake Champlain were found between 30 and 40 m during summer days (4 to 6 ° C) and between 10 and 15 m from the surface at night at temperatures from 4 to 20 º C (Simonin et al. 2012). In comparison, alewives, which are more tolerant of warmer water temperatures, have been collected in Lake Champlain in the top 6 m of the water column, in temperatures ranging from 15 to 23 ºC (Simonin et al. 2012). Larval yellow perch are often found in the top 9 m of the lake during their pelagic phase (Granet 2000, McNaught 2002, Edwards 2010), limiting habitat overlap with smelt but not

alewives. In our simulations, we accounted for predator thermal tolerances with the addition of the temperature dependent predator attack rate. The habitat overlap between alewives and pelagic larval yellow perch likely results in higher predation rates than those lakes with predators having a colder water optimum for consumption, such as Crystal Lake. We captured this in our baseline model simulations as Lake Michigan total predation rate on larval yellow perch was nearly 25 % higher than that in Crystal Lake.

Water temperature had the highest influence on larval yellow perch growth and pelagic phase duration in both Lakes (Figure 28). When we switched the Lake Michigan model from colder Lake Michigan to warmer Crystal Lake temperatures, the mean growth rate of larval yellow perch increased 18.0 % and subsequent pelagic phase duration decreased by an average of 8 days (Figure 28B) compared to the baseline Lake Michigan simulations (Chapter 3 Dissertation). Similarly, switching to the colder Lake Michigan water in our Crystal Lake model reduced the mean larval yellow perch growth rate by 17.6 % and increased the mean pelagic phase by 9.2 days (Figure 28D). These results were expected as temperature is a major factor influencing fish growth (Kitchell & Stewart 1977). Supporting this finding is a study on larval Eurasian perch (*Perca fluviatilis*) that were raised in 20 °C water and subsequently had increased growth rates compared to individuals raised in 15 °C water (Wang & Eckmann 1994). Furthermore, Honsey et al. (2016) suggested that yellow perch recruitment is dependent upon spring-summer air temperatures and reported stronger yellow perch year classes in the Great Lakes region during periods of warmer air temperatures.

Our model simulations suggest that the differences in prey composition between Lake Michigan and Crystal Lake may not be as important to larval yellow perch growth (Figure 28) and survival (Figure 29) rates as temperature and predator type, respectively. The prey

community sampling conducted by Granet (2000), McNaught (2002) and Edwards (2010) determined a higher mean total zooplankton density in Lake Michigan compared to Crystal Lake, however more preferred prey species for larval yellow perch, such as *Daphnia, Bosmina* and calanoid copepods, were less abundant (Table 6). Switching the prey community composition in the Lake Michigan simulations to that of Crystal Lake only increased the mean survival rate of the cohort by 0.41 % (Figure 29A). The increased preferred prey composition reduced starvation by 12.5 % (Figure 29C); however, total predation increased by 12.2 % (Figure 29D).

Additionally, larval yellow perch growth rate only increased by 0.01 mm / day resulting in a 1.4 day reduction in pelagic phase duration (Figure 29B) in these prey composition simulations. In the Granet (2000), McNaught (2002) and Edwards (2010) samplings, Crystal Lake averaged over twice as many calanoid and cyclopoid copepods as Lake Michigan. However, a further comparison of their sample data revealed similar maximum densities for calanoid and cyclopoid copepods: 89 and 39 individuals per L for Crystal Lake and 78 and 21 individuals per L for Lake Michigan, respectively (Granet 2000, McNaught 2002, Edwards 2010). It is possible that a small portion of the Lake Michigan cohort is able to seek out and locate or are passively aggregated with dense patches of prey similar to patch densities in Crystal Lake. Once located in a dense prey patch, these individuals in Lake Michigan could grow at a similar rate as those found in Crystal Lake. These findings suggest that even if the forage base in Lake Michigan changed to a similar composition as Crystal Lake, low recruitment of larval yellow perch would continue due to predation pressure from alewife.

Overall, our simulations suggest that not one single component on its own can explain the low survival rate of pelagic larval yellow perch in Lake Michigan (1.46 %; Figure 29A). Our model predicts a 25.34 % greater survival rate (18.4 x) for the population in Crystal Lake

compared to Lake Michigan. The combined effects of the individual Crystal Lake habitat components when applied to the Lake Michigan model was not enough to account for the difference in survival rate (Figure 29D): prey composition (+ 0.41 %) survival in Lake Michigan; temperature (+ 1.82 %); predator type (+ 4.98 %). Similarly, the combined individual effects of the Lake Michigan components applied to the Crystal Lake baseline model over-estimates the difference of survival between the two systems (Figure 29D): prey composition (- 6.81 %) survival in Crystal Lake; temperature (- 19.0 %); predator type (- 22.10 %). In our simulations where two Crystal Lake habitat components were applied to the Lake Michigan model, the combined individual effects (+ 28.1 % in larval yellow perch survival) indicate that synergistic effects are occurring in our model between more optimal water temperatures, a higher quality forage base and reduced predation.

When predators were allowed to attack at a maximum rate, absent of the temperature dependent function, survival of pelagic larval yellow perch in both systems declined as expected; however Crystal Lake exhibited a much larger reduction in comparison to Lake Michigan. In these simulations, Crystal Lake only had 2x greater survival rate compared to Lake Michigan (Figure 38; Appendix). This is in comparison to the 18.4 x greater survival rate in Crystal Lake versus Lake Michigan that we determined in our baseline simulations when predators were susceptible to lake temperature effects (Figure 29A). This response is because alewives are able to tolerate warmer temperatures than rainbow smelt (Hanson et al. 1997). Crystal Lake surface temperatures average 21.1 ° C throughout the pelagic period of larval yellow perch (Table 6) which exceeds the temperature threshold of 18 ° C (CTL, Table 7) for which rainbow smelt consumption rate begins to decline. In comparison, Lake Michigan temperatures average 17.8 ° C which falls in between the optimal temperature threshold for alewife consumption rate (16 to

18 ° C; Table 7) and below the upper temperature threshold of 25 ° C. These simulations suggest that the 25.3 % higher survival rate in Crystal Lake compared to Lake Michigan baseline simulation is largely due to the warmer water temperatures creating a refuge for the pelagic larval yellow where they may avoid predation by rainbow smelt.

When the environmental conditions (temperature, forage base, predation rate) are more favorable to supporting a stronger larval yellow perch population, the individuals are likely able to cope with additional impacts by stressors (Forbes et al. 2003, Lenihan et al. 2003, Thrush et al. 2008), such as MeHg. When incorporating the swimming speed and feeding efficiency effects of MeHg at even the highest concentration, 0.30 μM, our simulations suggest the larval yellow perch cohort in Crystal Lake would sustain a faster growth rate (Figure 30A) and higher survival rate (Figure 30B) than those in Lake Michigan exposed to lower MeHg concentrations (0 or 0.03 μM MeHg). This suggests that a more suitable habitat in terms of water temperature and prey availability, such as the one found in Crystal Lake, allows larval yellow perch populations to cope with multiple stressors including natural abiotic and biotic factors and anthropogenic stressors such as MeHg.

Our model assumes that yellow perch have not adapted to the habitat differences between these two systems and behave in similar fashion. We assumed that the fish in the two systems would have similar prey type selectivity indices (Chesson's α), swimming speed, and predator detection and avoidance parameters. Crystal Lake, originally a bay of Lake Michigan, became isolated over 2000 years ago (Crystal Lake Watershed Association 2005). It is possible that yellow perch have evolved differently in response to the habitat transformations between Lake Michigan and Crystal Lake. For example, Parker et al. (2009) suggested that both habitat and diet can influence morphological changes in response to paradigms of ecological function

including predator avoidance and feeding efficiency. They identified morphological and genetic distinctions between one year old yellow perch inhabiting deep, open-water nearshore areas of Lake Michigan in comparison to those living in the shallow, littoral zones and wetland areas. Fish living in deeper areas of the lake tended to have longer, deeper bodies with larger dorsal fins which were hypothesized to provide an adaptive response to increased predation. Additionally, dietary differences between the populations also indicated morphological changes, such as gill raker and pectoral fin length, associated with specific prey capture abilities. Additionally, we assumed that the pelagic phase would end when a fish reached 30 mm in total length. Beletsky et al. (2007) suggested that the pelagic phase of larval yellow perch in Lake Michigan may be much longer than that of those inhabiting smaller inland lakes, which would lead to even further reduced survival estimates. Future research should be conducted to see if similar morphological and pelagic duration differences exist between pelagic larval yellow perch found in Lake Michigan and Crystal Lake which may have implications for comparing two populations using an IBM that assumes no adaptation has occurred.

Other model limitations exist which should be addressed in future model versions. Our estimates of pelagic phase survival were under the assumption that the pelagic period ends once an individual reaches a total length of 30 mm. The lower growth rate in Lake Michigan compared to Crystal Lake may have an effect on the pelagic phase duration as fish up to 70 mm have been found in the pelagic zone of Lake Michigan (Dettmers et al. 2005). Longer pelagic phase duration may result in lower survival rates due to increased vulnerability to predation and starvation. We also assumed that zooplankton patches would exhaust equally between the two lakes because the total prey density in Lake Michigan (114.16 ± 138.93 individuals/L) was similar to that of Crystal Lake (85.68 ± 111.91 individuals/L). Additionally, rainbow smelt and

alewives are both known to feed on zooplankton (Crowder 1980). Our model assumes that differences in predator type did not have an effect on zooplankton patch longevity. Future studies should seek to determine if differences in prey composition and predator type have an overall effect on zooplankton patch exhaustion.

In order to determine the effect of predator type on larval yellow perch survival, we assumed that total predator density in Crystal Lake was equal to that reported for Lake Michigan. Additionally, our model assumed that only one main predator type existed within each lake as these species were reported to be the primary predators in these systems. If rainbow smelt, or another predatory species, are found in higher densities in Crystal Lake compared to the alewife density in Lake Michigan, our model results may over estimate pelagic yellow perch survival in Crystal Lake.

Lastly, our model was not spatially explicit and all individuals within a simulation experienced the same water temperature on a given day which was determined from a lake-wide daily average (Great Lakes Coastwatch 2014). Seasonal and interannual variability in surface water temperatures exist in Lake Michigan (Beletsky & Schwab 2001) which could affect overall model growth and survival estimates. For example, Honsey et al. (2016) reported years with spring-summer air temperatures were positively correlated with higher yellow perch recruitment in the Great Lakes.

In conclusion, the IBM described in Chapter 3 (Dissertation) was a useful tool to test the potential effects of invasive predator introductions, food web changes, and other environmental components on larval yellow perch survival in Lake Michigan. While alewife predation and water temperature had the largest individual influence on survival and growth, respectively, our model simulations determined that synergistic effects between multiple ecological components

may be driving the low recruitment of yellow perch in Lake Michigan. For example, the warmer water temperatures in Crystal Lake provide the larval yellow perch a refuge against cold water species such as the rainbow smelt. In comparison, our model suggests that the introduction of alewives into Lake Michigan has increased larval yellow perch predation rates leading to a loss of recruitment due to their higher thermal preferences compared to rainbow smelt. Thus, reducing alewife predation constraints would be beneficial to improving yellow perch recruitment in Lake Michigan. Additionally, when the environment is more favorable to promoting high survival and fast growth rates, the cohort has a better chance of surviving exposure to additional stressors, such as contaminants.

GENERAL CONCLUSION

This project highlighted the importance of using a multi-tiered experimental approach and framework in order to assess the effects of stressors within the Great Lakes and their potential impacts on fish populations. The models developed by this research encompass two important life stages in fish and each model allows for a linkage of sublethal effects within individuals to population-relevant indices. The results of these types of modeling exercises can be incorporated into population models to forecast long-term effects on a population following exposure to both biotic and abiotic stressors.

Computational models that link *in vitro* effects of chemical exposure to *in vivo* adverse outcomes are needed in order to reduce the workload of evaluating the adverse effects of the > 85,000 individual chemicals and their mixtures using traditional *in vivo* assays. Once validated, the vitellogenesis model can be used in combination with the U.S. Environmental Agency's ToxCast™ program to help prioritize chemicals for further toxicological analyses. Additionally, with our simulations on potential estrogen receptor compensation mechanisms, we've shown that these models can be useful in generating hypotheses to direct future research. Likewise, the utility and adaptability of the IBM make it a useful tool for generating and testing hypotheses of both abiotic and biotic stressor effects on larval fish recruitment that may be occurring in the Great Lakes region and beyond.

APPENDIX

Supplementary Equations

$$F(T)_{C,warm} = V^X * e^{(X-(1-V))} \quad (1)$$

Where:

$$V = \frac{CTM - T}{CTM - CTO}$$

$$X = \frac{Z^2 * (1 + \left(1 + \frac{40}{Y}\right)^{0.5})^2}{400}$$

$$Z = \ln CQ * (CTM - CTO)$$

$$Y = \ln CQ * (CTM - CTO + 2)$$

$$F(T)_{C,warm} = K_A * K_B \quad (2)$$

Where:

$$K_A = \frac{CK1 * L1}{1 + CK1 * (L1 - 1)}$$

$$L1 = e^{G1-(T-CQ)}$$

$$G1 = \frac{1}{CTO - CQ} * \ln(\frac{0.98 * (1 - CK1}{CK1 * 0.02})$$

$$K_B = \frac{CK4 * L2}{1 + CK4 * (L2 - 1)}$$

$$L2 = e^{G2-(CTL-T)}$$

$$G2 = \frac{1}{CTL - CTM} * \ln(\frac{0.98 * (1 - CK4}{CK4 * 0.02})$$

$$F(T)_R = V^X * e^{(X-(1-V))} \quad (3)$$

Where:

$$V = \frac{RTM - T}{RTM - RTO}$$

$$X = \frac{Z^2 * (1 + \left(1 + \frac{40}{Y}\right)^{0.5})^2}{400}$$

$$Z = \ln RQ * (RTM - RTO)$$

$$Y = \ln RQ * (RTM - RTO + 2)$$

Supplementary Tables:

Table 9: Baseline values and definitions for all parameters used in the female yellow perch vitellogenesis model. Compartments of the model included the hypothalamus (H), pituitary (P), gonad (G), liver (L), and blood (B).

C	Compound	Parameter	Definition	Value	Units	Species	Reference
H	GABA	GABA	Basal GABA concentration	24	nmol/mg	*Rattus norvegicus* (male)	Smolders et al. 1997
		V_{GABA}	Maximum uptake rate	0.402	nmol/mg/h	*Rana temporaria* (unsexed)	Voaden et al. 1974
		K_{GABA}	Half-saturation of uptake	25000	nmol/mg/h	*Rana temporaria* (unsexed)	Voaden et al. 1974
		Inh_{GABA}	Inhibition of DA synthesis	0.58	NA	NA	Assumed
	$GABA_A$	$GABA_A$	Basal receptor concentration	0.125	nM	NA	Assumed
		ka_{GABA}	Association rate to receptor	17.2	1/10^6 M/h	*Rattus norvegicus* (male)	Chu et al. 1990
		kd_{GABA}	Dissociation Rate from receptor	5.796	1/h	*Rattus norvegicus* (male)	Chu et al. 1990
		$kelim_{GABA-A}$	Elimination rate of receptor	80	1/h	NA	Assumed
		$kind_{GABA-A}$	Induction rate of receptor	0.024	1/h	NA	Assumed
	GABA-T	V_{GABAT}	Maximum degradation rate	4.05	nmol/mg/h	*Carassius auratus* (unsexed)	Lam 1972
		K_{GABAT}	Half Saturation of degradation	1670	nmol/mg/h	*Mus domesticus* (unsexed)	Bardakdjian 1979
	DA	DA	Basal DA concentration	2.2	nmol/mg	*Rattus norvegicus* (male)	Smolders et al. 1997
		V_{DA}	Maximum uptake rate	3.96	nmol/mg/h	*Carassius auratus* (unsexed)	Sarthy et al. 1978
		K_{DA}	Half-saturation of uptake	261	nmol/mg/h	*Carassius auratus* (unsexed)	Sarthy et al. 1978
		Inh_{DA}	Inhibition of GABA synthesis	0.8	NA	NA	Assumed
	D2	D2	Basal receptor concentration	0.125	nM	NA	Assumed
		ka_{DA}	Association rate to receptor	12.84	1/10^6 M/h	*Coturnix japonica* (male)	Kubikova 2009
		kd_{DA}	Dissociation rate from receptor	3.42	1/h	*Coturnix japonica* (male)	Kubikova 2009
		$kelim_{D2}$	Elimination rate of receptor	10	1/h	NA	Assumed
		$kind_{D2}$	Induction rate receptor	0.048	1/h	NA	Assumed
	MAO	V_{MAO}	Maximum degradation rate	39.9	nmol/mg/h	*Carassius auratus* (female)	Hall et al. 1972
		K_{MAO}	Half saturation of degradation	60630	nmol/mg/h	*Carassius auratus* (female)	Hall et al. 1972
	GnRH	$kdeg_{GH}$	Degradation rate	1.032	1/h	NA	Assumed

Table 9 Continued:

P	LH	$kdeg_{LH}$	Degradation rate	2.032	1/h	NA	Assumed
G	T	T	Basal T concentration	0.0822	ng/ml	NA	Assumed, 1.2% of total
		V_T	Maximum rate production	0.12	ng/ml/h	NA	Assumed
		K_T	Half saturation of production	0.3	ng/ml	*Micropogonias undulatus* (model)	Murphy et al. 2009
		H_T	Hill coefficient	1.8	unitless	*Micropogonias undulatus* (model)	Murphy et al. 2009
		$kdeg_T$	Degradation rate	1.386	1/h	*Micropogonias undulatus* (model)	Murphy et al. 2009
	E2	E2	Basal E2 concentration	0.00816	ng/ml	NA	Assumed, 1.2% of total
		V_E	Maximum rate production	1.5	ng/ml/h	NA	Assumed
		K_E	Half saturation of production	0.052	ng/ml	*Micropogonias undulatus* (model)	Murphy et al. 2009
		H_E	Hill coefficient	4	unitless	NA	Assumed
		$kdeg_E$	Degradation rate	1.386	1/h	*Micropogonias undulatus* (model)	Murphy et al. 2009
		$Stim_{E2DA}$	Stimulation rate of DA	0.1	1/h	NA	Assumed
		Inh_{E2GABA}	Inhibition rate of GABA	0.1	1/h	NA	Assumed
B	SBP	SBP	Basal SBP concentration	400	nM	*Micropogonias undulatus* (model)	Murphy et al. 2009
		ka_T	Association rate of T to SBP	5.6687	1/10^9 M/h	*Micropogonias undulatus* (model)	Murphy et al. 2009
		kd_T	Dissociation rate of T to SBP	27.72	1/h	*Micropogonias undulatus* (model)	Murphy et al. 2009
		ka_E	Association rate of E2 to SBP	17.743	1/h	*Micropogonias undulatus* (model)	Murphy et al. 2009
		kd_E	Dissociation rate of E2 to SBP	5.6687	1/10^9 M/h	*Micropogonias undulatus* (model)	Murphy et al. 2009
L	ER	E2	Basal ER concentration	0.125	nM	*Micropogonias undulatus* (model)	Murphy et al. 2009
		kdegu	Degradation rate of free ER	0.00058	1/h	*Micropogonias undulatus* (model)	Murphy et al. 2009
		kdega	Degradation rate of activated ER	0.012	1/h	*Micropogonias undulatus* (model)	Murphy et al. 2009
		k1	Association rate of E2 to ER	7.43	1/10^8 M/h	*Micropogonias undulatus* (model)	Murphy et al. 2009
		k_1	Dissociation rate of E2 to ER	0.81	1/h	*Micropogonias undulatus* (model)	Murphy et al. 2009
	VTG	k3	VTG production rate	3.465	1/h	*Micropogonias undulatus* (model)	Murphy et al. 2009

Table 10: Model parameters and range for one-factor-at-a-time (OFAT) sensitivity analysis. Parameters in the hypothalamus (H), pituitary (P) and gonad (G) compartment (C) of the vitellogenesis model were adjusted from their nominal value over a wide range to determine relationship to the model output, cumulative vitellogenin (Figure 31; Appendix).

C	Symbol	Description	Units	Nominal Value	Range for OFAT
H	InhGABA	Inhibition of DA synthesis	unitless	0.58	0.02 - 0.97
	InhDA	Inhibition of GABA synthesis	unitless	0.8	0.1 - 1.0
	kindG	Induction rate of receptor	1/h	0.024	0 - 0.89
	kindD	Induction rate receptor	1/h	0.048	0 - 0.89
	kelimG	Elimination rate of receptor	1/h	80	0 - 100
	kelimD	Elimination rate of receptor	1/h	10	0 - 89
	VGABA	Maximum uptake rate	nmol/mg/h	0.4	0.1 - 50
	KGABA	Half-saturation of uptake	nmol/mg/h	25000	5 - 50000
	VDA	Maximum uptake rate	nmol/mg/h	3.96	1 - 50
	KDA	Half-saturation of uptake	nmol/mg/h	261	25 - 500
	VGABAT	Maximum degradation rate	nmol/mg/h	4.05	1 - 60
	VMAO	Maximum degradation rate	nmol/mg/h	39.9	1 - 60
	KMAO	Half saturation of degradation	nmol/mg/h	60630	500 - 120000
	KGABAT	Half Saturation of degradation	nmol/mg/h	1670	600 - 120000
	kaG	Association rate to receptor	1/10^6 M/h	17.2	1 - 30
	kdG	Dissociation Rate from receptor	1/h	5.8	1 - 30
	kaD	Association rate to receptor	1/10^6 M/h	12.8	1 - 30
	kdD	Dissociation rate from receptor	1/h	3.4	1 - 30
	kdegGH	Degradation rate of GnRH	1/h	1.032	0.1 - 4
P	kdegLH	Degradation rate of LH	1/h	2.032	0.1 - 4
G	VE	Maximum rate production	ng/ml/h	1.5	0.05 - 10
	KE	Half saturation of production	ng/ml	0.052	0.05 - 10
	HE	Hill coefficient	unitless	4	0.1 - 10
	VT	Maximum rate production	ng/ml/h	0.12	0.05 - 4
	KT	Half saturation of production	ng/ml	0.3	0.05 - 4
	HT	Hill coefficient	unitless	1.8	0.5 - 4

Supplementary Figures:

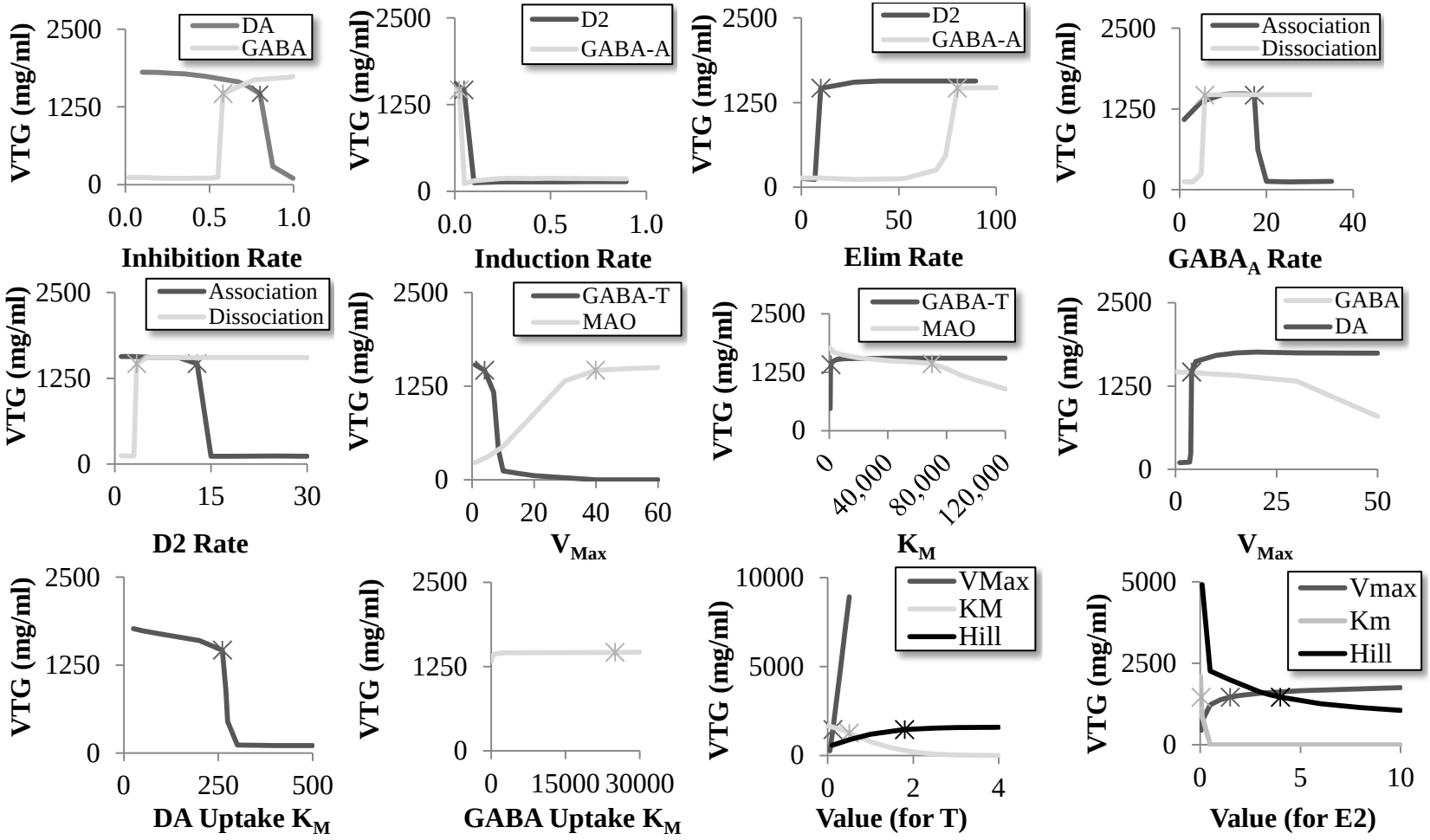

Figure 31: One-factor-at-a-time (OFAT) analysis for parameters that were changed or added to the fish vitellogenesis model (Murphy et al. 2009). Parameters (X-axis) were individually varied over a wide range (Table 10; Appendix) and cumulative vitellogenin (VTG; Y-axis) was compared between parameter value model simulations. * indicates the nominal value for the respective parameter used in the vitellogenesis simulations.

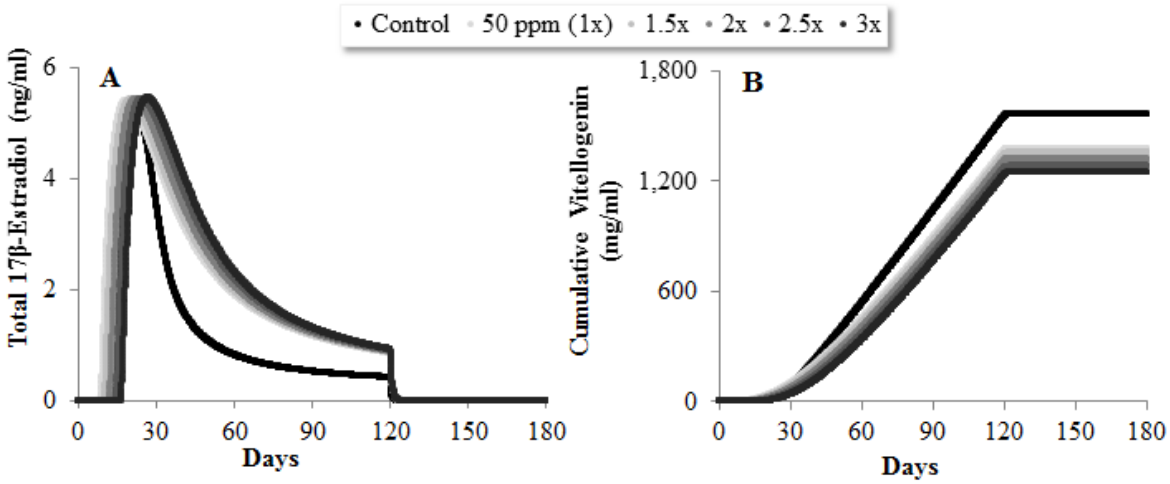

Figure 32: Using the vitellogenesis model as a means to test the assumption that MeHg exposure increases γ-aminobutyric acid transaminase (GABA-T) activity in the hypothalamus of female yellow perch. Simulations included a control absent of MeHg and exposure to 50.0 ppm MeHg using *in vitro* neurochemical effects on hypothalamic $GABA_A$ and D2 receptor binding and monoamine oxidase activity and liver estrogen receptor β concentration. Simulations included the assumption that 50.0 ppm MeHg exposure would increase GABA-T activity by either 1.5, 2.0, 2.5 or 3.0x compared to the control. Comparisons were made on the simulated concentration of 17β-estradiol (A) and cumulative vitellogenin production (B).

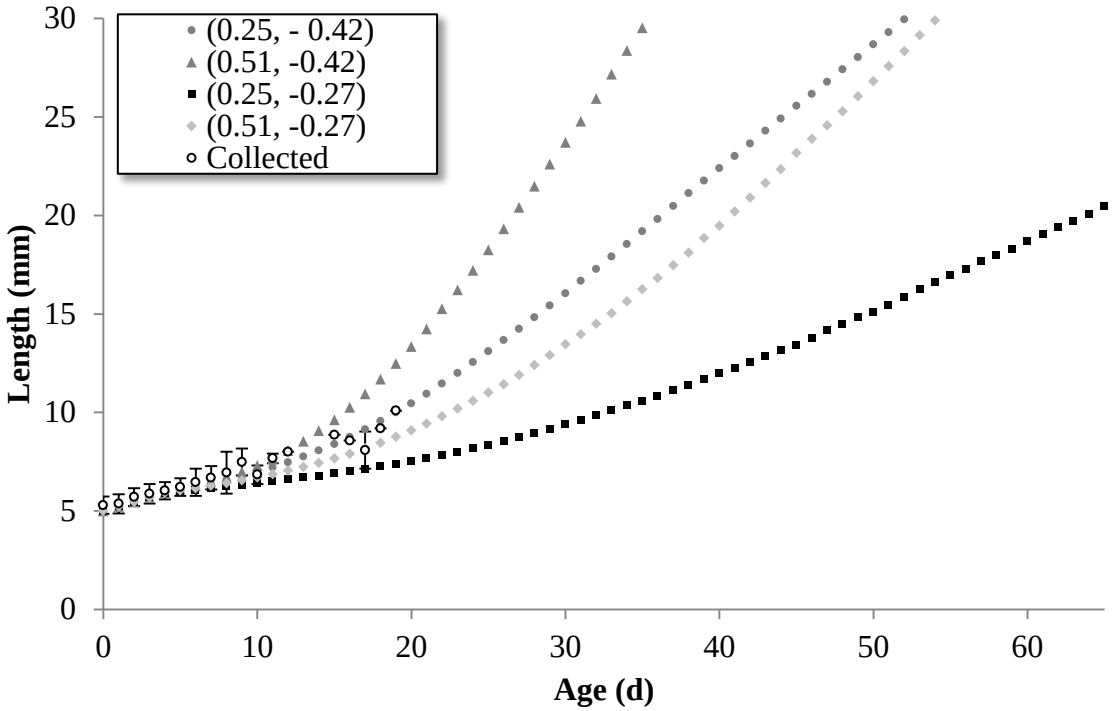

Figure 33: **Calibration of growth by adjusting the maximum consumption (Cmax) parameters α and β.** Cmax = α * W-β x p x W x F(T), where W was the mass (g) of the larval fish, p was the observed consumption rate and F(T) was a function of lake temperature. The open circles are larval yellow perch growth data collection from Lake Michigan from 1998 to 2002 (Granet 2000, McNaught 2002, Edwards 2010). The triangles and squares are Cmax parameters for young-of-the-year (YOY) and adult yellow perch, respectively, proposed by Post (1990). The circles and diamonds are adjustments using a combination of both adult and YOY parameters.

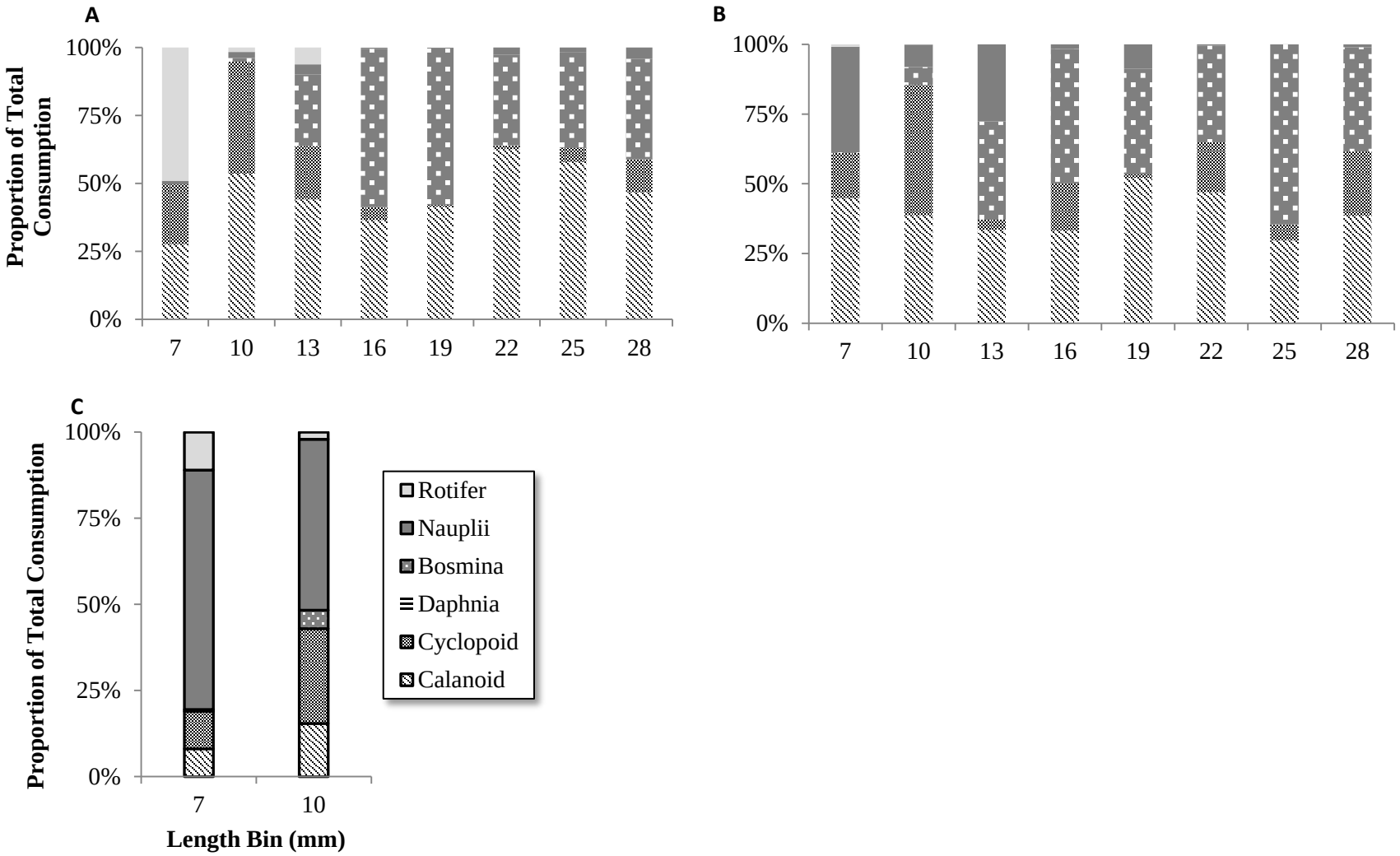

Figure 34: **Calibration of larval yellow perch diet by adjusting the Chesson's α diet parameters for nauplii and rotifers.** A represents modeled diet using Chesson's α values reported by Fulford et al. (2006b); B represents modeled diet following an adjustment to the nauplii and rotifer Chesson's α value; C represents diet proportion data for larval yellow perch collected from Lake Michigan from 1998 to 2002 (Granet 2000, McNaught 2002, Edwards 2010).

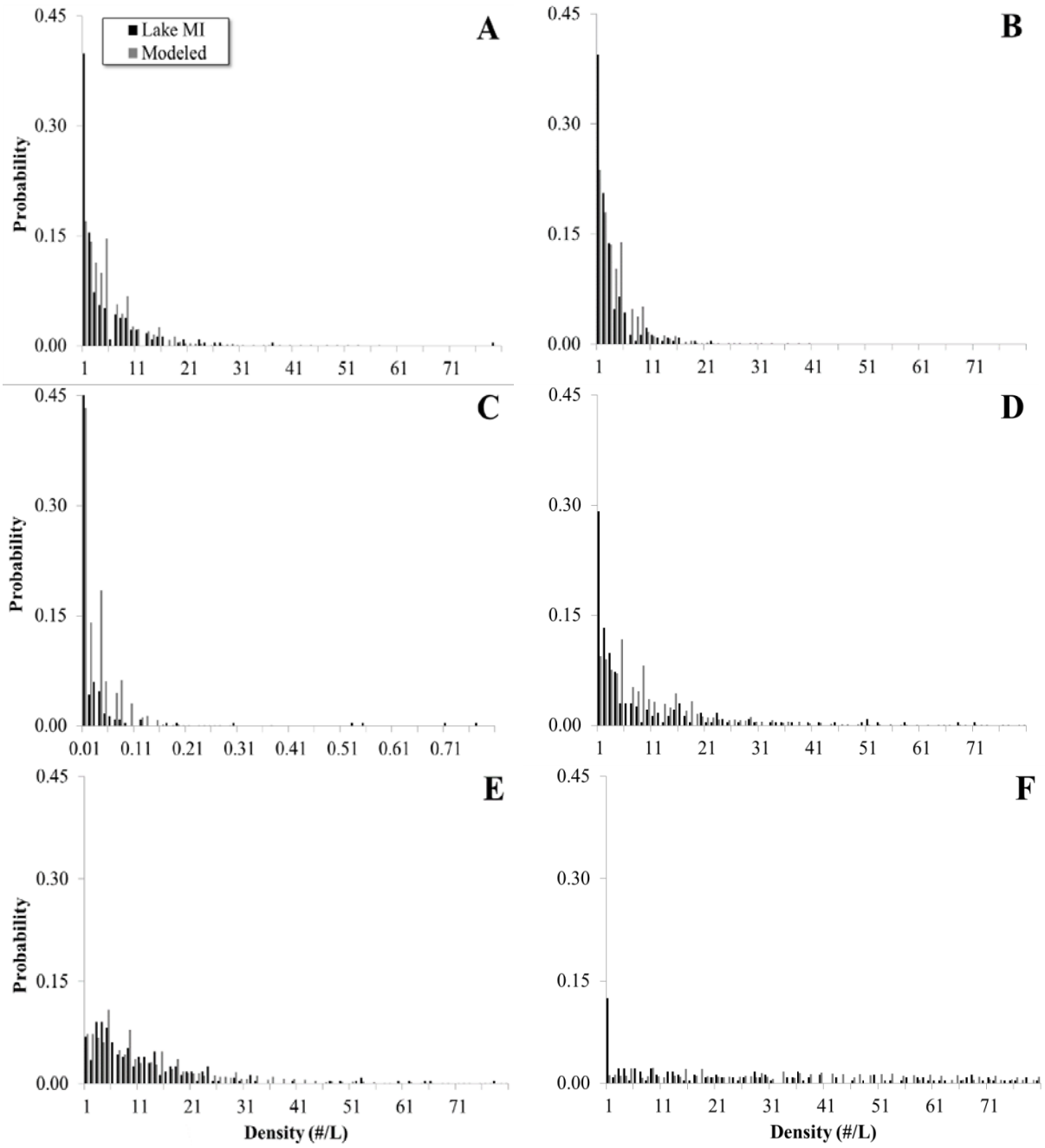

Figure 35: Comparison of modeled and observed Calanoid (A), Cyclopoid (B), *Daphnia* (C), *Bosmina* (D), Nauplii (E) and Rotifer (F) density (# organisms / L) probability distributions in Lake Michigan. Zooplankton tow sampling was conducted in Lake Michigan from 1998 to 2002 (Granet 2000, McNaught 2002, Edwards 2010).

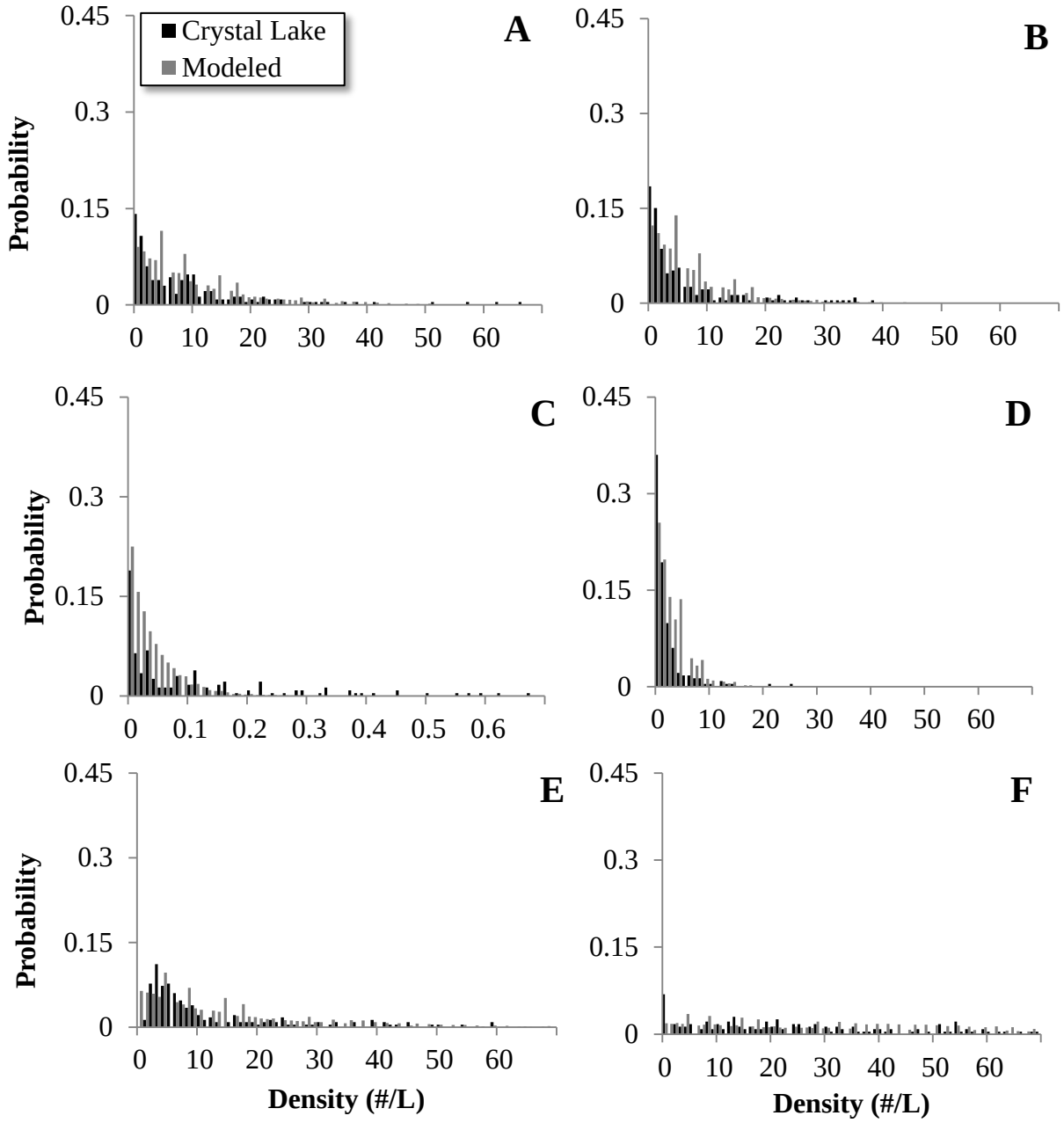

Figure 36: Comparison of modeled and observed Calanoid (A), Cyclopoid (B), *Daphnia* (C), *Bosmina* (D), Nauplii (E) and Rotifer (F) density (# organisms / L) probability distributions in Crystal Lake. Zooplankton tow sampling was conducted in Crystal Lake (Benzie County, MI) from 1998 to 2002 (Granet 2000, McNaught 2002, Edwards 2010).

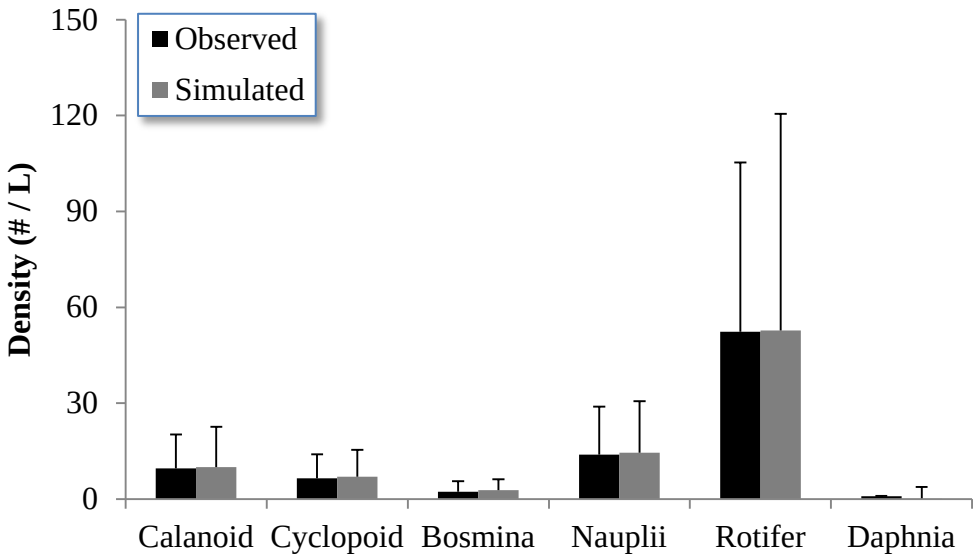

Figure 37: Comparison of modeled and observed mean prey type (Calanoid and Cyclopoid copepods, *Bosmina spp.*, copepod nauplii, rotifers and *Daphnia spp.*) densities (# individuals per liter) in Crystal Lake. Zooplankton tow sampling was conducted in Crystal Lake (Benzie County, MI) from 1998 to 2002 (Granet 2000, McNaught 2002, Edwards 2010). Error bars are + 1 standard deviation.

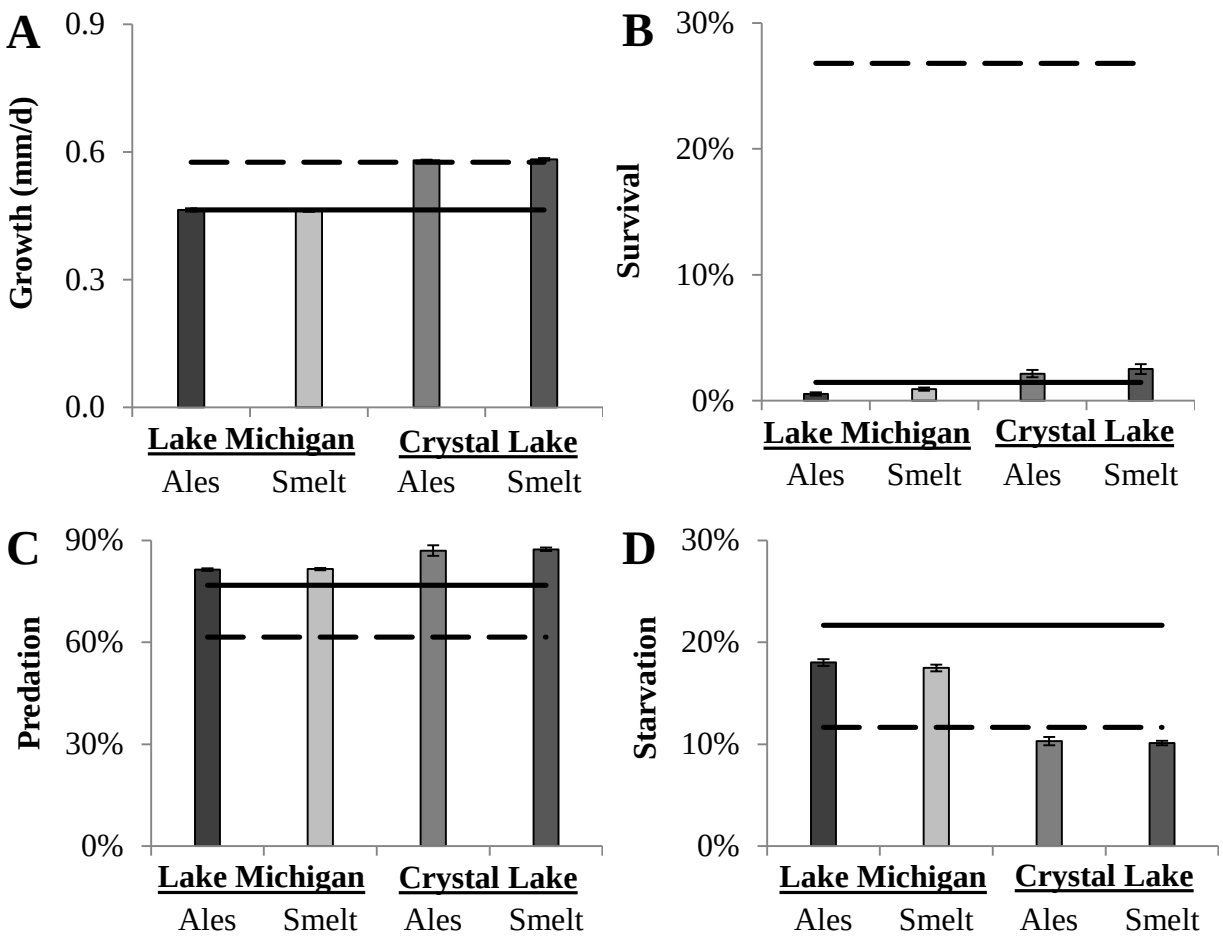

Figure 38: Simulated mean growth rate (A; mm/d), survival rate (B; %), total predation rate (C; %), and starvation rate (D; %) of a yellow perch cohort in two systems. Lake Michigan (——) and Crystal Lake (– –) after turning off the temperature dependent effect on predator attack rate (represented by the bars). Baseline simulations (represented by the lines) were conducted for a cohort consisting of 10,000 newly hatched yellow perch with the systems normal main predator being dependent upon water temperature: Crystal Lake (Smelt) and Lake Michigan (Alewife [Ales]). Separate simulations were conducted with each predator species as the main predator in each system. Larval yellow perch survived the simulation by reaching 30 mm in length and transforming to the demersal larval stage. Error bars are ± 1 standard deviation of five simulations.

REFERENCES

REFERENCES

Adams, S.M. (2005) Assessing cause and effect of multiple stressors on marine systems. *Marine Pollution Bulletin, 51,* 649 - 657.

Ali, M., Sreekrishnan, T.R. (2001) Aquatic toxicity from pulp and paper mill effluents: A review. *Advances in Environmental Research, 5(2),* 175 - 196.

Alvarez, M, Murphy, C.A., Rose, K.A., McCarthy, I.D., Fuiman, L.A. (2006). Maternal body burdens of methylmercury impair survival skills of offspring in Atlantic croaker (*Micropogonias undulates*). *Aquatic Toxicology, 80,* 329 – 337.

Anglade, I., Tramu, G., Kah, O. (1991).Neuroanatomical substrate for dopamine-sGnRH (gonadotropin-releasing hormone) interactions in the forebrain of goldfish (*Carassius auratus*). Proceedings, Fourth International Symposium on the Reproductive Physiology of Fish. In: Scott, A.P., et al. (Eds.), Fish Symp. 91, Sheffield, UK, p. 60.

Ankley, G.T., Jensen, K.M., Kahl, M.D., Korte, J.J., Makynen, E.A. (2001) Description and evaluation of a short-term reproductive test with the fathead minnow (*Pimephales promelas*). *Environmental Toxicology and Chemistry, 20(6),* 1276 - 1290.

Ankley, G.T., Bennett, R.S., Erickson, R.J., Hoff, D.J., Hornung, M.W., Johnson, R.D., Mount, D.R., Nichols, J.W., Russom, C.L., Schmieder, P.K., Serrano, J.A., Tietge, J.E. & Villeneuve, D.L. (2010). Adverse outcome pathways: A conceptual framework to support ecotoxicology research and risk assessment. *Environmental Toxicology & Chemistry, 29,* 730–741

Armstrong, B.M., Lazorchak, J.M., Murphy, C.A., Haring, H.J., Jensen, K.M., Smith, M.E. (2015) Determining the effects of a mixture of an endocrine disrupting compound, 17α-ethinylestradiol, and ammonia on fathead minnow (*Pimephales promelas*) reproduction. *Chemosphere, 120,* 108 - 114.

Arini, A., Head, J.A., Murphy, C.A., Carvan, M.J., Goetz, R., Klinger, R.H., Nam, D-H., Basu, N. (2016). Neuroendocrine biochemical effects in methylmercury-exposed yellow perch. *Comparative Biochemistry and Physiology, Part C, 187,* 10 – 18.

Arukwe, A. & GoskØyr, A. (2003). Eggshell and egg yolk proteins in fish: hepatic proteins for the next generation: oogenetic, population, and evolutionary implications of endocrine disruption. *Comparative Hepatology, 2,* 1 – 21.

Atchison, W.D., Hare, M.F. (). Mechanisms of methylmercury-induced neurotoxicity. (1994). *The Journal of the Federation of American Societies for Experimental Biology, 8(9),* 622 – 629.

Bardakdjian, J., Tardy, M., Pimoule, C., Gonnard, P. (1979). GABA metabolism in cultured glial cells. *Neurochemical Research, 4(4),* 518 – 527.

Basu, N., A. M. Scheuhammer, R. D. Evans, M. O'Brien, and L. H. M. Chan. (2007). Cholinesterase and monoamine oxidase activity in relation to mercury levels in the cerebral cortex of wild river otters. *Human and Experimental Toxicology, 26,* 213-220.

Basu, N., Ta C.A., Waye A., Mao, J., Hewitt, M., Arnason, J.T., Trudeau, V.L. (2009). Pulp and paper mill effluents contain neuroactive substances that potentially disrupt neuroendocrine control of fish reproduction. *Environmental Science and Technology, 43,* 1635-1641.

Becker, R.A., Ankley, G.T., Edwards, S.W., Kennedy, S.W., Linkov, I., Meek, B., Sachana, M., Segner, H., Van Der Burg, B., Villeneuve, D.L., Watanabe, H., Barton-Maclaren, T.S. (2015) Increasing scientific confidence in adverse outcome pathways: application of tailored bradford-hill considerations for evaluating weight of evidence. *Regulatory Toxicology and Pharmacology, 72,* 514-537.

Beletsky, D., Mason, D.M., Schwab, D.J., Rutherford, E.S., Janssen, J., Clapp, D.F., Dettmers, J.M. (2007). Biophysical model of larval yellow perch advection and settlement in Lake Michigan. *Journal of Great Lakes Research, 33,* 842 – 866.

Belknap, A.M., Solomon, K.R., MacLatchy, D.L., Dube, M.G., Hewitt, L.M. (2006) Identification of compounds associated with testosterone depressions in fish exposed to bleached kraft pulp and paper mill chemical recovery condensates. *Environmental Toxicology and Chemistry, 25(9),* 2322 - 2333.

Bellehumeur, K. (2010). Consequences of sublethal polychlorinated biphenyl exposure on the swimming performance of rainbow trout, *Oncorhynchus mykiss*. A master's thesis submitted to the University of Ottawa, Ottawa, ON.

Bengtsson, B-E. (1980). Long-term effects of PCB (Clophen A50) on growth, reproduction, and swimming performance in the minnow, *Phoxinus phoxinus*. *Water Research, 14,* 681 – 687.

Bhavsar, S.P., Gewurtz, S.B., Mcgoldrick, D.J., Keir, M.J., Backus, S.M. (2010). Changes in mercury levels in Great Lakes fish between 1970s and 2007. *Environmental Science and Technology, 44,* 3273 – 3279.

Birge, W.J,, Black, J.A., Westerman, A.G., Hudson, J.E. (1979). The effects of mercury on reproduction of fish and amphibians. In Nriagu, J.O. ed. The Biogeochemistry of Mercury in the Environment. Amsterdam: Elsevier/North Holland, 629 – 655.

Blazer, V.S., Pinkney, A.E., Jenkins, J.A., Iwanowicz, L.R., Minkkinen, S., Draugelis-Dale, R.O., Uphoff, J.H. (2013). Reproductive health of yellow perch *Perca flavescens* in

selected tributaries of the Chesapeake Bay. *Science of the Total Environment, 447,* 198 – 209.

Blum, J.J., Reed, M.C., Janovick, J.A., Conn, P.M. (2000). A mathematical model quantifying GnRH-induced LH secretion from gonadotropes. *American Journal of Physiological Endocrinology and Metabolism, 278,* 263 – 272.

Bortolato, M., Chen, K., Shih, J.C. (2008). Monoamine oxidase inactivation: From pathophysiology to therapeutics. *Advanced Drug Delivery Reviews, 60,* 1527 – 1533.

Braband, A. (1995). Intra-cohort cannibalism among larval stages of perch (*Perca fluviatilis*). *Ecology of Freshwater Fish, 4,* 70 – 76.

Brandt, S.B., Mason, D.M., Macneill, D.B., Coates, T., Gannon, J.E. (1987). Predation by alewives on larvae of yellow perch in Lake Ontario. *Transactions of the American Fisheries Society, 116(4),* 641 – 645.

Brazner, J., DeVita, W. (1998). PCBs, DDE, and mercury in young-of-the-year littoral fishes in Green Bay, Lake Michigan. *Journal of Great Lakes Research, 24(1),* 83 – 92.

Brazo, D.C., Tack, P.I., Liston, C.R. (1975). Age, growth, and fecundity of yellow perch, *Perca flavescens,* in Lake Michigan near Ludington, Michigan. *Transactions of the American Fisheries Society, 104(4),* 726 – 730.

Breck, J.E., Gitter, M.J. (1983). Effect of fish size on the reactive distance of bluegill (*Lepomis macrochirus*) sunfish. *Canadian Journal of Fisheries and Aquatic Sciences, 40,* 162 – 167.

Broeke, G, Voorn, G., Ligtenberg, A. (2016). Which sensitivity analysis method should I use for my agent-based model? *Journal of Artificial Societies and Social Simulation, 19(1),* 1 – 35.

Carvan III, M.J., Incardona, J.P., Rise, M.L. (2008) Meeting the challenges of aquatic vertebrate ecotoxicology. *BioScience, 58(11),* 1015 - 1025.

Castaneda, T.R., Marquez de Prado, B.., Prieto, D., Mora, F. (2004). Circadian rhythms of dopamine, glutamate, and GABA in the striatum and nucleus accumbens of the awake rate: modulation by light. *Journal of Pineal Research,* 177 – 185.

Chang, J.P., Peter, R.E. (1983). Effects of Pimozide and Des Gly10,[D-Ala6]Luteinizing Hormone-Releasing Hormone Ethylamide on Serum Gonadotropin Concentrations, Germinal Vesicle Migration, and Ovulation in female Goldfish, *Carassius auratus. General and Comparative Endocrinology, 52,* 30 – 37.

Chen, C., Amirbahman, A., Fisher, N., Harding, G., Lamborg, C., Nacci, D., Taylor, D. (2008). Methylmercury in marine ecosystems: Spatial patterns and processes of production, bioaccumulation, and biomagnification. *Ecosystem Health, 5,* 399 – 408.

Chu, D.C.M., Albin, R.L., Young, A.B., Penney, J.B. (1990). Distribution and kinetics of GABAB binding sites in rat central nervous system: A quantitative autoradiographic study. *Neuroscience, 34(2),* 341 – 357.

Clapp, D.F., Dettmers, J.M. (2004). Yellow perch research and management in Lake Michigan: evaluating progress in a cooperative effort, 1997 – 2001. Fisheries, 29(11), 11 – 19.

Creque, S.M., Czesny, S.J. (2012). Diet overlap of non-native alewife with native yellow perch and spottail shiner in nearshore waters of southwestern Lake Michigan, 2000 – 2007. Ecology of Freshwater Fish, 21, 201 – 221.

Crowder, L.B. (1980). Alewife, rainbow smelt and native fishes in Lake Michigan: Competition or predation? *Environmental Biology of Fishes, 5(3),* 225 – 233.

Crystal Lake Watershed Association. (2005). The chronology of the Crystal Lake watershed. Available at http://www.clwa.us/PDF/CLWAStudies05041205.pdf

Crump, K.L., Trudeau, V.L. (2009). Mercury-induced reproductive impairment in fish. *Environmental Toxicology and Chemistry, 28(5),* 895 – 907.

Cushing, D.H. (1983). Are fish larvae too dilute to affect the density of their food organisms? *Journal of Planktonic Research, 5,* 847 – 854.

Dabrowski, K., Ciereszko, A., Ramseyer, I., Culver, D., Kestemont, P. (1994). Effects of hormonal treatment on induced spermiation and ovulation in the yellow perch (*Perca flavescens*). *Aquaculture, 120,* 171 – 180.

Dahlberg, M.D. (1979). A review of the survival rates of fish eggs and larvae in relation to impact assessment. *Marine Fisheries Reviews, 41,* 1 – 12.

DeBofksy, A.R., Klingler, R.H., Mora, F.X., Walz, M., Shepherd, B., Larson, J.K., Anderson III, D., Yang, L., Goetz, F., Basu, N., Head, J., Tonellato, P., Murphy, C.M., Carvan III, M.J. Female reproductive impacts of dietary methylmercury in yellow perch (*Perca flavescens*) and zebrafish (*Danio rerio*). In Review.

Depew, D.C., Basu, N., Burgess, N.M., Campbell, L.M., Devlin, E.W., Drevenick, P.E., Hammerschmidt, C.R., Murphy, C.A., Sandheinrich, M.B., Wiener, J.G. (2012). Toxicity of dietary methylmercury to fish: Derivation of ecologically meaningful threshold concentrations. *Environmental Toxicology and Chemistry, 31(7),* 1536 – 1547.

Depledge, M.H. (1994). The rational basis for the use of biomarkers as ecotoxicological tools. In Fossi, M.C., Leonzio, C. Nondestructive biomarkers in vertebrates. Lewis, Boca Raton, FL. 271 – 295.

Dettmers, J.M., Raffenberg, M.J., Weis, A.K. (2003). Exploring zooplankton changes in southern Lake Michigan: implications for yellow perch recruitment. *Journal of Great Lakes Research, 29,* 355 – 364.

Dettmers, J.M., Janssen, J., Pientka, B., Fulford, R.S., Jude, D.J. (2005). Evidence across multiple scales for off-shore transport of yellow perch (*Perca flavescens*) larvae in Lake Michigan. *Canadian Journal of Fish and Aquatic Sciences, 62,* 2683 – 2693.

Dey, S., Choudhurry, M.D., Das, S. (2013). A review on toxicity of paper mill effluent on fish. *Bulletin of Environmental, Pharmacology and Life Sciences, 2(3),* 17 – 23.

Dill, L.M. (1983). Adaptive flexibility in the foraging behavior of fishes. *Canadian Journal of Fisheries and Aquatic Sciences, 40,* 398 – 408.

Drevnick, P.E., Sandheinrich, M.B. (2003). Effects of dietary methylmercury on reproductive endocrinology of fathead minnows. *Environmental Science and Technology, 37(19),* 4390 – 4396.

Driscoll, C.T., Mason, R.P., Chan, HM, Jacob, D.J., Pirrone, N. (2013). Mercury as a global pollutant: Sources, pathways, and effects. *Environmental Science and Technology, 47,* 4967 – 4983.

Dube, M.G., MacLatchy, D.L. (2000). Endocrine responses of *Fundulus heteroclitus* to effluent from a bleached-kraft pulp mill before and after installation of reverse osmosis treatment of a waste stream. *Environmental Toxicology and Chemistry, 19(11),* 2788 - 2796.

Edwards, M.D. (2010). A diet analysis and selectivity of juvenile and adult alewives (*Alosa pseudoharengus*) in NE Lake Michigan. Master's Thesis. Central Michigan University. 78 pp.

Engevold, P.M., Young, E.B., Sandgren, C.D., Berges, J.A. (2015). Pressure from top and bottom: Lower food web responses to changes in nutrient cycling and invasive species in Lake Michigan. *Journal of Great Lakes Research, 41(S3),* 86 – 94.

Enmark, E., Gustafsson, J-A. (1999). Oestrogen receptors – an overview. *Journal of Internal Medicine, 246,* 133 - 138.

Fabrizio, M.C., Adams, J.V., Curtis, G.L. (1997). Assessing prey populations in Lake Michigan: comparison of simultaneous acoustic-midwater trawling and bottom trawling. *Fisheries Research, 33,* 37 – 54.

Field, L.J., MacDonald, D.D., Norton, S.B., Ingersoll, C.G., Severn, C.G., Smorong, D., Lindskoog, R. (2002). Predicting amphipod toxicity from sediment chemistry using logistic regression models. *Environmental Toxicology and Chemistry, 21(9),* 1993 – 2005.

Fleeger, J.W., Carman, K.R., Nisbet, R.M. (2003). Indirect effects of contaminants in aquatic ecosystems. *The Science of the Total Environment, 317,* 207 – 333.

Folt, C., Schulze, P.C., Baumgartner, K. (1993). Characterizing a zooplankton neighbourhood: Small-scale patterns of association and abundance. *Freshwater Biology, 30(2),* 289 – 300.

Forbes, V.E., Palmqvist, A., Bach, L. (2006). The use and misuse of biomarkers in ecotoxicology. *Environmental Toxicology and Chemistry, 25(1),* 272 – 280.

Forney, J.L. (1971). Development of dominant year classes in a yellow perch population. *Transactions of the American Fisheries Society, 100(4),* 739 – 749.

Friedmann, A.S., Costain, E.K., MacLatchy, D.L., Stansley, W., Washuta, E.J. (2002). Effect of mercury on general and reproductive health of largemouth bass (*Micropterus salmoides*) from three lakes in New Jersey. *Ecotoxicology and Environmental Safety, 52,* 117 – 122.

Fritz, E.S., Garside, E.T. (1975). Comparison of age composition, growth, and fecundity between two populations each of *Fundulus heteroclitus* and *F. diaphanous* (Pices: Cyprinodontidae). *Canadian Journal of Zoology, 53,* 361 - 369.

Froehlich, C.Y.M., Kline, R.J. (2015). Using fish population metrics to compare the effects of artificial reef density. *PLOS One, 10(9).* 1 – 16.

Fulbright, T.E., Lewitt, D.G. (2007). Wildlife science: Linking ecological theory and management applications. CRC Press, Boca Raton, FL.

Fulford, R.S. (2003). Food web interactions of larval yellow perch, *Perca flavescens*, in Lake Michigan: Implications for recruitment. PhD Dissertation submitted to North Caroline State University.

Fulford, R.S., Rice, J.A., Miller, T.J., Binkowski, F.P. (2006a). Elucidating patterns of size-dependent predation on larval yellow perch (*Perca flavescens*) in Lake Michigan: An experimental and modeling approach. *Canadian Journal of Fisheries and Aquatic Sciences, 63,* 11 – 27.

Fulford, R.S., Rice, J.A., Miller, T.J., Binkowski, F.P., Dettmers, J.M., Belonger, B. (2006b). Foraging selectivity by larval yellow perch (*Perca flavescens*): implications for understanding recruitment in small and large lakes. *Canadian Journal of Fisheries and Aquatic Sciences, 63,* 28 – 42.

Fuller, P. & Neilson, M. (2015). *Perca flavescens*. USGS Nonindigenous Aquatic Species Database, Gainesville, FL. Available at http://nas.er.usgs.gov/queries/factsheet.aspx?SpeciesID=820 Revision Date: 5/29/2012

Fynn-Aikins, K., Gallagher, E., Reussler, S., Wiebe, J., Gross, T.S. (1998). An evaluation of methylmercury as an endocrine disruptor in largemouth bass. *Abstracts*, SETAC 19th Annual meeting, Charlotte, NC, USA. p 146.

Gerhardt, A. (2007). Aquatic behavioral ecotoxicology: Prospects and limitations. *Human Ecological Risk Assessment, 13* 481 – 491.

Goetz, F.W., Rise, M.L., Rise, M., Goetz, G.W., Binkowski, F., Shepherd, B.S. (2009). Stimulation of growth and changes in the hepatic transcriptome by 17β-estradiol in the yellow perch (*Perca flavescens*). *Physiological Genomics, 38,* 261 – 280.

Gillies, K., Krone, S.M., Nagler, J.J., Schultz, I.R. (2016). A computational model of the rainbow trout hypothalamus-pituitary-ovary-liver axis. *PLOS Computational Biology,12(4),* e1004874.

Goodyear, C.S., Edsall, T.A., Dempsey, O., Moss, G.D., Polanski, P.E.(1982). Atlas of the spawning and nursery areas of the Great Lakes fishes. Volume four: Lake Michigan. U.S. Fish and Wildlife Service, Washington, DC FWS/OBS-82/52.

Gordon, T.C. (1982). Instantaneous growth rates and distribution of larval fish in the vicinity of Locust Point, western Lake Erie. CLEAR technical report.

Granet, J.J.A. (2000). A comparative study of growth and survival of yellow perch in Lake Michigan and Crystal Lake, Michigan. Master's Thesis. Central Michigan University. 66 pp.

Grandjean, P., Weihe, P., White, R.F., Debes, F. (1998). Cognitive performance of children prenatally exposed to "safe" levels of methylmercury. *Environmental Research, Section A, 77,* 165 – 172.

Groh, K.J., Carvalho, R.N., Chipman, J.K., Denslow, N.D., Hadler, M., Murphy, C.A., Roelofs, D., Rolaki, A., Schirmer, K., Watanabe, K.H. (2015) Development and application of the adverse outcome pathway framework for understanding and predicting chronic toxicity: II. A focus on growth impairment in fish. *Chemosphere, 120,* 778 - 792.

Great Lakes Coastwatch. (2014). Long term average surface water temperatures (1992 – 2013 data): Lake Michigan. Available at http://coastwatch.glerl.noaa.gov/statistic/dat/avgtemps-m_1992-2013.dat

Grimm, V., Berger, U., Bastiansen, F., Eliassen, S., Ginot, V., Giske, J., Goss-Custard, J., Grand, T., Heinz, S.K., Huse, G., Huth, A., Jepsen, J.U., Jørgensen, C., Mooij, W.M., Müller, B., Pe'er, G., Piou, C., Railsback, S.F., Robbins, A.M., Robbins, M.M., Rossmanith, E., Rüger, N., Strand, E., Souissi, S., Stillman, R.A., Vabø, R., Visser, U., DeAngelis, D.L. (2006). A standard protocol for describing individual-based and agent-based models. *Ecological Modelling, 198, (1-2),* 115-126.

Grimm, V., Berger, U., DeAngelis, D.L., Polhill, J.G., Giske, J., Railsback, S.F. (2010). The ODD protocol: A review and first update. *Ecological Modeling, 221,* 2760 – 2768.

Hall, T.R., Urena, G., Figueroa, H.R. (1962). In vivo and in vitro effects of temperature on monoamine oxidase activity in brain and other tissues of the goldfish, *Carassius auratus* L. *Computational Biochemistry and Physiology, 73C,* 175 – 180.

Hallam, T.G., Lassiter, R.R., Li, J., McKinney, W. (1990). Toxicant-induced mortality in models of *Daphnia* populations. *Environmental Toxicology and Chemistry, 9,* 597 – 623.

Hammerschmidt, C.R., Sandheinrich, M.B., Wiener, J.G. Rada, R.G. (2002). Effects of dietary methylmercury on reproduction of fathead minnows. *Environmental Science and Technology, 36,* 877 – 883.

Hammerschmidt, C.R., Wiener, J.G., Frazier, B.E., Rada, R.G. (1999). Methylmercury content of eggs in yellow perch related to maternal exposure in four Wisconsin lakes. *Environmental Science and Technology, 33,* 999 – 1003.

Hammond, G.L. (2016). Plasma steroid-binding proteins; primary gatekeepers of steroid hormone action. *Journal of Endocrinology, 230,* R13 – R25.

Hanson, P.C., Johnson, T.B., Schindler, D.E., Kitchell, J.F. (1997). Fish bioenergetics 3.0 for windows. University of Wisconsin Sea Grant Institute. Madison, Wisconsin.

Harvey, B.C., Railsback, S.F. (2007). Estimating multi-factor cumulative watershed effects on fish populations with an individual-based model. *Fisheries, 32(6),* 292 – 298.

Holmstrup, M., Bindesbol, A.-M., Oostingh, G.J., Duschl, A., Scheil, V., Kohler, H.-R., Loureiro, S., Soares, A.M.V.M., Ferreira, A.L.G., Kienle, C., Gerhardt, A., Laskowski, R., Kramarz, P.E., Bayley, M., Svendsen, C., Spurgeon, D.J. (2010) Interactions between effects of environmental chemicals and natural stressors: A review. *Science Of The Total Environment, 408, 3746 - 3762.*

Honsey, A.E., Bunnell, D.B., Troy, C.D., Fielder, D.G., Thomas, M.V., Knight, C.T., Chong, S.C., Hook, T.O. (2016). Recruitment synchrony of yellow perch (*Perca flavescens,* Percidae) in the Great Lakes region, 1966 – 2008. *Fisheries Research, 181,* 214 – 221.

Hooper, M.J., Ankley, G.T., Cristol, D.A., Maryoung, L.A., Noyes, P.D., Pinkerton, K.E. (2013) Interactions between chemical and climatic stressors: A role for mechanistic toxicology in assessing climate change risks. *Environmental Toxicology and Chemistry, 32(1),* 32–48.

Houde, E.D. (1969). Sustained swimming ability of larvae of walleye (*Stizostedion vitreum vitreum*) and yellow perch (*Perca flavescens*). *Journal of the Fisheries Research Board of Canada, 26(6),* 1647 – 1659.

Houde, E.D. (1997). Patterns and consequences of selective processes in teleost early life histories. Pages 169 – 193 in Chambers, R.C., Trippel, E.A. Early life history and recruitment in fish populations. Chapman and Hall, New York, NY.

Houde, E.D. (2001). Fish larvae. Pages 286 – 296 in: Steele, J.H., Thorpe, S.A., Turekian, K.K. Elements of physical oceanography: A derivative of the encyclopedia of ocean sciences. New York, BY. Academic Press.

Ito, S.I., Kishi, M.J., Kurita, Y., Oozeki, Y., Yamanaka, Y., Megrey, B.A., Werner, F.E. (2004). Initial design for a fish bioenergetics model of Pacific saury coupled to a lower trophic ecosystem model. *Fish Oceanography, 13(1),* 111 – 124.

Janssen, J., Luebke, M.A. (2004). Preference for rocky habitat by age-0 yellow perch and alewives. *Journal of Great Lakes Research, 30,* 93 – 99.

Jensen, K.M., Korte, J.J., Kahl, M.D., Pasha, M.S., Ankley, G.T., (2001). Aspects of basic reproductive biology and endocrinology in the fathead minnow (*Pimephales promelas*). *Computational Biochemistry and Physiology C, 128,* 127-141.

Johnston, E.L., Roberts, D.A. (2009). Contaminants reduce the richness and evenness of marine communities: A review and meta-analysis. *Environmental Pollution, 157,* 1745 – 1752.

Kavlock, R.J., Austin, C.P., & Tice, R,R. (2009). Toxicity testing in the 21st century: implications for human health risk assessment. Risk Analysis, 29(4), 485–497.

Kirubagaran, R., Joy, K.P. (1990). Changes in brain monoamine levels and monoamine oxidase activity in the catfish, *Clarias batrachus,* during chronic treatments with mercurial. *Bulletin of Environmental Contamination and Toxicology, 45,* 88 – 93.

Kitchell, J.F., Stewart, D.J. (1977). Applications of a bioenergetics model to yellow perch (*Perca flavescens*) and walleye (*Stizostedion vitreum vitreum*). *Journal of Fisheries Research Board of Canada, 34,* 1922 – 1935.

Knudsen, T.B., Houck, K.A., Sipes, N.S., Singh, A.V., Judson, R.S., Martin, M.T., Weissman, A., Kleinstreuer, N.C., Mortensen, H.M., Reif, D.M., Rabinowitz, J.R., Setzer, R.W., Richard, A.M., Dix, D.J., Kavlock, R.J. (2011) Activity profiles of 309 ToxCast™ chemicals evaluated across 292 biochemical targets. *Toxicology, 282,* 1-15.

Kolpin, D.W., Furlong, E.T., Meyer, M.T., Thurman, E.M., Zaugg, S.D., Barber, L.B., Buxton, H.T. (2002) Pharmaceuticals, hormones, and other organic wastewater contaminants in U.S. streams, 1999-2000: A national reconnaissance. *Environmental Science and Technology, 36,* 1202 - 1211

Kovacs, T.G., Martel, P.H., O'Connor, B.I., Hewitt, L.M., Parrott, J.L., McMaster, M.E., MacLatchy, D.L., Van Der Kraak, G.J., Van Den Heuvel, M.R. (2013) A survey of Canadian mechanical pulp and paper mill effluents: Insights concerning the potential to

affect fish reproduction. *Journal of Environmental Science and Health, Part A, 48(10*), 1178 - 1189.

Kramer, V.J., Etterson, M.A., Hecker, M., Murphy, C.A., Roesijadi, G., Spade, D.J., Spromberg, J.A., Wang, M., & Ankley, G.T. (2011). Adverse outcome pathways and ecological risk assessment bridging to population-level effects. *Environmental Toxicology and Chemistry, 30(1):* 64 – 76.

Kubikova, L., Vyboh, P., Kost'al, L. (2009). Kinetics and pharmacology of the D1 and D2 like dopamine receptors in Japanese quail brain. *Cellular and Molecular Neurobiology, 29,* 961 - 970

Kurreck, J., Stein, C.A. (2015). Molecular medicine: an introduction. Wiley-Blackwell, Weinheim, Germany.

Lam, D.M.K. (1972). The biosynthesis and content of gamma-aminobutyric acid in the goldfish retina. *Journal of Cell Biology, 54*, 225 – 231.

Lauder, J.M. (1993) Neurotransmitters as growth regulatory signals: role of receptors and second messengers. *Trends in Neurosciences, 16(6)*, 233 – 240.

Laurence, G.C. (1982). Nutrition and trophodynamics of larval fish review, concepts, strategic recommendations and opinions. *Fish Ecology III,* University of Miami Technical Report 82008, 123 – 147.

Laws, E.A. (2000). Aquatic pollution: An introductory text. 3rd Edition. Wiley-Interscience. New York, 639 pp.

Leaños-Castañeda, O. & Van Der Kraak, G. (2007). Characterization of estrogen receptor subtypes, ERα and ERβ, mediating vitellogenesis production in the liver of rainbow trout. *Toxicology and Applied Pharmacology, 224*, 116 – 125.

Lenihan, H.S., Peterson, C.H., Kim, S.L., Conlan, K.E., Fairey, R., McDonald, C., Grabowski, J.H., Oliver, J.S. (2003). Variation in marine benthic community composition allows discrimination of multiple stressors. *Marine Ecology Progress Series, 261,* 63 – 73.

Letcher, B.H., Rice, J.A., Crowder, L.B., Rose, K.A. (1996). Variability in survival of larval fish: disentangling components with a generalized individual-based model. *Canadian Journal of Fisheries and Aquatic Sciences, 53,* 787 - 801

Levavi-Sivan, B., Biran, J., Fireman, E. (2006). Sex steroids are involved in the regulation of gonadotropin-releasing hormone and dopamine D2 receptors in the female tilapia pituitary. *Biology of Reproduction, 75,* 642 – 650.

Levavi-Sivan, B., Bogerd, J., Mananos, E.L., Gomez, A., Lareyre, J.J. (2010). Perspectives on fish gonadotropins and their receptors. *General and Comparative Endocrinology, 165,* 412 – 437.

Li, Z., Kroll, K.J., Jensen, K.M., Villeneuve, D.L., Ankley, G.T., Brian, J.V., Sepulveda, M.S., Orlando, E.F., Lazorchak, J.M., Kostich, M., Armstrong, B., Denslow, N.D., & Watanabe, K.H. (2011). A computational model of the hypothalamic-pituitary-gonadal axis in female fathead minnows (*Pimephales promelas*) exposed to 17α-ethinylestradiol and 17β-trenbolone. *BMC Systems Biology, 5,* 63 – 85.

Lynn, S.G., Birge, W.J., Shepherd, B.S. (2008). Molecular characterization and sex-specific tissue expression of estrogen receptor α (esr1), estrogen receptor βa (esr2a) and ovarian aromatase (cyp19a1a) in yellow perch (*Perca flavescens*). *Comparative Biochemistry and Physiology, Part B, 149,* 126 – 147.

Mackas, D.L., Denman, K.L., Abbott, M.R. (1985). Plankton patchiness: Biology in the physical vernacular. *Bulletin of Marine Science, 37(2),* 652 – 674.

Macek, K.J. (1968). Reproduction in brook trout (*Salvelinus fontinalis*) fed sublethal concentrations of DDT. *Journal of Fisheries Research Board of Canada,* 25(9), 1787 – 1796.

Macho, L., Kvetnansky, R., Culman, J., Fickova, M. (1986). Neurotransmitter levels in the hypothalamus during postnatal development in rates. *Experimental & Clinical Endocrinology, 88(2),* 142 – 150.

Madenjian, C.P., Bunnell, D.B., Desorcie, T.J., Chriscinske, M.A., Kostich, M.J., Adams, J.V. (2012). Status and trends of prey fish populations in Lake Michigan, 2011. *USGS Report,* presented at Great Lakes Fisheries Commission Lake Michigan Committee Meeting, Windsor, ON.

Maffucci, J.A., Gore, A.C. (2009) Hypothalamic neural systems controlling the female reproductive life cycle: gonadotropin-releasing hormone, glutamate and GABA. *International Review of Cell and Molecular Biology, 274,* 69 - 127.

Manning, N.F., Bossenbroek, J.M., Mayer, C.M., Bunnell, D.B., Tyson, J.T., Rudstam, L.G., Jackson, J.R. (2014). Modeling turbidity type and instantaneous effects on the growth and starvation mortality of age-0 yellow perch. *Canadian Journal of Fish and Aquatic Sciences, 71,* 1544 – 1553.

Marsden, J.E., Robillard, S.R. (2004). Decline of yellow perch in Southwestern Lake Michigan, 1987 – 1997. *North American Journal of Fisheries Management, 24(3),* 952 – 966.

Mason, R.P., Sullivan, K.A. (1997). Mercury in Lake Michigan. *Environmental Science and Technology, 31,* 942 – 947.

Mayer, F.L., Krause, G.F., Buckler, D.R., Ellersieck, M.R., Lee, G. (1994). Predicting chronic lethality of chemicals to fishes from acute toxicity test data: concepts and linear regression analysis. *Environmental Toxicology and Chemistry, 13(4),* 671 – 678.

McCarty, H.B., Miller, K., Brent, R.N., Schofield, J. (2004). Results of the Lake Michigan Mass Balance Study: Mercury Data Report. *Environmental Protection Agency Great Lakes National Program Office,* Chicago, IL. Report # EPA 905 R-01-012

McGeer, P.L., Eccles, J.C., McGeer, E.G. (2013). Molecular neurobiology of the mammalian brain. Plenum Press, New York.

McNaught, S. (2002). [Lake Michigan and Crystal Lake yellow perch survey]. Central Michigan University. Unpublished raw data.

Megard, R.O., Kuns, M.M., Whiteside, M.C., Downing, J.A. (1997). Spatial distributions of zooplankton during coastal upwelling in western Lake Superior. *Limnology and Oceanography, 42,* 827 – 840.

Mercado-Silva, N., Olden, J.D., Maxted, J.T., Hrabik, T.R., Vander Zanden, M.J. (2006). Forecasting the spread of invasive rainbow smelt in the Laurentian Great Lakes region of North America. *Conservation Biology, 20(6),* 1740 – 1749.

Michigan Department of Environmental Quality. (2013). Fish contaminant monitoring program online database. Available at http://www.deq.state.mi.us/fcmp/default.asp

Miehls, S.M., Dettmers, J.M. (2011). Factors influencing habitat shifts of age-0 yellow perch in southwestern Lake Michigan. *Transactions of the American Fisheries Society, 140(5),* 1317 – 1329.

Miller, D.H., Jensen, K.M., Villeneve, D.L., Kahl, M.D., Makynen, E.A., Durhan, E.J., Ankley, G.T. (2007). Linkage of biochemical responses to population-level effects: a case study with vitellogenin in the fathead minnow. *Environmental Toxicology and Chemistry,* 26, 521 – 527.

Miller, R.R. (1957). Origin and dispersal of the alewife, *Alosa pseudoharengus,* and the gizzard shad, *Dorosoma cepedianum,* in the Great Lakes. *Transactions of the American Fisheries Society, 86,* 96 – 111.

Mills, E.L., Forney, J.L. (1981). Energetics, food consumption, and growth of young yellow perch in Oneida Lake, New York. *Transactions of the American Fisheries Society, 110,* 479–488.

Monosson, E. (2005) Chemical mixtures: Considering the evolution of toxicology and chemical assessment. *Environmental Health Perspectives, 113(4),* 383 - 390.

Mora, F.X. (2015). Neurobehavioral and gene expression effects of early embryonic methylmercury exposure in yellow perch (*Perca flavescens*) and zebrafish (*Danio rerio*) larvae. PhD Dissertation. University of Wisconsin-Milwaukee.

Murphy, C.A, Nisbet, RN, Atnzcak, P., Garcia-Reyero, N., Gergs, A., Lika, K. Mathews, T., Muller E., Nacci, D. Peace, A. Remien, C, Schulz, I., Watanabe, K. Linking the adverse outcome pathway to dynamic energy budgets: a conceptual model. In Garcia-Reyero, N, and Murphy, C.A, (eds). Systems Biology approaches for advancing the adverse outcome pathway for risk assessment. Springer, in press.

Murphy, C.A., Rose, K.A., & Thomas, P. (2005). Modeling vitellogenesis in female fish exposed to environmental stressors: predicting the effects of endocrine disturbance due to exposure to a PCB mixture and cadmium. *Reproductive Toxicology, 19,* 395 – 409.

Murphy, C.A., Rose, K.A., Alvarez, M., Fuiman, L.A. (2008). Modeling larval fish behavior: Scaling the sublethal effects of methylmercury to population-relevant endpoints. *Aquatic Toxicology, 86,* 470 – 484.

Murphy, C.A., Rose, K.A., Rahman, M.S., & Thomas, P. (2009). Testing and applying a fish vitellogenesis model to evaluate laboratory and field biomarkers of endocrine disruption in Atlantic croaker exposed to hypoxia. *Environmental Toxicology and Chemistry, 28*, 1288–1303.

Murphy, E., MacEachen, C., Whittle, D.M., Keir, M.J., Gorrie, J.F. (2007). State of the Great Lakes 2007 - Indicator #121: Contaminants in whole fish. Environment Canada and the U.S. Protection Agency. Report No. EPA 905-R-07-003.

Mylonas, C.C., Zohar, Y. (2007). Promoting oocyte maturation, ovulation, and spawning in farmed fish. In Babin, P.J., Cerdà, J., Lubzens, E. eds, The Fish Oocyte: From Basic Studies to Biotechnological Applications. Springer Netherlands, Dordrecht, pp 437-474.

National Research Council. (2007). Toxicity testing in the 21st century: A vision and a strategy. Washington, DC: National Academies Press.

National Research Council (2007) Toxicity testing in the 21st century: A vision and a strategy. National Academies Press, Washington, DC.

Nelson, E.R., Habibi, H.R. (2013). Estrogen receptor function and regulation in fish and other vertebrates. *General and Comparative Endocrinology*, *192,* 15 – 24.

Omori, M., Hamner, W.M. (1982). Patchy distribution of zooplankton: Behavior, population assessment and sampling problems. *Marine Biology, 72,* 193 – 200.

Organisation for Economic Co-operation and Development (2013) Guidance document on developing and assessing adverse outcome pathways: series on testing and assessment No. 184. Available at

http://www.oecd.org/officialdocuments/publicdisplaydocumentpdf/?cote=env/jm/mono(2013)6&doclanguage=en.

Parker, A.D., Stepien, C.A., Sepulveda-Villet, O.J., Ruehl, C.B., Uzarski, D.G. (2009). The interplay of morphology, habitat, resource use, and genetic relationships in young yellow perch. *Transactions of the American Fisheries Society, 138,* 899 – 914.

Pepin, P. (1989). Predation and starvation of larval fish: A numerical experiment of size and growth dependent survival. *Biological Oceanography, 6,* 23 – 44.

Peter, R. E., Chang, J. P., Nahorniak, C. S., Omeljaniuk, R. J., Sokolowska, M., Shih, S. H., Billard, R. (1986). Interactions of catecholamines and GnRH in regulation of gonadotropin secretion in teleost fish. *Recent Progress Hormone Research. 42,* 513–548.

Peter, R.E., Yu, K-L., Marchant, T.A., Rosenblum, P.M. (1990)> Direct neural regulation of the teleost adenohypophysis. *Journal of Experimental Zoology Part A: Ecological Genetics and Physiology, 256, S4,* 84 – 89.

Pettersson, K., Grandien, K., Kuiper, G.G.J.M., Gustafsson, J-A. (1997). Mouse estrogen receptor β forms estrogen response element-binding heterodimers with estrogen receptor α. *Molecular Endocrinology, 11(10),* 1486 – 1496.

Popesku, J.T., Martyniuk, C.J., Mennigen, J., Xiong, H., Zhang, D., Xia, X., Cossins, A.R., & Trudeau, V.L. (2008). The goldfish (*Carassius auratus*) as a model for neuroendocrine signaling. *Molecular and Cellular Endocrinology, 293,* 43 – 56.

Post, J.R. (1990). Metabolic allometry of larval and juvenile yellow perch (*Perca flavescens*): In situ estimates and bioenergetics models. *Canadian Journal of Fisheries and Aquatic Sciences, 47,* 554 – 560.

Reimchen, T.E. (1988). Inefficient predators and prey injuries in a population of giant stickleback. *Canadian Journal of Zoology, 66,* 2036 – 2044.

Richardson, J.E. (2004). Winnicut dam removal feasibility study: Hydraulic fish passage and alternative analysis. New Hampshire Department of Environmental Services. Report prepared for Woodlot Alternatives, Inc. Topsham, Maine.

Rice, J.A., Miller, T.J., Rose, K.A., Crowder, L.B., Marschall, E.A., Trebitz, A.S., DeAngelis, D.L. (1993). Growth rate variation and larval survival: Inferences from an individual-based size-dependent predation model. *Canadian Journal of Fisheries and Aquatic Sciences, 50,* 133 – 142.

Richter, C.J.J., Eding, E.H., Goos, H.J.TH., De Leeuw, R., Scott, A.P. (1987). The effect of pimozide/LHRHa and 17α-hydroxyprogesterone on plasma steroid levels and ovulation in the African catfish, *Clarias gariepinus. Aquaculture, 63,* 157 – 168.

Ruby, S.M., Idler, D.R., So, Y.P. (1986) The effect of sublethal cyanide exposure on plasma vitellogenin levels in rainbow trout (*Salmo gairdneri*) during early vitellogenesis. *Archives of Environmental Contamination and Toxicology, 15,* 603-607.

Sabo-Attwood, T., Kroll, K.J., & Denslow, N.D. (2004). Differential expression of largemouth bass (*Micropterus salmoides*) estrogen receptor isotypes alpha, beta and gamma by estradiol. *Molecular and Cellular Endocrinology, 218,* 107 – 118.

Santucci Jr., V.J., Eggold, B.T., Kalish, T.G., Price, J., Gorenflo, T.K. (2014). Lake Michigan yellow perch summit summary report. Report prepared by the Lake Michigan Committee for the UIC Forum, Chicago, IL.

Sarthy, P.V., Lam, D.M.K. (1979). The uptake and release of [3H] Dopamine in the goldfish retina. *Journal of Neurochemistry, 32,* 1269 – 1277.

Schael, D.M., Rudstam, L.G., Post, J.R. (1991). Gape limitation and prey selection in larval yellow perch (*Perca flavescens*), freshwater drum (*Aplodinotus grunniens*), and black crappie (*Pomoxis nigromaculatus*). *Canadian Journal of Fisheries and Aquatic Sciences, 48,* 1919 – 1925.

Scott, G.R., Sloman, K.A. (2004). The effects of environmental pollutants on complex fish behavior: integrating behavioural and physiological indicators of toxicity. *Aquatic Toxicology, 68,* 369 – 392.

Shroyer, S.M., McComish, T.S. (2000). Relationship between alewife abundance and yellow perch recruitment in southern Lake Michigan. *North American Journal of Fisheries Management, 20,* 220 – 225.

Siefert, R.E.. (1972). First food of larval yellow perch, white sucker, bluegill, emerald shiner, and rainbow smelt. *Transactions of the American Fisheries Society, 101(2),* 219 – 225.

Simonin, P.W, Parrish, D.L., Rudstam, L.G., Sullivan, P.J., Pientka, B. (2012). Native rainbow smelt and nonnative alewife distribution related to temperature and light gradients in Lake Champlain. *Journal of Great Lakes Research, 38,* 115 – 122.

Searcy, S.P., Sponaugle, S. (2000). Variable larval growth in a coral reef fish. *Marine Ecology Progress Series, 206,* 213 – 226.

Sepulveda, M.S., Quinn, B.P., Denslow, N.D., Holm, S.R., Gross, T.S. (2003) Effects of pulp and paper mill effluents on reproductive success of largemouth bass. *Environmental Toxicology and Chemistry, 22(1),* 205 – 213.

Smith, L.E., Carvan III, M.J., Dellinger, J.A., Ghorai, J.K., White, D.B., Williams, F.E., Weber, D.N. (2010). Developmental selenomethionine and methylmercury exposures affect zebrafish learning. *Neurotoxicology and Teratology, 32,* 246 – 255.

Smith, M.J., Jennes, L. (2001). Neural signals that regulate GnRH neurons directly during the oestrous cycle. *Reproduction, 122,* 1 – 10.

Smolders, I., Bogaert, L., Ebinger, G., Michotte, Y. (1997). Muscarinic modulation of striatal dopamine, glutamate, and GABA release, as measured with in vivo Microdialysis. *Journal of Neurochemistry,68,* 1942 – 1948.

Stone, R.B., Pratt, H.L., Parker Jr., R.O., Davis, G.E. (1979). A comparison of fish populations on an artificial and natural reef in the Florida keys. *Marine Fisheries Reviews, 41(9),* 1-11

Sulistyo, I., Rinchard, J., Fontaine, P., Gardeur, J-N., Capdeville, B. (1998). Reproductive cycle and plasma levels of sex steroids in Female Eurasian perch *Perca fluviatilis*. *Environmental Science and Biology Faculty Publications,* Paper 15, Brockport State University, NY, NY.

Sun, K., Krause, G.F., Mayer, F.L., Ellersieck, M.R., Basu, A.P. (1995). Predicting chronic lethality of chemicals to fishes from acute toxicity test data: Theory of accelerated life testing. *Environmental Toxicology and Chemistry, 14(10),* 1745 – 1752.

Sundling, K., Craciun, G., Schultz, I., Hook, S., Nagler, J., Cavileer, T., Verducci, J., Liu, Y., Kim, J., Hayton, W. (2014). Modeling the endocrine control of vitellogenin production in female rainbow trout. *Mathematical Biosciences and Engineering, 11(3),* 621 – 639.

Szabo, A., Ruby, S.M., Rogan, F., Amit, Z. (1991) Changes in brain dopamine levels, oocyte growth and spermatogenesis in rainbow trout, *Oncorhynchus mykiss*, following sublethal cyanide exposure. *Archives of Environmental Contamination and Toxicology, 21,* 152-157.

Szymański P, Markowicz M, Mikiciuk-Olasik E (2012) Adaptation of high-throughput screening in drug discovery – toxicological screening tests. International Journal of Molecular Sciences 13(1):427-452.

Tarby, M.J. (1974). Characteristics of yellow perch cannibalism in Oneida Lake and the relation to first year survival. *Transactions of the American Fisheries Society, 103(3),* 462 – 471.

Terasawa, E. (1994). Steroid modulation of pulsatile LHRH release in the Rheses monkey. *Hormones and Behavior, 28,* 408 – 416.

Thompson G, Swain J, Kay M et al (2001) The treatment of pulp and paper mill effluent: a review. Bioresource Technology 77:275 – 286.

Thrush, S.F., Hewitt, J.E., Hickey, C.W., Kelly, S. (2008). Multiple stressor effects identified from species abundance distributions: interactions between urban contaminants and species habitat relationships. *Journal of Experimental Marine Biology and Ecology, 366,* 160 – 168.

Tonello, M.A. (2015). Michigan Department of Natural Resources Status of the Fishery Resource Report: Crystal Lake, Benzie County. Report No. 2015-202, 1 – 27.

Treimann, D.M. (2001). GABAergic mechanisms in epilepsy. *Epilepsia, 42,* 8 - 12.

Trudeau, V.L., Sloley, B.D., Peter, R.E. (1993). GABA stimulation of gonadotropin-II release in goldfish: involvement of GABAA receptors, dopamine, and sex steroids. *The American Journal of Physiology: Regulatory, Integrative and Comparative Physiology, 265,* R348 – 355.

Trudeau, V.L. (1997). Neuroendocrine regulation of gonadotropin-II release and gonadal growth in the goldfish, *Carassius auratus. Reviews of Reproduction, 2,* 55 – 68.

Trudeau, V.L., Spanswick, D., Fraser, E.J., Lariviere, K., Crump, D., Chiu, S., MacMillan, M., & Schulz, R.W. (2000). The role of amino acid neurotransmitters in the regulation of pituitary gonadotropin release in fish. *Biochemistry and Cell Biology, 78,* 241-59.

Trudel, M., Rasmussen, J.B. (2001). Predicting mercury concentration in fish using mass balance models. *Ecological Applications, 11(2),* 517 – 529.

Tsehaye, I., Jones, M.L., Bence, J.R., Brenden, T.O., Madenjian, C.P., Warner, D.M. (2014). A multispecies statistical age-structured model to assess predator-prey balance: application to an intensively managed Lake Michigan pelagic fish community. *NRC Research Press, 71,* 627 – 644.

Turskchak, B. (2013). Changes in the Lake Michigan trophic structure: As revealed by stable C and N Isotopes. M.S. Thesis submitted to the University of Wisconsin-Milwaukee.

United States Environmental Protection Agency (2012) Research in Action: Exposure Biomarkers in Aquatic Organisms. Available at http://www.epa.gov/nerleerd/research/exposurebiomarkers.html. Accessed 25 Dec 2015:

United States Environmental Protection Agency. (2015). The toxic substances control act (TSCA) chemical substance inventory. Available at https://www.epa.gov/tsca-inventory.

van den Pol, A.N. (2010). Excitatory neuromodulator reduces dopamine release, enhancing prolactin secretion. *Neuron, 65(2),* 147 – 149.

Van Der Kraak, G., Zacharewski, T., Janz, D.M., Sanders, B.M., & Gooch, J. W. (1998). Comparative endocrinology and mechanisms of endocrine modulation in fish and wildlife. In Principles and processes for evaluating endocrine disruption in wildlife, Kendall, R.J., Dickerson, R.L., Suk, W.A., Giesy, J.P., Eds. SETAC Press, Pensacola, FL, 97-119.

Van Der Kraak, G. (2009). The GnRH system and the neuroendocrine regulation of reproduction. *Fish Neuroendocrinology, 28,* 115 – 149.

Van Oosten, J. (1937). The dispersal of smelt, *Osmerus mordax* (Mitchill), in the Great Lakes region. *Transactions of the American Fisheries Society, 66(1),* 160 – 171.

Venton, B.J., Zhang, H., Garris, P.A., Phillips, P.E.M., Sulzer, D., & Wightman, R.M. (2003). Real-time decoding of dopamine concentration changes in the caudate-putamen during tonic and phasic firing. *Journal of Neurochemistry, 87,* 1284 – 1295.

Villeneuve, D., Volz, D.C., Embry, M.R., Ankley, G.T., Belanger, S.E., Leonard, M, Schirmer, K., Tanguay, R., Truong, L., Wehmas, L. (2013). Discovering and annotating adverse outcome pathways for early fish development. *Environmental Toxicology and Chemistry, 33(1),* 158 – 169.

Voaden, M.J., Marshall, J., Murani, N. (1974). The uptake of [3H]-amino butyric acid and [3H] glycine by the isolated retina of the frog. *Brain Research, 67,* 115 – 132.

Wang, N., Eckmann, R. (1994). Effects of temperature and food density on egg development, larval survival and growth of perch (*Perca fluviatilis* L.). *Aquaculture, 122,* 323 – 333.

Warner, D.M., Farha, S.A., O'Brien, T.P., Ogilvie, L., Claramunt, R.M., Hanson, D. (2014). Status of pelagic prey fishes in Lake Michigan, 2013. Report prepared for the U.S. Geological Survey. Reston, VA.

Watanabe, K., Anderson, M., Basu, N., Carvan, MJ 3rd, Crofton, K.M., King, K.A., Suñol, C., Tiffany-Castiglioni, E., & Schultz, I.R. (2011). Defining and modeling known adverse outcome pathways: Domoic acid and neuronal signaling as a case study. *Environmental Toxicology and Chemistry, 30(1),* 9-21.

Watanabe, K.H., Li, Z., Kroll, K.J., Villeneuve, D.L., Garcia-Reyero, N., Orlando, E.F., Sepulveda, M.S., Collette, T.W., Ekman, D.R., Ankley, G.T., & Denslow, N.D. (2009). A computational model of the hypothalamic-pituitary-gonadal axis in male fathead minnows exposed to 17α-ethinylestradiol and 17β-estradiol. *Toxicological Sciences, 109(2),* 180 – 192.

Watanabe, M., Fukuda, A., Nabekura, J. (2014). The role of GABA in the regulation of GnRH neurons. *Frontiers in Neuroscience, 8,* 1-9.

Waye, A., Annal, M., Tang, A., Picard, G., Harnois, F., Guerrero-Analco, J.A., Saleem, A., Hewitt, L.M., Milestone, C.B., MacLatchy, D.L. (2014A) Canadian boreal pulp and paper feedstocks contain neuroactive substances that interact in vitro with GABA and dopaminergic systems in the brain. *Science Of The Total Environment, 468,* 139 - 315-325.

Waye, A., Lado, W.E., Martel, P.H., Arnason, J.T., Trudeau, V.L. (2014B) Ovulation but not milt production is inhibited in fathead minnows (*Pimephales promelas*) exposed to a reproductively inhibitory pulp mill effluent. *Reproductive Biology and Endocrinology, 12*, 1-43.

Weber, M.J., Dettmers, J.M., Wahl, D.H. (2011). Growth and survival of age-0 yellow perch across habitats in Southwestern Lake Michigan: Early life history in a large freshwater environment. *Transactions of the American Fisheries Society, 140,* 1172 – 1185.

Weis, J.S., Candelmo, A. (2012). Pollutants and fish predator/prey behavior. A review of laboratory and field approaches. *Current Zoology, 58(1),* 9 – 20.

Weis, P., Weis, J.S. (1974). DDT causes changes in activity and schooling behavior in goldfish. *Environmental Research, 7,* 68 – 74.

Wells, L., McLain, A.L. (1972). Lake Michigan: Effects of exploitation, introductions, and eutrophication on the salmonid community. *Journal of Fisheries Research Board of Canada, 29,* 889 – 898.

Wheeler, D.D., Hollingsworth, R.G. (1979). A model of GABA transport by cortical synaptosomes from the Long-Evans rat. *Journal of Neuroscience Research, 4,* 265 – 289.

Whiteside, M.C., Swindoll, C.M., Doolittle, W.L. (1985). Factors affecting the early life history of yellow perch, *Perca flavescens*. *Environmental Biology of Fishes, 12(1),* 47 – 56.

Wiener, J.G., Sandheinrich, M.B., Bhavsar, S.P., Bohr, J.R., Evers, D.C., Monson, B.A., Schrank, C.S. (2012). Toxicological significance of mercury in yellow perch in the Laurentian Great Lakes region. *Environmental Pollution, 161,* 350 – 357.

Wydoski, R.S., Whitney, R.R. (2003). Inland Fishes of Washington. University of Washington Press. Seattle Washington. 193 – 198.

Xu, X., Lamb, C., Smith, M., Schaefer, L., Carvan III, M.J., Weber, DN. (2012). Developmental methylmercury exposure affects avoidance learning outcomes in adult zebrafish. *Toxicology and Environmental Health Sciences, 4(5),* 85 – 91.

Young, K.V., Dower, D.E., Pepin, P. (2009). A hierarchical analysis of the spatial distribution of larval fish prey. *Journal of Planktonic Research, 1(1),* 1 – 14.

Zakes, Zdislaw, Demska-Zakes, K. (2005). Artificial spawning of pikeperch (*Sander lucioperca (L.))* stimulated with human chorionic gonadotropin (HCG) and mammalian GNRH analogue with a dopamine inhibitor. *Archives of Polish Fisheries, 13(1),* 63 – 75.

Żarski, D., Horváth, A., Held, J.A., Kucharczyk, D. (2015). Artificial Reproduction of Percid Fishes. In Kestemont P, Dabrowski K, Summerfelt CR, eds, Biology and Culture of Percid Fishes: Principles and Practices. Springer Netherlands, Dordrecht, p. 123-161.

Zhang, X, Hecker, M, Jones, P.D., Newsted, J., Au, D., Kong, R., Wu, R.S.S., Giesy, J.P. (2008). Responses of the medaka HPG axis PCR array and reproduction to prochloraz and ketoconazole. *Environmental Science and Technology, 42,* 6762 – 6769.

Zhou, T., Scali, R., Weis, J.S. (2001). Effects of methylmercury on ontogeny of prey capture ability and growth in three populations of larval *Fundulus heteroclitus*. *Archives of Environmental Contamination and Toxicology, 41,* 47 – 54.

Zohar, Y., Munoz-Cueto, J.A., Elizur, A., & Kah. O. (2010). Neuroendocrinology of reproduction in teleost fish. *General and Comparative Endocrinology, 165,* 43